1987

Spatial and temporal variation of snow accumulation in the central Karakoram, northern Pakistan

Cameron Parker Wake
Wilfrid Laurier University

CANADIAN THESES

THÈSES CANADIENNES

NOTICE

The quality of this microfiche is heavily dependent upon the quality of the original thesis submitted for microfilming. Every effort has been made to ensure the highest quality of reproduction possible.

If pages are missing, contact the university which granted the degree.

Some pages may have indistinct print especially if the original pages were typed with a poor typewriter ribbon or if the university sent us an inferior photocopy.

Previously copyrighted materials (journal articles, published tests, etc.) are not filmed.

Reproduction in full or in part of this film is governed by the Canadian Copyright Act, R.S.C. 1970, c. C-30.

AVIS

La qualité de cette microfiche dépend grandement de la qualité de la thèse soumise au microfilmage. Nous avons tout fait pour assurer une qualité supérieure de reproduction.

S'il manque des pages, veuillez communiquer avec l'université qui a conféré le grade.

La qualité d'impression de certaines pages peut laisser à désirer, surtout si les pages originales ont été dactylographiées à l'aide d'un ruban usé ou si l'université nous a fait parvenir une photocopie de qualité inférieure.

Les documents qui font déjà l'objet d'un droit d'auteur (articles de revue, examens publiés, etc.) ne sont pas microfilmés.

La reproduction, même partielle, de ce microfilm est soumise à la Loi canadienne sur le droit d'auteur, SRC 1970, c. C-30.

THIS DISSERTATION HAS BEEN MICROFILMED EXACTLY AS RECEIVED

LA THÈSE A ÉTÉ MICROFILMÉE TELLE QUE NOUS L'AVONS REÇUE

NL-339 (r. 86/06)

Canada

SPATIAL AND TEMPORAL VARIATION OF SNOW ACCUMULATION IN THE CENTRAL KARAKORAM, NORTHERN PAKISTAN

By

Cameron Parker Wake
B.Sc. Hon., University of Ottawa, 1984

THESIS
Submitted to the Department of Geography
in partial fulfilment of the requirements
for the Master of Arts degree
Wilfrid Laurier University
1987

ISBN 0-315-37956-1

ACKNOWLEDGEMENTS

I would like to express my appreciation to Dr. Kenneth Hewitt, Dr. Mike English and Dr. Houston Saunderson for guidance in this study; and to Dr. Paul Mayewski, Dr. Mary-Joe Spencer and Mark Twickler of the Glacier Research Group at the University of New Hampshire for valuable discussions and assistance during the preparation and laboratory analysis phases of this research. In addition the use of the laboratories at the University of New Hampshire is greately appreciated. Dr. W. Dansgaard at the Geophysical Isotope Laboratory, University of Copenhagen kindly conducted the oxygen isotope analyses; Dr. L. Thompson at the Institute of Polar Studies, Ohio State University kindly provided the microparticle and conductivity analyses.

Many thanks to the expedition members which included Barry Roberts, Shambi Khan, Rajib Shah, Hussain, Mohammed and Claude David. I would like to specially thank Pamela Carnochan for drafting the figures as well as both Pam and David Butz for moral support. The manuscript was typed by Lisa Bowyer.

This research is part of the Snow and Ice Hydrology Project which is a collaborative project funded jointly by the Canadian International Development Research Centre, the Water and Power Development Authority in Pakistan, and Wilfrid Laurier University, Waterloo, Canada.

ABSTRACT

Runoff from the Upper Indus Basin depends upon snowfall at high elevations in the northern mountains of Pakistan. However, very little is known concerning the amount of snowfall in the major source area, the high Karakoram, or its spatial and temporal distribution.

Glaciers contain well preserved records of snow accumulation and provide a unique tool for retrieving data. A number of studies on temperate and tropical glaciers indicate that variations in chemical content and microparticle concentrations delineates seasonal stratigraphy. In addition, the chemical record of the snowpack can usually be used to determine the source of precipitation.

Field work in the Central Karakoram during the summer of 1986 consisted of a physical analysis of, and sample collection from seven snowpits, one snow/firn core and seven fresh snowfall events. Snowmelt samples have been analysed for ion concentrations (including Na, Cl, NO2, NO3, PO4,& SO4) and oxygen isotope ratios. A limited number of samples were analysed for microparticle concentrations, conductivity and total beta activity.

Seasonal trend can be delineated for all of the snowpits and the upper 12.2 m of the snow/firn core from an analysis of the time-series profiles (Figures 5.1, 5.2 & 5.3). The net annual accumulation (Table 6.1 A & B) provides the basis for interpretation of the spatial and temporal variation in snow accumulation in the Karakoram. Glaciochemical dating techniques are seen as an effective and efficient technique to determine net annual accumulation in high altitude alpine environments. Sampling over a range of geographic locations and elevations provides valuable information concerning the altitudinal and lateral variation in snow accumualtion.

TABLE OF CONTENTS

LIST OF TABLES

LIST OF FIGURES

CHAPTER 1

INTRODUCTION

1.1 PREAMBLE

Pakistan depends heavily upon the waters of the Upper Indus Basin (U.I.B.) for power generation, irrigation and water supply. Runoff from the U.I.B. depends primarily upon snowfall at higher elevations along the northern portion of the watershed. The tremendous arc of the Karakoram Mountains, which extends over 350 km, holds the greatest concentration of snow and ice in Asia (Hewitt 1986; Figure 1.1). On average, 70-80% of the total annual runoff from the U.I.B. originates as snow and ice melt in the Karakoram. The bulk of this meltwater runoff occurs during the summer season from mid-June to mid-September. The overwhelming role the Karakoram plays in the hydrology of the U.I.B. draws attention to the snow conditions in this mountain range.

Unfortunately very little is known concerning the mountainous headwaters of the Indus. A concerted research effort concentrating on the glacial hydrology of the U.I.B. was begun in 1985 as part of the Snow and Ice Hydrology Project (S.I.H.P.). This is a collaborative project funded jointly by the Canadian International Development Research Centre, the Water and Power Development Authority in Pakistan, and Wilfrid Laurier University, Waterloo, Canada. The main goal of the S.I.H.P. is to improve our understanding of glacial conditions in the U.I.B. with a view towards developing a monitoring and forecasting network so that Pakistan can better manage its limited water resources.

The present study is concerned with moisture input into the region, which represents one crucial component of the hydrological system in the U.I.B.

Most of the precipitation in the Karakoram occurs at elevations above 3000 m.a.s.l (above sea level). It is this precipitation, in the form of snow, that creates the only large moisture surplus for the region. However, precipitation records for the U.I.B. come from weather stations which lie below 3000 m. mostly in semi-arid and valley locations. The stations are in the main towns and subject to the powerful topoclimatic effects of valley wind systems (Butz and Hewitt, 1986).

Accumulation zones of glaciers often contain well preserved records of snowfall and provide a unique opportunity for retrieving data. Traditional work attempted to delineate annual stratigraphy by interpreting the physical characteristics of the snowpack. Melting events during the summer result in the concentration of surface debris into a single, distinct, dirty horizon and the formation of ice layers. However, this interpretation is problematic. For example, temperate and tropical glaciers that experience two seasons of accumulation, two or more periods of melting, or intensified periods of debris transport are likely to develop snowpacks which display two or more dirty horizons and/or several ice layers within each year of snow accumulation.

More recent studies of polar and high altitude alpine glaciers indicate that a wide range of geochemical dating techniques can accurately and confidently identify annual stratigraphy within snowpits and snow/ice cores. These glaciochemical dating techniques are discussed in detail in Section 1.3. In regions that experience two seasons of accumulation, the chemical record of the snowpack provides additional information that can be used to delineate the seasonal snowpack stratigraphy and therefore determine the relative seasonal contribution of snow. In addition, the chemical record can usually be employed

to determine the source of precipitation. This is of particular interest in glacier basins where moisture is derived from two different sources.

Previous studies that have employed glaciochemical dating techniques in high altitude glacier basins have concentrated on recovering a chemical record from one, or possibly two locations. In general, these studies focus upon the temporal variation of snow accumulation, of stable isotope ratios, and of ion concentrations, in order to produce a paleoclimatic record.

The basis of snow accumulation research in the Karakoram is to look at snow accumulation as a fundamental component of the hydrology of the Upper Indus Basin. This presents the opportunity to use glaciochemical dating techniques to determine both the temporal and spatial variation of snow accumulation in the Karakoram in relation to the hydrology of the region. This is accomplished by developing a sampling network that covers a range of elevations and geographic locations within a glacier basin. This type of network is essential to pick out the altitudinal and lateral variation in snow accumulation. In essence, this study attempts not only to determine the spatial and temporal variation in snow accumulation within the Karakoram to produce a paleoclimatic record, but also to apply a unique and sensitive technique to hydrological studies in alpine environments.

1.2 RESEARCH OBJECTIVES

The goal of this research is to delineate annual snowpack stratigraphy and determine the rate of snow accumulation in the Biafo Glacier Basin. This is done by interpreting the variation with depth of the physical characteristics (density, position of ice layers and debris band, and microparticle

concentrations) and chemical content (sodium, chloride, nitrate, sulfate, oxygen isotopes, and total β activity) of the snowpack, at several locations over a range of elevations. This information will then be used to determine the temporal, spatial and altitudinal variations of annual snow accumulation From such data it is possible to:

1. provide a first estimate of annual moisture input to the Biafo Glacier Basin;
2. determine the short term response of the hydrological system to variations in summer and winter snow accumulation;
3. provide basic data concerning moisture input to calibrate hydrological forecasting models (Ferguson, 1986; Quick, pers. comm.);
4. determine the provenance of moisture and its seasonal variation and;
5. provide an input, from a data sparse area, to a global data set developed to improve our understanding of atmospheric circulation and the Earth's geochemical cycle.

1.3 LITERATURE REVIEW

1.3.1 Snow accumulation measurements in the Karakoram, Hindu Kush and Western Himalaya.

The Karakoram mountains, the major contributor of runoff from the U.I.B., remain one of the least studied glaciated areas on Earth. Only one study, limited both in scope and analytical technique, has attempted to measure accumulation rates in the accumulation areas of Karakoram glaciers. In 1973 the Batura Investigation Group (1979) recorded a net winter accumulation of 1.03 m water equivalent (w.e.) at 4840 m on the Batura Glacier. (Figure 2.1 illustrates the location of the snow accumulation studies discussed in this

section.) A stratigraphic analysis of ice layers in two different crevasse walls at 5000 m revealed an apparent net annual accumulation rate ranging from 1.03 - 1.25 m w.e. over the previous 5 years.

Mayewski et al. (1984) drilled a 16.6 m core on Sentik Glacier, Ladakh Himalaya at an elevation of 4908 m. Core chronology was determined by correlating a maximum total β activity (found in the depth range 15.4-15.9 m) with the increased concentration of total β activity found in the atmosphere due to 1963 series of thermonuclear weapons testing. The results indicate an average annual net accumulation of 0.62 m w.e., which is lower than the 0.90 m of rainfall recorded at the valley bottom station adjacent to the core site. Maximum precipitation in this region is a result of the Indian summer monsoon circulation which occurs during July and August.

During 1965, Gilbert et al. (1969) worked on a one square kilometre northwest facing cirque glacier in the Hindu Kush. Annual layers in the bergshrund at 5000 m were delineated by naturally occurring, yellow-brown discoloured ice, interpreted as the summer surface. For an 8 year period of record, the mean net accumulation rate was 1.30 m w.e. with a range from 0.30 to 2.30 m w.e. The late summer firn line occurs at 4,900 m. They suggest that most of the snowfall occurs during late winter and spring.

A 5 km^2 north facing valley glacier, the Gara Glacier, in the Western Himalaya was studied by Raina, Kaul and Singh (1977). They determined the net balance for the 1974-75 season over the entire glacier (4700-5600 m). A positive balance was recorded above the 5050 m level. The mean net accumulation of 5 elevation bands from 5400 - 5600 m was 2.25 m w.e. The majority of snowfall occurs during the winter with as much as 6 m of snow

accumulation. They indicate that the basin receives very little precipitation during the monsoon period. The timing of maximum precipitation contrasts sharply with the results of Mayewski et al. (1984), who suggest that maximum precipitation occurs during the summer monsoon. Of the two regions studied, Gara glacier lies further to the south (Figure 1.2), and therefore closer to the effects of the summer monsoon circulation.

In a study of snow and ice conditions on the Pamir firn plateau, Dyurgerov et al. (1980) found that snow falls throughout the year at elevations of 5500 to 7000 m. The average rate of snow accumulation for this elevation band is 1.20 m.

1.3.II Glaciochemical Dating Techniques

Ice core studies in Antarctica, Greenland and the Canadian Arctic have provided the opportunity to trace the chemical evolution of precipitation and therefore develop a long-term data base free from local anthropogenic influences. Identification of the seasonal and long term variation of stable and radioactive isotopes and ions, the seasonal signature of microparticles and distinct reference horizons has enabled researchers to:

1. establish a chronology for the cores and determine the rate of snow accumulation;
2. provide detailed records of past atmospheric conditions; and
3. determine the source of the impurities.

Of special interest has been interpretations concerning the long term variation in global temperatures (Dansgaard et al., 1969), and the increased concentration of acid content in the upper portions of cores, attributed to

increased levels of anthropogenic emissions in the last few decades (for example: Koerner and Fisher, 1982; Neftel et al., 1985; Mayewski et al., 1986).

These glaciochemical techniques have been successfully applied to studies of temperate and tropical glaciers (see Table 1.1). The inherent difficulties involved in the interpretation of cores from temperate and tropical glaciers prove to be greater than for polar ice sheets. In order to confidently date and interpret the glaciochemistry of ice cores recovered from tropical and temperate regions, the glaciers must experience rather stringent conditions that will preserve the seasonal signatures of the chemical constituents. This implies a climatic regime of regular snowfall throughout the year combined with minimal post depositional alteration of the record. The extent to which post depositional alteration can affect the chemical record in temperate and tropical snowpacks is discussed in detail in Chapter 4.

A variety of chemical and physical properties have been used by various investigators in order to identify seasonal snowpack stratigraphy in tropical and temperate glaciers. The techniques employed in these studies are listed in Table 1.1 and are discussed below.

Total β activity, Tritium

Stratospheric fallout of radioactive debris from thermonuclear bomb testing, which began in 1952, produced a series of easily recognizable reference horizons in glaciers (Picciotto and Wilgain, 1963). These horizons, identified by sharp peaks in the total β activity and tritium profile, have been recognized in Antarctica, Greenland, the Yukon Territories, the Himalayas and the Alps. The variety of widespread locations indicates the global extent of

this reference horizon.

Miller et al. (1965) collected snowmelt samples from a 20 m section of crevasse wall at an elevation of 6160 m in the accumulation area of Khumbu Glacier, near Mount Everest. A chronology was established for the 20 m of record from the identification of four tritium peaks produced by nuclear weapons test series in 1954 and 1958 (U.S.A.); 1961 and 1962 (U.S.S.R.). Mean annual net accumulation was 1.70 m w.e. Applying the chronology established with the tritium reference horizons, they noted that on average, each annual layer displays two distinct stratigraphic layers. This is attributed to two accumulation seasons: direct snowfall accumulation during the summer monsoon and minimal snowfall supplemented by wind deposition of snow during the winter.

Ambach et al. (1976) investigated the total β activity profile from two 12 m cores drilled in the accumulation area of Kesselwandferner in the Oetztal Alps, Austria. They discovered that summer ablation horizons were characterized by high values of total β activity, even during periods of comparatively low atmospheric fallout. Records from three locations in Austria indicate a decrease, by approximately a factor of ten, in the total β activity of precipitation for the period 1966–1973, as compared to that of 1961–64. Ambach et al. (1968) and Prantl et al. (1974) have proposed a model to explain the formation of high β active deposits in summer ablation horizons. Their work is summarized below. The total β activity of snow results mainly from radioactive substances attached to aerosols enclosed in snowflakes. Atmospheric radioactivity is at its annual peak during the spring, and therefore spring precipitation is characterized by a higher than average total β activity.

Melting and evaporation during the summer causes the aerosols to agglomerate on the surface, forming a horizon of concentrated radioactive material. The concentration of beta active particles of this aerosol layer is further enhanced by dry fallout during the months when the surface is exposed. Both studies also indicate that following burial, a further redistribution of radioactive material occurs. Radioactive substances from overlying deposits are transported downwards with meltwater or rain, and are retained by the summer ablation horizons. These horizons consist of aerosols and dust that have a higher absorption and retention rate of various radioactive substances, and therefore act as an adsorption filter for the percolating meltwater. Percolating meltwater does not wash out the total β activity profile, but concentrates and intensifies it. While this model fits their data, neither study incorporates any data which relates high β active deposits with dust layers. The authors do not discuss the amount of meltwater produced in the snowpack under investigation. However, the redistribution of radioactive material following burial presumably only occurs in areas that experience periods of substantial downward percolation of meltwater or rain, as it requires water to percolate through at least one winter's snow accumulation.

The distribution of tritium concentrations from a separate core were also studied by Ambach et al. (1976). The peak in tritium concentrations in the core was assigned to the 1963 accumulation year by relating it to the 1963 maximum tritium content measured in precipitation. This indicates a mean net annual accumulation of 1.8 m of snow from 1963 to 1972. This corresponds well with the results determined from the total β activity profile.

Stable Isotopes

Seasonal variations of stable isotopes in precipitation have been used widely to establish a chronology for snowpacks and snow/firn cores. The following discussion is a summary after Dansgaard (1964) and Patterson (1980). The isotopic composition of water changes during natural cycles of evaporation and condensation. Isotope fractionation during phase transitions results in characteristic seasonal and spatial distributions. The content of heavy isotopes in precipitation increases with condensation temperature and are therefore dependent on both the season and orographic altitude of precipitation. Water molecules with a heavier isotope content (D, ^{18}O) evaporate less readily from a liquid and condense more readily from vapor. Precipitation from any given air mass becomes progressively depleted in heavy isotopes as it travels further from its source.

The ratios of heavy to light isotopes (ie $^{18}O/^{16}O$; D/H) are more easily measured than absolute concentrations. The results are given as a relative deviation, δ, of the heavy isotope content of a sample from that of a standard (standard mean ocean water) in parts per thousand ($^{o}/oo$). As the heavy isotope content of precipitation decreases, the δ value decreases.

Early investigations of the stable isotopes in temperate regions (Epstein and Sharp, 1959; Sharp, Epstein and Vidziunas, 1960; Macpherson and Krouse, 1967; Judy, Meiman and Friedman, 1970; and Friedman and Smith, 1970) concentrated on the isotopic content of the previous winter's snowpack and glacier ice. These studies identified the altitude effect on the heavy isotope content in precipitation and minima and maxima δ values corresponding to winter and summer precipitation, respectively. However, no attempt was made

to date the snowpack using this information. These studies emphasized the homogenization of the isotopic record at locations and elevations that experience significant meltwater percolation.

Jouzel et al. (1977) measured the δD, tritium and total β activity in a 16 m snow core taken at an elevation of 4785 m on Mount Blanc. Meteorological data indicate that the air temperature is almost always below 0° C and accumulation occurs in both summer and winter. Annual variations in both tritium and total β activity were attributed to stratospheric-tropospheric exchange; peaks occur in spring or early summer. Two series of ice lenses were observed at depths which correspond to zones of high deuterium content, interpreted as the summer strata. Both the tritium and β activity profiles confirm the chronology established with the deuterium record, which indicates a mean annual snow accumulation of 2.8 m w.e. This study shows that stable isotope, tritium and total β activity records recovered from high elevations on temperate alpine glaciers can be used to accurately delineate snowpack stratigraphy.

The drilling and recovery in March of 1979 of three cores at an elevation of 3150 m on Vernagtferner, Oetztal Alps, Austria is discussed by Oerter, Reinnarth and Rufli (1982). During the drilling program borehole I filled with water at clearly defined depths, indicating the existence of a seasonal water table in the firn. The chemical profiles from cores drilled again in 1983 at the same location display a strong smoothing in comparison with the profiles from the 1979 core for depths of 17-20 m. This homogenization process is explained by isotopic and chemical exchange between meltwater and the firn occurring below the upper limit of the seasonal water table

(Oerter et al. 1985). Tritium measurements on cores I and II (81 and 45 m deep, respectively) from Verngtferner display clear peaks, formed during the period of extensive nuclear weapon testing 1953–62 (Oerter and Rauert, 1982). Cores I and II show mean annual net accumulation rates of 0.70 and 0.90 m w.e., respectively.

Both the stable isotope record and the oscillations in the deuterium 'excess d' were used to date the core (Stichler et al., 1982). The 'excess d' of the snow cover is altered by isotopic fractionation due to evaporation, condensation and melting at the surface, after the snow is deposited. The decrease that occurs in the 'excess d' content of the snow as a result of processes that predominate in summer are used to identify snow layers exposed during the summer. From the 'excess d' profile Stichler et al. (1982) calculated a mean annual accumulation rate between 0.77 and 0.85 m. w.e. A rise in temperature in the second half of the 1940's, as measured at a meteorological station 8 km away, is clearly reflected by a corresponding rise in isotopic ratios of the core.

Oeschger et al. (1977) present the first results from two cores drilled to depths of 55 and 65 m on the Colle Gnifetti (4450 m), Monte Rosa, Swiss Alps (final results are presented by Schotterer et al. (1981) in German). The area is subject to high winds and portions of the precipitation may be missing due to strong wind erosion. Some chronological indications were given by the distribution of ice layers over the whole core length. Both the tritium and oxygen isotope profiles show seasonal variation. Pronounced tritium peaks were related to periods of extensive nuclear weapons testing and provide reference horizons for dating the upper 21 m of the core. This technique

indicates that 21 m of the core represents 70 years of record, corresponding to a mean annual net accumulation rate of 0.30–0.35 m w.e. Only 35 annual cycles are apparent in the $\delta\ ^{18}O$ profile, indicating the oxygen isotope cycles occurring in precipitation are not fully preserved at the sampling site. The cause of this discrepancy is related to irregular snow accumulation over a whole years period, due either to strong wind erosion or little precipitation during certain seasons. The electric conductivity profile displays maxima that coincide with peaks in the $\delta\ ^{18}O$ profile. ^{210}Pb profiles were also used to date the core (Gaggeler et al., 1983).

In a 4 m snowpit dug at Colle Gnifetti Haeberli et al. (1983) investigated a wide range of parameters which in combination provided a key for identifying snowpack/core stratigraphy. This location is extremely wind exposed. Their conclusions concerning the value of the parameters as stratigraphic indicators are summarized below. Clear ice layers are good indicators of summer layers as they indicate melting processes at or near the surface during warm summer temperature. Of three summer seasons recorded in this pit, only two contained ice layers. These melt layers are easily distinguished from wind crusts. Peaks in tritium concentrations occur in spring or early summer layers. However, annual variations do not always exist. Haeberli et al. (1983) state that the $\delta\ ^{18}O$ values cannot be used alone to develop a stratigraphic interpretation as high values indicate either a summer surface or precipitation from a warm air mass and low values indicate either a winter layer or precipitation from a cold (continental) air mass. High values for electric conductivity correspond well with dust layers. However, neither of these parameters display distinct annual variations. Low dust content in the snowpack does not necessarily correspond to low atmospheric dust

concentrations, but could result from the deposition of fresh snow which was not subject to redistribution by the wind. While pollen values do exhibit annual variation, it is not consistent. A chronology was produced by considering all parameters together, which suggests an accumulation rate of 0.40 m w.e. and 0.65 m w.e. for the years 1976/77 and 1977/78, respectively.

If no portion of the snowpack record is missing, the stable isotope record should display broad seasonal variations with some superimposed anomalous peaks and troughs due to isolated precipitation events. The weak seasonal signal in the $\delta\ O^{18}$ values, pollen, tritium and dust concentration is probably due to extensive mixing and losses of surface snow due to the strong role wind plays in the redeposition of snow at Colle Gnifetti. This would result in the preservation of a discontinuous record of precipitation.

Holdsworth et al. (1984) dated 27 m of a firn core retrieved at 5340 m on Mt. Logan in the Yukon Territory using total β activity and tritium activity and $\delta^{18}O$ values. There is no melting at this site as the mean annual firn temperature is -28.5° C. Mean annual accumulation rates for the period 1957 to 1980 are 0.39 m w.e.

Other studies that have used stable isotopes along with other glaciochemical techniques to date cores, such as Mayewski et al. (1984) and Thompson et al. (1984; 1986), are discussed below, under the heading which relates to the main focus of the study.

Ion Concentrations

Only recently have ion concentration profiles been employed to identify

seasonal snow layers in high altitude temperate glaciers. Snowpit and core studies from high altitude temperate glaciers show that ion concentrations profiles from areas of snow accumulation provide a record of seasonal variations in atmospheric chemistry. Not only can these variations be used to delineate seasonal snowpack stratigraphy, but they provide valuable data concerning atmospheric circulation and its' seasonal variations.

Butler et al. (1983) analysed the chemistry (nitrate, phosphate, iron and reactive silicate) in a 7.4 m snow pit excavated at 2694 m on Athabasca Glacier, Alberta. They recognized trends in the NO_3/PO_4 and Si/Fe ratios, and interpreted these as seasonal trends in the chemical deposition, with maxima formed during spring/summer due to increased plant growth and soil exposure. This corresponds to a net annual mass balance of 1.5 and 2.4–2.7 m w.e. for 1978 and 1977, respectively.

Mayewski et al. (1984) interpreted a physical and chemical time series of a 16.6 m core recovered from Sentik Glacier (4908 m) in the Ladakh Himalaya. This study location was chosen because it is close to the northern limit of the summer monsoon in an area that is potentially susceptible to monsoonal fluctuations. Although melt events do occur, as evidenced by the presence of several ice bands, the quality and periodic variation of the chemical record indicates that these melting events have not obscured the seasonal chemical signature of the snowpack. Core chronology was determined using the β activity record by correlating a peak in the profile with the 1963 thermonuclear test level. Spectral analysis of chemical properties (chloride, sodium, reactive iron, reactive silicate, reactive phosphate, ammonium, $\delta^{18}O$, δ D, pH and total β activity) and physical properties (density and microparticles

in size ranges 0.5–0.63, 1.00–1.25 and 8–10/μm) revealed subannual periodicities for nearly all time series sets and strong annual periodicities for chloride, reactive silicate, reactive phosphate and small microparticles (0.5–0.63μm). Only trends in the density time series do not correspond with the trends in chemical properties or microparticle concentrations. Visible debris bands in the core do not match the core chronology established with the β activity record. This suggests that debris bands are not a good stratigraphic marker but rather are indicative of periods of intense ablation or high atmospheric dust concentrations. The identification of spectrally defined periodic events which coincide with subannual and annual snowpack stratigraphy in this study is of particular importance. It demonstrates that stratigraphic records recovered from high altitude temperate glaciers in the Himalayas can be used to determine annual net balance and provide information concerning former climate.

Lyons et al. (1985) discuss glaciochemical data from samples collected in 3 m snowpits at 5690 m on the Quelccaya Ice Cap in the Peruvian Andes. Reactive silicate, reactive iron, sodium, and microparticles (>0.63 μm) display similar trends in concentration with depth, which they attribute to a common source of weathered crustal material. Peak concentrations in all four parameters occur in the dry, winter season. This appears to be a function of the dominant winter wind direction which transports material from the high, dry Altiplano and the lower rate of snow accumulation.

The glaciochemical record of a 3m snowpit at an elevation of 2450 m on Heard Island in the South Indian Ocean was investigated by Spencer and others (1985). Chloride, sodium and sulfate display corresponding seasonal

trends and are therefore good seasonal indicators. A marine origin is suggested as the primary source for these three chemical species. Seasonal variation in ion concentration with depth is related to the seasonal extent of Antarctic sea ice distribution.

There is some question as to the validity of directly relating snowpack chemistry with atmospheric chemistry. Studies by Junge (1977), Boutron (1979), and Boutron and Lorius (1979) in clean air conditions in Antarctica, indicate that the chemical composition of the surface snow reflects the atmospheric chemistry during the precipitation event. On the other hand, Rahn and MacCaffrey (1979) recognized the effects of air-snow fractionation in Alaska. Current investigations concentrated on the air-snow fractionation process should solve this controversy. In addition, postdepositional processes can change the ion content of the snow (these are discussed in Chapter 4).

Microparticles

The analyses of microparticle concentrations from snowpits and cores in tropical and temperate glaciers exhibits a strong seasonal signal, suitable for dating purposes. Thompson, Hastenrath and Arnao (1979) recognized broad, parallel seasonal trends in microparticle concentrations oxygen isotope ratios and β activity of a 15 m long core taken at 5650 m on the Quelccaya Ice Cap. They determined the net accumulation for the eight years of record preserved in the snowpack. At this location the least negative δ values occur during the dry winter season. This is opposite to the seasonal variation commonly found in cores taken at higher latitudes.

Thompson et al. (1986) recovered two ice cores, 155 and 166 m deep,

from the Queiccaya Ice Cap. Both the visible stratigraphy and annual variations in microparticle concentrations (0.63 to 16.0 μm), conductivity and oxygen isotope ratios were used to date the cores. Visible dust layers, high microparticle concentrations, high conductivities and less negative $\delta\ ^{18}O$ ratios are characteristic of the dry season. However short term variations in each of the $\delta\ ^{18}O$, microparticle concentrations and conductivity records occur within a single year. This emphasizes the importance of measuring more than one variable in order to clarify the annual signal when ambiguities occur. With the long period of record the authors were able to identify long term trends in the isotope record which identifies decreased temperatures at the core site from 1530-1900 A.D. This trend corresponds well with the Little Ice Age (1530-1920; Sugden and John, 1976). In summary, very little is known concerning snow accumulation in the Karakoram. The data that does exist originates from valley bottom stations which do not reflect conditions at higher elevations. Fortunately, accumulation zones of glaciers in the Karakoram preserve a fossil record of snowfall. A number of different glaciochemical dating techniques have been employed in the snow accumulation areas of temperate and tropical glaciers around the world to identify seasonal layers and thus determine the annual rate of snow accumulation. Analysing a series of different glaciochemical parameters to date cores increases the confidence and accuracy of the results. Different impurity sources are incorporated into the snowpack by different mechanisms (Herron, 1982) and therefore can display peak concentrations at different times of the year. Cycles which are uncertain in one record may be clear in another. Records from different chemical profiles can also be cross-checked.

It is clear from a review of the literature that glaciochemical dating

techniques can be successfully employed in temperate and tropical glaciers to determine the rate of snow accumulation. With a large number of high altitude glaciers, the Karakoram represents one region of the world where these glaciochemical techniques can be applied. One can appreciate the importance of determining the rate of snow accumulation in the Karakoram as it is this moisture surplus which supports tens of millions of people in Pakistan.

TABLE 1.1 SUMMARY OF ACCUMULATION STUDIES ON TROPICAL AND TEMPERATE GLACIERS EMPLOYING GLACIOCHEMICAL DATING TECHNIQUES

Reference	SITE CHARACTERISTICS elev (m)	depth (m)	acc rate(m)	CHEMICAL PROPERTIES stable isotop	ion conc	cond	beta	trit	PHYSICAL PROPERTIES part	strat	LOCATION
Miller (1965)	6160	20	1.70					x			Khumbu Glacier, Nepal
Ambach (1976)	?	12	1.80				x	x			Kesselwandferner, Austrian Alps
Oerter (1982)	3150	81,45	0.80	x				x			Vernagtferner, Austrian Alps
Jouzel (1977)	4785	16	2.80	x			x				Mont Blanc, French Alps
Oeschger (1977)	4450	55,65	0.32	x		x		x			Monte Rosa, Swiss Alps
Haeberli (1983)	4450	4	0.52	x		x		x		x	Monte Rosa, Swiss Alps
Butler (1983)	2720	7	2.00		x						Athabasca Glacier, Canadian Rockies
Mayewski (1984)	4908	17	0.62	x	x		x		x		Sentik Glacier, Ladakh Himalaya
Lyons (1985)	5670	3	—		x		x		x		Quelccaya Ice Cap, Peru
Spencer (1985)	2450	3	—		x						Heard Island, South Indian Ocean
Thompson (1979)	5650	15	?	x			x		x	x	Quelccaya Ice Cap, Peruvian Andes
Thompson (1986)	5650	155,166	?	x		x			x	x	Quelccaya Ice Cap, Peruvian Andes
Holdsworth (1984)	5340	27	0.39	x			x	x			Mt Logan, Yukon Territory

Figure 1.1 GLACIERS AND DRAINAGE IN NORTH PAKISTAN

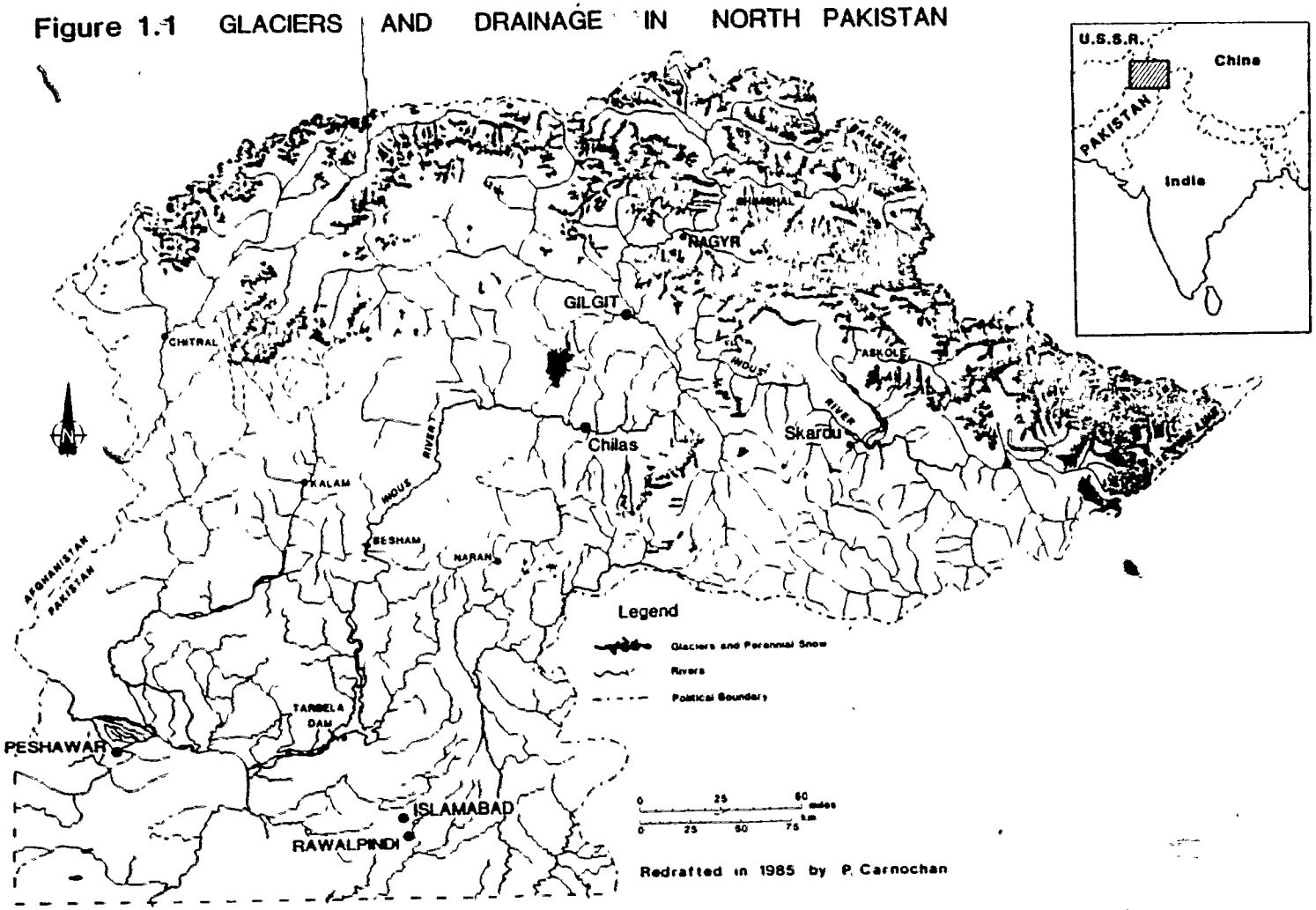

FIGURE 1.2

LOCATION OF SNOW ACCUMULATION STUDIES IN THE KARAKORAM, HINDU KUSH, WESTERN HIMALAYA & PAMIRS

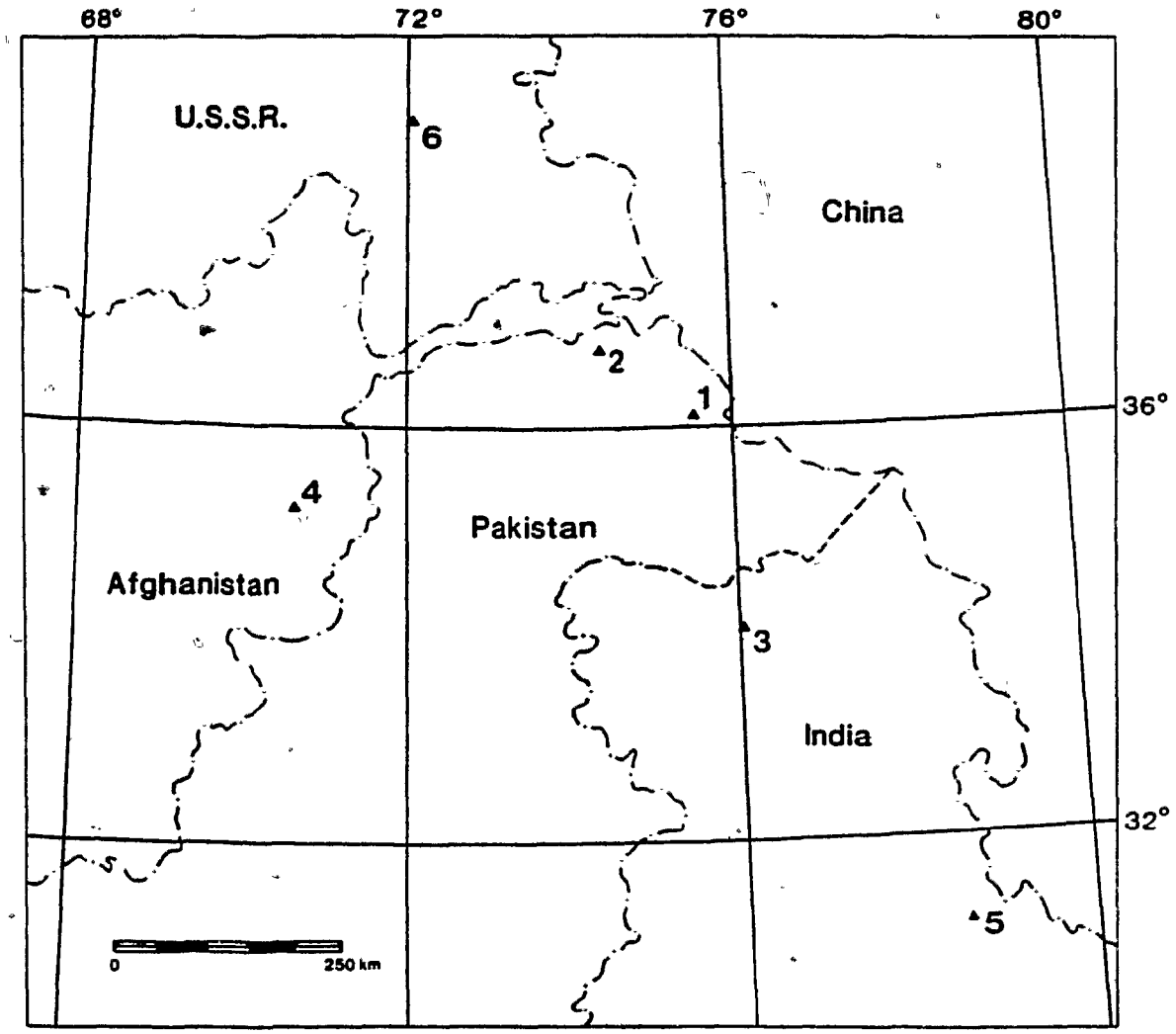

1. Biafo Glacier, Karakoram
2. Batura Glacier, Karakoram
3. Sentik Glacier, Ladakh Himalaya
4. Mir Samir West Glacier, Hindu Kush
5. Gara Glacier, Western Himalaya
6. Glacier near Kommunizma Peak, Central Pamirs

CHAPTER 2

CLIMATE AND GEOGRAPHY

2.1 OVERVIEW

The Upper Indus Basin (U.I.B.) is defined as the watershed above the Tarbela Resevoir, and comprises an area of approximately 164,000 km^2 (Figure 2.1). The Tarbela Resevoir is of fundamental importance for power generation, flood control, irrigation water and general water supply in Pakistan. Thirteen percent of the basin is covered by perennial snow and ice: glaciers are concentrated along the northern edge of the watershed in the Karakoram mountain range. Runoff from the U.I.B. is dominated by snow and ice melt.

During the 1960's the Water and Power Development Authority (WAPDA) set up a network of gauging stations in the U.I.B. The location of these stations is shown in Figure 2.1. Runoff data indicate that snow and ice melt from the Karakoram accounts for approximately 75% of the total runoff of the U.I.B. Four-fifths of this occurs during the warm summer season, from mid-June to mid-September. Figure 2.2 displays the runoff hydrographs for two gauging stations in the U.I.B. and clearly illustrates the seasonal nature of the runoff. The rising limb of the hydrograph is due primarily to melting of the seasonal snowpack in the foothills and at lower elevations within the glacierized basins. In June and July the transient snowline rises rapidly, exposing large areas of glacier ice. By early July, melting ice has become a significant contributor to runoff and subsequently dominates the runoff hydrograph from mid-July to mid-September.

Under the Indus Waters Treaty, the left bank tributaries of the Indus

River forms a smaller portion of Pakistan's water supplies. As India increases its use of the water from the left bank tributaries, this source of water for Pakistan will continue to decrease in the future. To a large extent, these traditional sources of water for the Punjab have been replaced by water from the Indus River through an extensive network of barrages and canals. This has increased Pakistan's dependence on water from the Indus, which has therefore increased their dependence on snow and ice melt in the Karakoram. It is only through an understanding of the snow and ice conditions and the terrain characteristics in the Karakoram, and a knowledge of the climatic variables which control melting, that Pakistan will be able to predict runoff into the Tarbela Reservoir.

The following discussion deals with the broad climatic controls of the region in general before focusing on the local climate and geography of the Karakoram. The last section of this chapter deals specifically with the Biafo Glacier Basin.

2.2 CLIMATE

2.2.1 Broad Climatic Controls

This discussion follows the summary of the broad pattern of climate of the U.I.B. given by Hewitt (1961), and of the Indian subcontinent by Boucher (1975) and Barry, Richard and Chorley (1982). The climate of the Karakoram is the product of global and regional influences. The exceptional elevation of the mountain range over a large area, the abrupt edges of the mountain block and thermal effects combine to isolate the region from the lower air masses of the Indian subcontinent. The orographic barrier of the range plays an

important role in the region's climate. The mountains extend into the mid troposphere and are directly affected by upper air circulation. The seasonal character of the upper air flow pattern influences the climate in the Karakoram.

The region is dominated by the influx of westerly air masses. Throughout the winter, the subtropical westerly jet stream steers depressions towards the Karakoram and Northern India. These lows appear to penetrate across the Middle East from the Mediterranean. It is from these westerly air masses that the bulk of precipitation in the Upper Indus Basin is thought to be derived. Boucher (1975) states that on average five disturbances a month affect northern India from December to April. However, conditions in winter are subject to great variability as they depend on the scale, frequency and intensity of westerly disturbances (Hewitt, 1961).

During the winter the jet stream is split into two distinct branches; one passing to the north and the other to the south of the Tibetan Plateau. Early studies attributed the bifurcation of the jet stream to the role of the Tibetan Plateau as a topographic barrier, but later work emphasized the thermal effects of the plateau acting as a high level heat source (ie. Lockwood, 1965).

In May and June the jet stream slowly weakens, and by mid-June is altogether diverted to the north of the plateau. As the southern branch of the westerly jet stream shifts north, an area of high pressure is established over the Tibetan Plateau due partly to surface heating by the sun. As warm air is less dense than cold air, pressure falls less rapidly with height over the Tibetan Plateau. The formation of the Tibetan anticyclone is concurrent with the development of a high level easterly jet stream over southern Asia (at ~15° N). At this time the summer monsoon begins to move across the Indian

subcontinent.

The effect that the reorganization of the upper air flow has on the climate of the Karakoram is unclear. The regional airstream continues to be influenced by the westerlies and westerly depressions may continue to effect the region. Temporary destruction of the Tibetan anticyclone can result in the incursion of monsoonal air masses into the Karakoram, resulting in heavy precipitation. The potential for fluctuations in the summer circulation creates an environment that is open to substantial variability.

We know from the records of numerous climbing expeditions in the Karakoram and from our own experiences that significant amounts of snowfall can occur in the northern portions of the basin during the summer. Finsterwalder (1960) reported that the summer monsoon crossed the Himalaya in early July of 1959 and resulted in heavy rainfall in the Hunza Valley and raging snowstorms at higher elevations. Snowfall during the late summer of 1985 and 1986 appear to have been examples of the influx of monsoonal air masses. However, there exists no reliable data to determine the frequency of these monsoonal incursions. The relative roles of westerly disturbances and incursions of monsoonal air masses on summer precipitation in the Karakoram is a question that is addressed in Chapter 5 of this thesis.

2.2.II Local Climate: The effect of altitude and topography

Seasonal variation plays a major role in all aspects of climate in the Karakoram. The annual variation in monthly averaged minimum and maximum temperatures and precipitation for Gilgit and Skardu is illustrated in Figure 2.3. The strong seasonal variation in the hydrological response of the Karakoram

due to melting snow and ice is a result of warm summer temperatures and a decrease in summer cloud cover over much of the region. Superimposed on the seasonal nature of climate in the Karakoram is the considerable variation of local climate due to the effects of altitude and topography. Outstanding features of this variability are the overwhelming increase in precipitation with elevation, rainshadow effects, the existence of dry valley wind systems and aspect.

The main river valleys in the Karakoram are extremely arid. The valley bottom towns of Gilgit and Skardu show a mean annual precipitation of 132 and 202 mm (Figure 2.3). In these valleys the potential for evaporation is high; water balance calculations indicate a strong negative balance for both Gilgit and Skardu (Butz and Hewitt, 1986). The combined effects of a negative water balance and dry valley wind systems create a severely desiccated landscape. These conditions persist up to 3000–3500 m. Any agriculture that does exist is supported by irrigation water from melting snow and ice at higher elevations. (Butz, 1987).

There are two clear effects on climate that occur with an increase in elevation from valley bottoms. First, as both the aerosol content and the water vapor pressure decrease with elevation, the direct solar radiation reaching the surface increases (Barry, 1981). The region in general has a high incident radiation level because of the rainshadow effect which reduces cloud cover, especially during the summer months. Secondly, temperature decreases with elevation. Whiteman (1985) calculated an environmental lapse rate of 6.5–7.8 °C/1000 m from mean monthly air temperature records from 11 stations over a range of elevation from 1260 to 3088 m.

Above 3000 m, precipitation increases rapidly with elevation. Orographic effects dominate the form and spatial distribution of precipitation. Work by the Batura Investigation group (1979) discovered net annual accumulation rates of 1.00 to 1.30 m w.e. at 5000 m on the Batura Glacier. It is this snowfall that supports the vast snowfields and large valley glaciers that characterize the Karakoram. Especially important in regards to the moisture balance in the Karakoram is the elevation zone of maximum precipitation. This is thought to be near the 5000 m level (Hewitt, 1961; Batura Investigation Group, 1979).

Aspect has a fundamental effect on local radiation income and temperature conditions. South facing slopes receive direct solar radiation for much longer periods during the day, resulting in a greater degree of melting. The transient snowline on south facing slopes at any given time during the ablation period is usually 500–1000 m higher than on north facing slopes. This has important implications for the hydrological response of snow-covered basins. A basin with a large percentage of south-facing slopes would produce meltwater sooner under clear sky conditions. While radiation is probably the key factor in controlling melting on south-facing slopes, air temperature is presumably more important on north-facing slopes (Hewitt, 1961). Glacier coverage, especially the number and extent of small cirque or hanging glaciers, is noticeably less on south-facing slopes.

Wind

During the summer of 1985 and 1986, a record of wind velocity was recorded at the Baintha meteorological station, located on the mainstream Biafo Glacier ice at an elevation of 4080 m (Figures 2.4 and 2.5). Downglacier

(katabatic) winds predominate, with wind speed commonly ranging from 3 to 7 metres per second (m/sec.). Short term wind measurements were undertaken in Lukpe Lawo in 1985 and at all snowpit locations during 1986. In the broad accumulation basins wind conditions were generally calm, and wind speed never exceeded 5 m/sec. Winds were always much stronger at higher elevation exposed areas such as 'Shark Col' (5660 m) and Khurdopin Pass (5800 m).

2.3 GEOGRAPHY OF THE KARAKORAM

2.3.i Regional Setting

The Karakoram lies in the northwest of a region that consists of a series of mountain ranges that extends over 2500 km from the eastern Himalaya to the Hindu Kush. This large positive land mass was created by continental collision and subsequent suturing of the Indian subcontinent and Eurasia (Molna and Taponnier, 1975). This resulted in crustal shortening accompanied by tremendous uplift to form the broad arc of mountain ranges. The Karakoram are bordered by the Great Himalaya to the southeast, the Kunlun Shan to the northeast, the Pamirs to the northwest and the Hindu Kush to the southwest.

The Karakoram consists of a series of well outlined ESE-WNW trending mountain ranges which parallel the main rock formations (Gansser, 1964). According to Wissman (1959) approximately 37% of the area is covered by perennial snow and ice. The ranges and glaciers of the region are summarized by Mercer (1975). The Great Karakoram represents the main crestline of the entire mountain system and includes three mountain massifs over 8000 metres

(K2, Gasherbrum and Broad peak) as well as more than 25 peaks over 7000 m. North of the Great Karakoram lies the Ghujerab mountains. To the south lies the lesser Karakoram with such noteable 7000+ m mountain massifs as Rakaposhi, Haramosh, Masherbrum and Saltoro-Kangri.

2.3.II Geomorphology

The U.I.B. in general and the Karakoram in particular are characterized by extreme relief and a dynamic environment. The 5940 m of relative relief from the peak of Rakaposhi (7790 m) to the Hunza River (1850 m) over a distance of 11 km makes this one of the steepest places on Earth. High elevation mountain blocks are dissected by deep main valleys which are occupied by the Indus River and its right bank tributaries. Relative relief in these valleys is often greater than 4000 m. Within the mountain blocks themselves high sharp ridges descend by steep slopes to tributary valleys. Relative relief here is commonly greater than 2000 m. Plateau features are rare.

Three periods of widespread glaciation in the U.I.B. during the Pleistoscene have left thick deposits of glacial and glacial-fluvial sediments in the main valleys (Hewitt, 1961). These deposits are cut by the main rivers thereby creating terraces which usually lie 100-200 m above the level of the river. Transport of debris by meltwater streams from higher elevation catchments has built large alluvial fans on top of the thick valley deposits. The relatively flat areas represented by alluvial fans combined with the availability of water makes these areas prime locations for settlements and agricultural activity.

The combination of available relief, steep slopes, large scale of debris accumulation and climate result in mass movements of debris and catastrophic events. The evidence of mass movements is ubiquitous. Slope failure increases in importance with altitude as precipitation and weathering activity increase. (Goudie et al., 1984). At higher elevation avalanching snow and ice predominates. These avalanches have the potential to transport substantial quantities of debris.

Large quantities of debris are deposited in the river valleys by a combination of slope processes and glacial erosion. On average, about 250 million tonnes of sediment are delivered to the Tarbela Reservoir every year. This results in a denudation rate for the whole mountain range of over 1500 tonnes $km^{-2}yr^{-1}$. (Ferguson, 1984).

2.3.III Glaciers

The main crestline of the Karakoram, extending from Batura Mustagh (7,795 m) in the west through K2 (8,611 m) to Sasir Kangri (7672 m) in the east holds the greatest concentration of perennial snow and ice in Asia (Figure 1.1). From this topographic high flow some of the world's longest glaciers outside of polar regions. Of the glaciers that lie within the Karakoram, over 15 are longer than 20 km. Five of these are longer than 50 km in length. The glacier cover on the Indus flank of the Greater Karakoram is almost 60% (Hewitt, 1961).

Glaciers in the Karakoram extend through a wide range of climatic environments. Accumulation zones extend from ~4500 to 7000 m, show a

negative mean annual temperature and receive over one metre water equivalent of solid precipitation per year. Most glaciers have extremely high gradient accumulation areas. Accumulation in this type of glacier system is predominantly by avalanching snow and ice. Conversely, glacier snouts reach into subtropical desert conditions at elevations in the range 2300 to 3000 m (Goudie et. al., 1984). A substantial number of these glaciers have flowed across major river valleys and created ice dammed lakes. The subsequent failure of the ice dam creates large catastrophic floods. There is evidence of 35 disastrous ice-dam bursts since 1862 (Hewitt, 1982).

2.4 STUDY LOCATION: THE BIAFO GLACIER BASIN

The Biafo glacier descends south-west from the main crest of the Greater Karakoram in the central portion of the range. The glacier itself is a large valley glacier stretching over 59 km. The Biafo Glacier basin covers an area of 852 square kilometers, of which 64% is covered by perennial snow and ice (Appendix A lists the glacier inventory data for the Biafo basin.) There exists a reliable topographic map of the Biafo Hispar glacial region produced by the Royal Geographical Society (Mott, 1950). A schematic version of this map is shown in Figure 2.4. A topographic map of the Biafo Basin, redrawn from the original Shipton survey maps, appears in Figure 2.5. The area-altitude relationships for the glacier covered area of the Biafo basin are illustrated in Figure 2.6. Features of the ablation and accumulation areas of the Biafo glacier are discussed below.

2.4.1 Ablation Zone

The Ablation Zone of the Biafo Glacier below the firn line occupies

approximately 1/3 of total glacierized portion of the basin. The snout of the glacier descends to an elevation of 3400 m, reaching into a semi-arid climate. Terminus fluctuations are described in detail by Hewitt (1986). Briefly, from 1899 to about 1909 the terminus advanced by approximately 3–4 km. From 1909–1961 it experienced gradual retreat. There was little change in the position of the snout in the 1960's and 70's. Since then the terminus has advanced about one kilometre to its present position. Hewitt (1964) argues from geomorphological evidence that the Biafo Glacier had at one time formed a glacier dam across the Braldu, confirming a report by local residents to Godwin Austen (1864).

The lower 20–30% of the ablation zone is covered in supraglacial debris. This is less than the estimated 50% debris cover on the Hispar Glacier or 90% debris cover on the Baltoro Glacier and reflects the role of direct precipitation, as opposed to avalanching, as the predominant form of accumulation for this glacier. Clean ice predominates in the upper half of the ablation zone. Two adjacent large medial moraines, presumably derived from the junction of Lukpe Lawo and Sim Gang ice, surface approximately 7 km down from the firn line. In the lower half of the ablation zone several more medial moraines appear. The margins of the Biafo are covered in thick supraglacial debris; stagnant ice is a common feature here. Both the medial and lateral moraines broaden and thicken downstream, eventually spreading out to cover the entire glacier surface. While the relationship between debris cover and ablation rate is a complicated one, the overall effect of this debris cover is to reduce ablation, allowing the glacier to descend even lower into semi-arid regions.

Surface movement measurements at three profiles in the ablation zone indicate a 'block schollen' type of motion. The velocity of the glacier increases rapidly away from the margins and then remains constant across most of the width. Maximum surface movement in the middle of the ablation zone is approximately 130 m per year. A report discussing the surface movement measurement program and results appears in Appendix B.

The depth of the winter snow cover in the ablation zone is extremely variable, presumably due to wind drifting. Hollows may accumulate as much as 1-2 m of snow while positive features, such as medial moraines, show only a thin veneer of snow cover.

Observations during our summer measurement program indicate that the ablation season extends from mid June to mid September. Field measurements show average summer ablation rates, in relatively clean ice, of about 60 mm per day, although this can vary considerably with aspect, elevation and the concentration of fine particles on the ice (a fine dust cover is found nearly everywhere, presumably transported to the glacier surface by the wind.) Measurements indicate that the ablation rate on the medial moraine under extensive debris cover is roughly 1/2 that in relatively clean ice; seasonal snow cover melts at approximately 1/3 the rate of relatively clean ice. With a rough knowledge of these parameters, an even rougher estimate of water production from the ablation zone can be calculated (see Table 2; note that this does not include off glacier seasonal snowmelt). These calculations indicate that for a 90 day ablation period, the melting of snow and ice in the ablation zone of the Biafo Glacier produces on the order of 0.7 km^3 of water. This represents 1% of the total runoff of the U.I.B. measured at Besham Qila from

0.1% of the total basin area. While this is an extremely gross estimation, it provides us with a first estimate of the water production of the ablation zone of the Biafo Glacier.

From our observations during 1985 and 1986 and a study of the available Landsat imagery, the firn line in recent years is found at approximately 4650 m on the Biafo Glacier (close to the location of the 'Equilibrium Line' snowpit, illustrated in Figure 2.5). It is lowest on the south-west margin of the glacier and gradually increases in elevation, by as much as 250 m, towards the north-east margin. A triangular patch of ice becomes exposed in the late summer on the north margin of the Sim Gang. This is due to the thermal effects of the adjacent south facing wall. It is precisely at the firn line elevation that the surface morphology of the Biafo glacier transforms. Below this line the glacier flows in a constricted valley, 2-3 km wide. Above this line the glacier valley opens up into a broad, relatively flat plateau. A small increase in the elevation of the late summer firn line would expose substantial areas of glacier ice in the broad, flat plateau area. Considering the three-fold increase in the ablation rate of ice compared to snow, a larger area of exposed glacier ice would increase runoff late in the melt season. The combination of morphology and present location of the firn line makes the Biafo Glacier very sensitive to climate changes that could increase the elevation of the firn line, such as an increase in temperature or decrease in solid precipitation.

2.4.II Accumulation Zone

The Biafo Glacier flows from a broad, gently sloping accumulation zone

consisting of two large accumulation basins; the Sim Gang Glacier to the west and Lukpe Lawo (also referred to as 'Snow Lake') to the north (Figure 2.5). These basins are separated by steep narrow ridges which occupy a small percentage of the area in the accumulation zone. While avalanches of snow and ice descend onto the Sim Gang Glacier and Lukpe Lawo from the surrounding steep walls, the area represented by elevations at which avalanching predominates accounts for less than 15% of the accumulation zone. The majority of precipitation falls onto the broad, relatively low elevation surface of the accumulation zone, which accounts for an overwhelming 85% of the area in the accumulation zone and 2/3 of total basin glacier cover (Figure 2.6) . Direct precipitation is the predominant form of nourishment. In this regard, the Biafo Glacier appears to be the exception in relation to other valley glaciers in the Central Karakoram. However, because of the minimal influence of avalanches on overall accumulation rates, the basin does provide an ideal location for determining the altitudinal, lateral and temporal distribution of snow accumulation.

Debris cover is rare in the accumulation basins. Exceptions include the cones of dirty avalanches and a surface moraine deposit adjacent to the north wall of the Sim Gang glacier. The predominance of clean accumulation zone reflects the minor role avalanches play in the nourishment of the glacier basin.

While the accumulation basins are relatively flat, they show considerable microrelief in the form of hollows and dunes. These are concentrated downstream from ice falls and are presumably a result of differential melting of the chaotic mass of ice at the bottom of the ice falls and perhaps due to the drifting of snow by the wind. The geometry of the Biafo accumulation

zone creates a large heat trap. Daytime maximum temperatures in the accumulation basins are as high as 20°C. Pools and lakes are found as high as 5000 m in some of the hollows described above.

TABLE 2.1 ESTIMATE OF MELTWATER PRODUCTION FROM THE BIAFO GLACIER

PERIOD OF MELTING	SNOWLINE ELEV(m)	AREA* SNOW	AREA* ICE	AREA* DEBRIS	MELTWATER+ FROM SNOW	MELTWATER+ FROM ICE	MELTWATER+ FROM DEBRIS	TOTAL MELTWATER PRODUCTION+
June 15-30	4200	60	70	40	18	63	18	99
July 1-31	4500	30	100	40	19	186	37	242
Aug 1-31	4650	10	120	40	6	223	37	266
Sept 1-15	4570	20	110	40	6	99	18	123
								730 TOTAL

+ 10^6 m^3

* Ablation area with firn line at 4650 m = 170 km^2

Ablation rates: snow-20 mm/day; ice-60 mm/day; debris-30 mm/day.

FIGURE 2.1

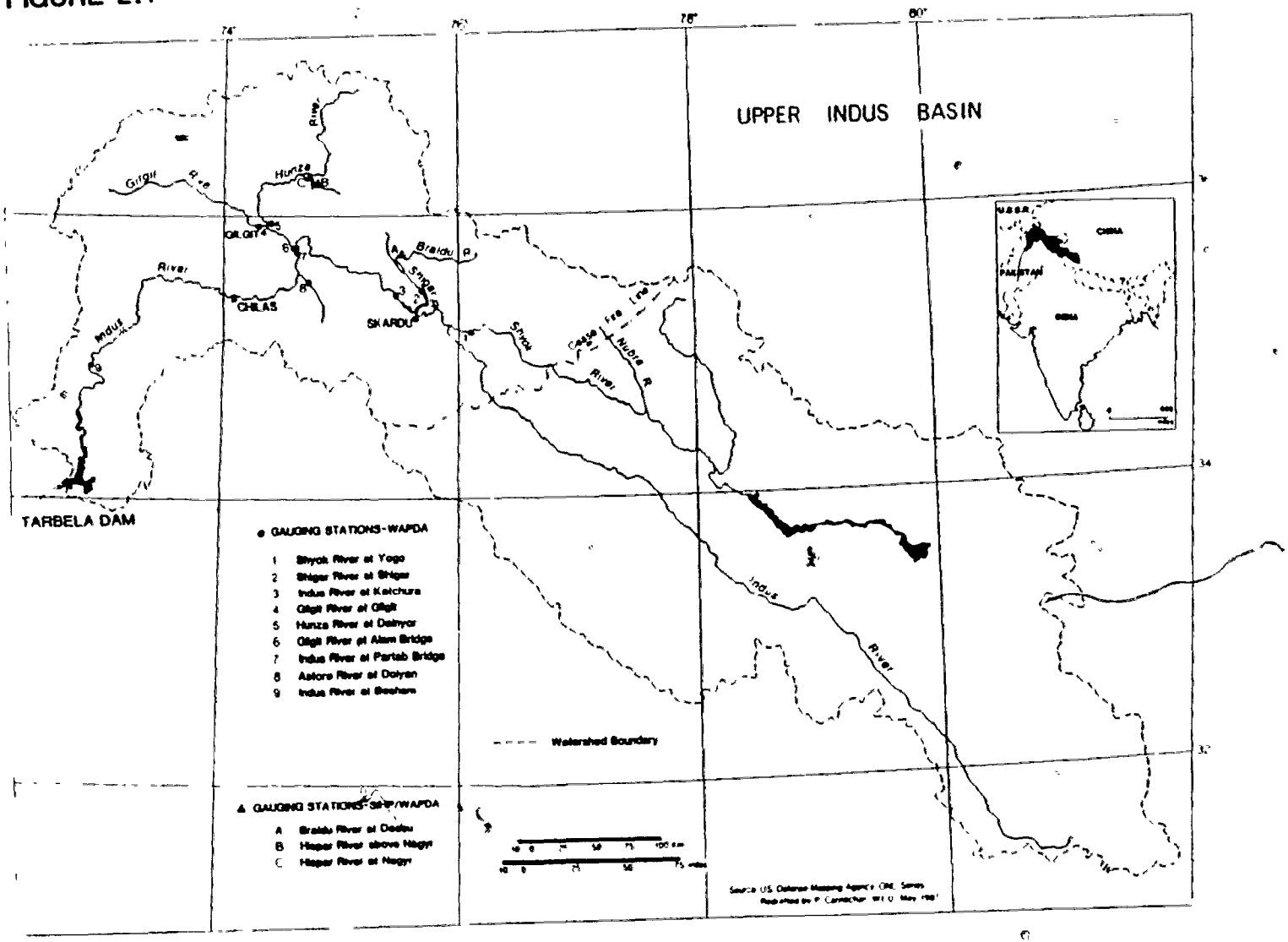
UPPER INDUS BASIN
Gilgit River
Hunza River
Braldu R.
Shigar R.
Indus River
GILGIT
CHILAS
SKARDU
Shyok River
Nubra R.
Leh
TARBELA DAM
GAUGING STATIONS-WAPDA
1 Shyok River at Yogo
2 Shigar River at Shigar
3 Indus River at Kachura
4 Gilgit River at Gilgit
5 Hunza River at Dainyor
6 Gilgit River at Alam Bridge
7 Indus River at Partab Bridge
8 Astore River at Doiyan
9 Indus River at Besham
Watershed Boundary
GAUGING STATIONS-SHP/WAPDA
A Braldu River at Dasbu
B Hisper River above Nagyr
C Hisper River at Nagyr
USSR
CHINA
PAKISTAN
INDIA

FIGURE 2.2 INDUS RIVER
TOTAL MONTHLY DISCHARGE
1985

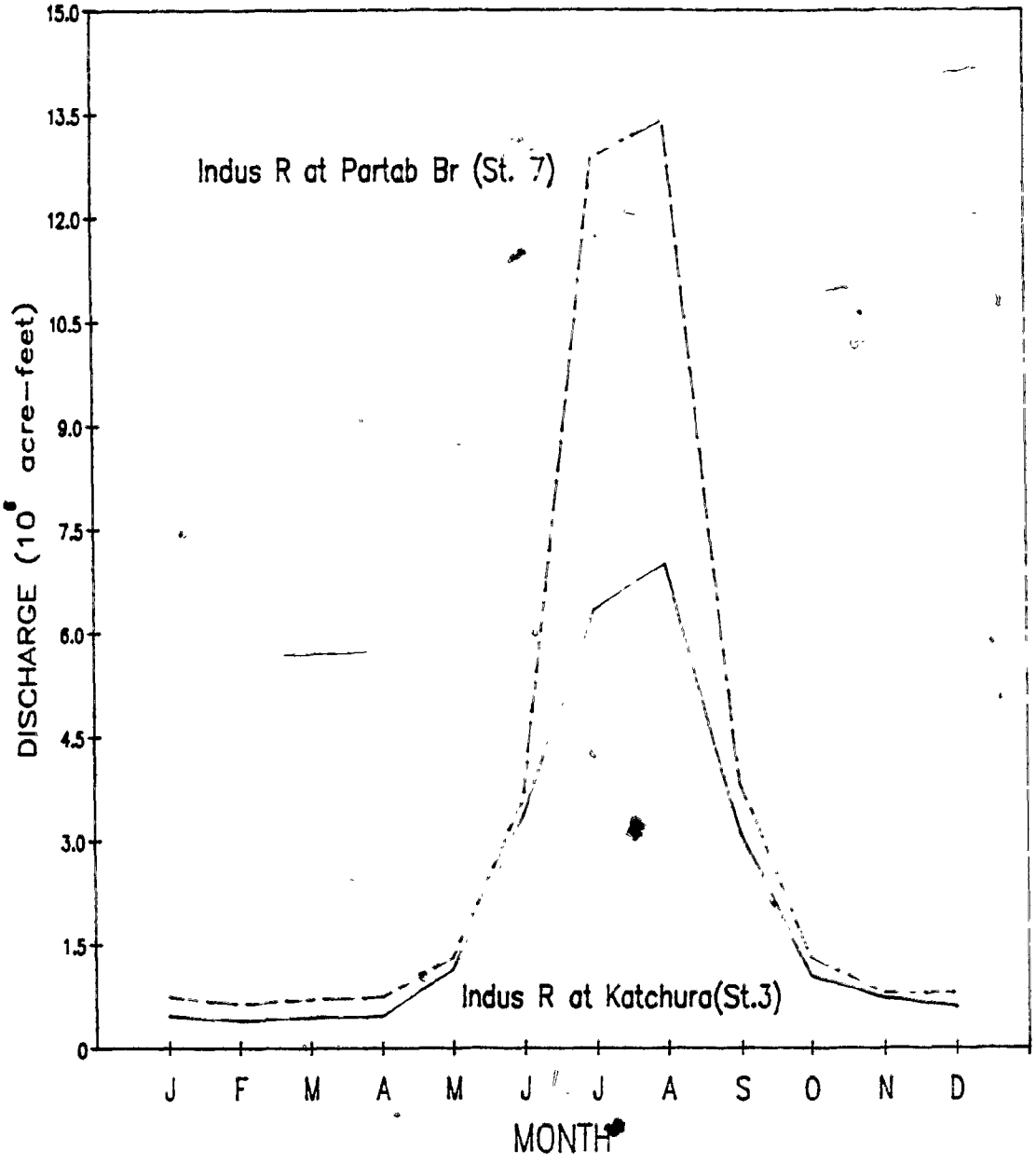

FIGURE 2.3

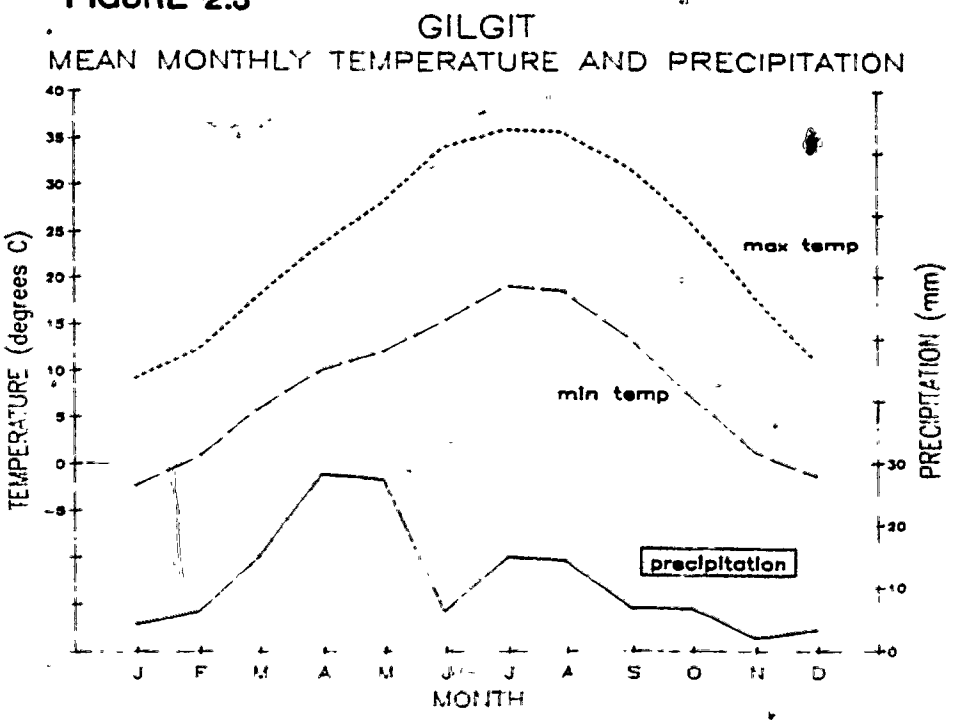
GILGIT
MEAN MONTHLY TEMPERATURE AND PRECIPITATION
TEMPERATURE (degrees C)
PRECIPITATION (mm)
max temp
min temp
precipitation
J F M A M J J A S O N D
MONTH

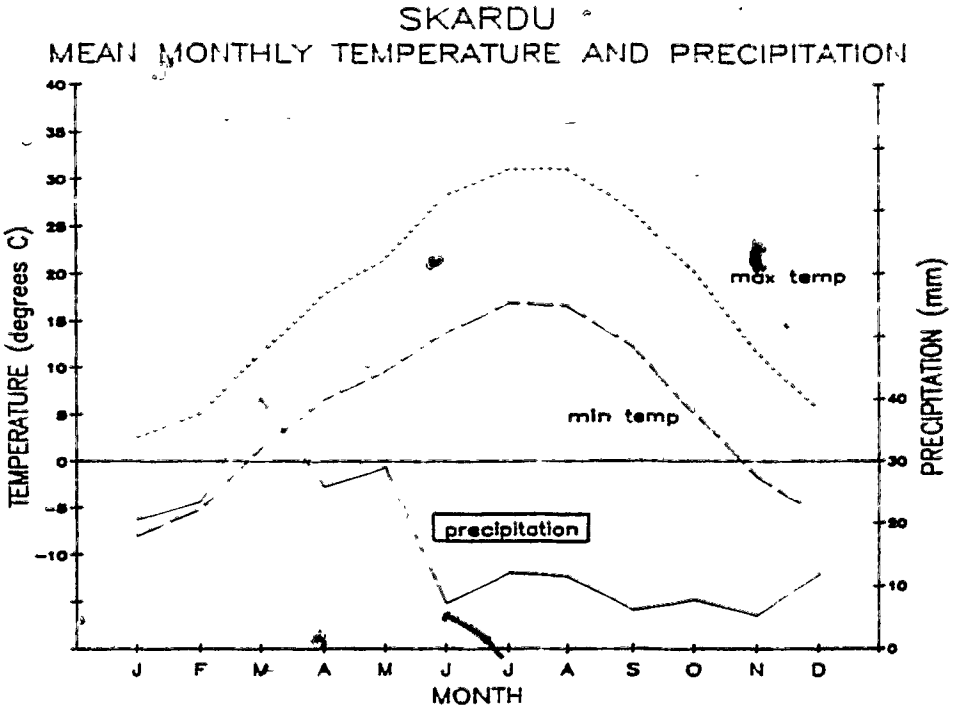
SKARDU
MEAN MONTHLY TEMPERATURE AND PRECIPITATION
TEMPERATURE (degrees C)
PRECIPITATION (mm)
max temp
min temp
precipitation
J F M A M J J A S O N D
MONTH

FIGURE 2.4

HISPAR-BIAFO GLACIER SYSTEMS
CENTRAL KARAKORAM

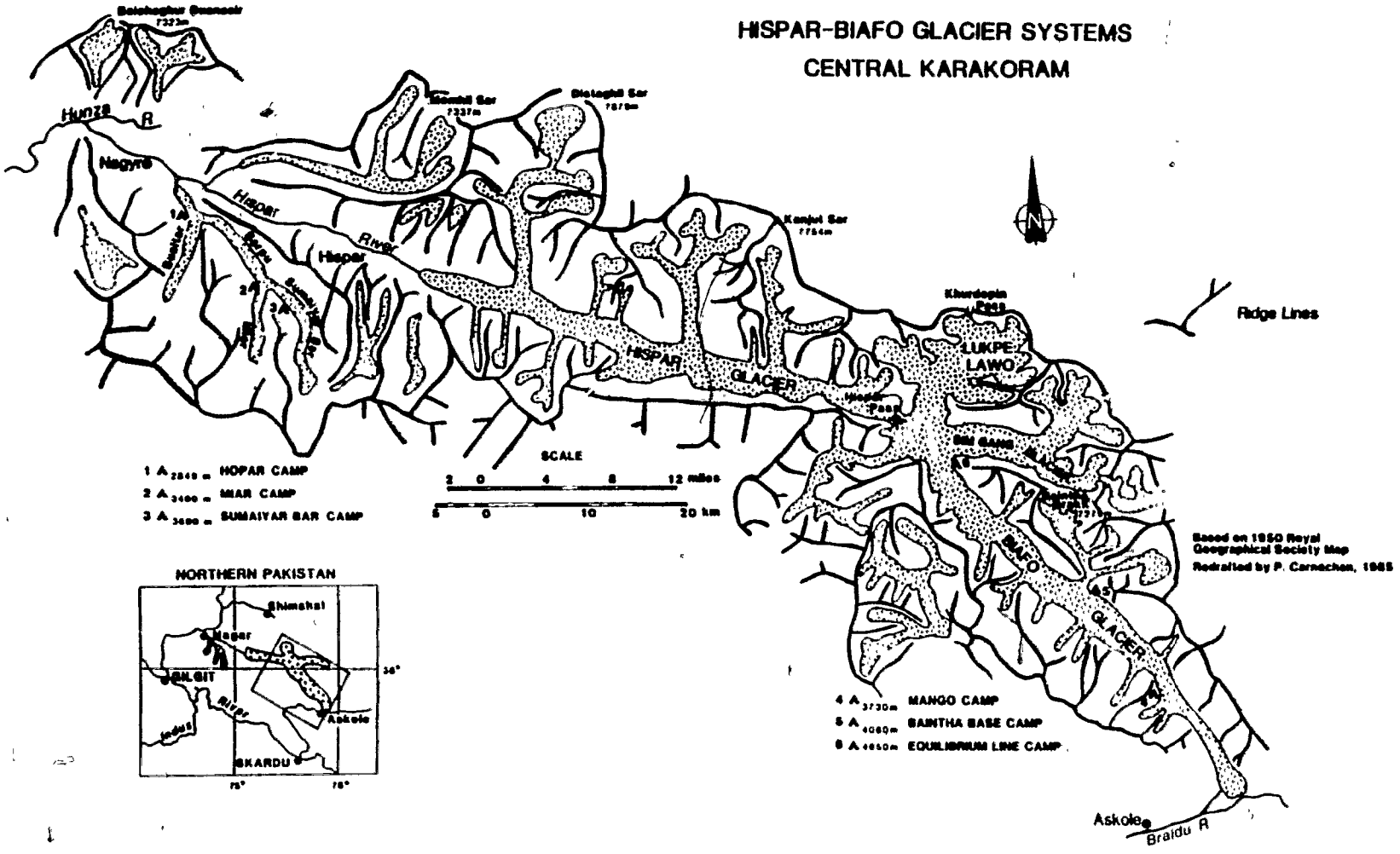

FIGURE 2.5

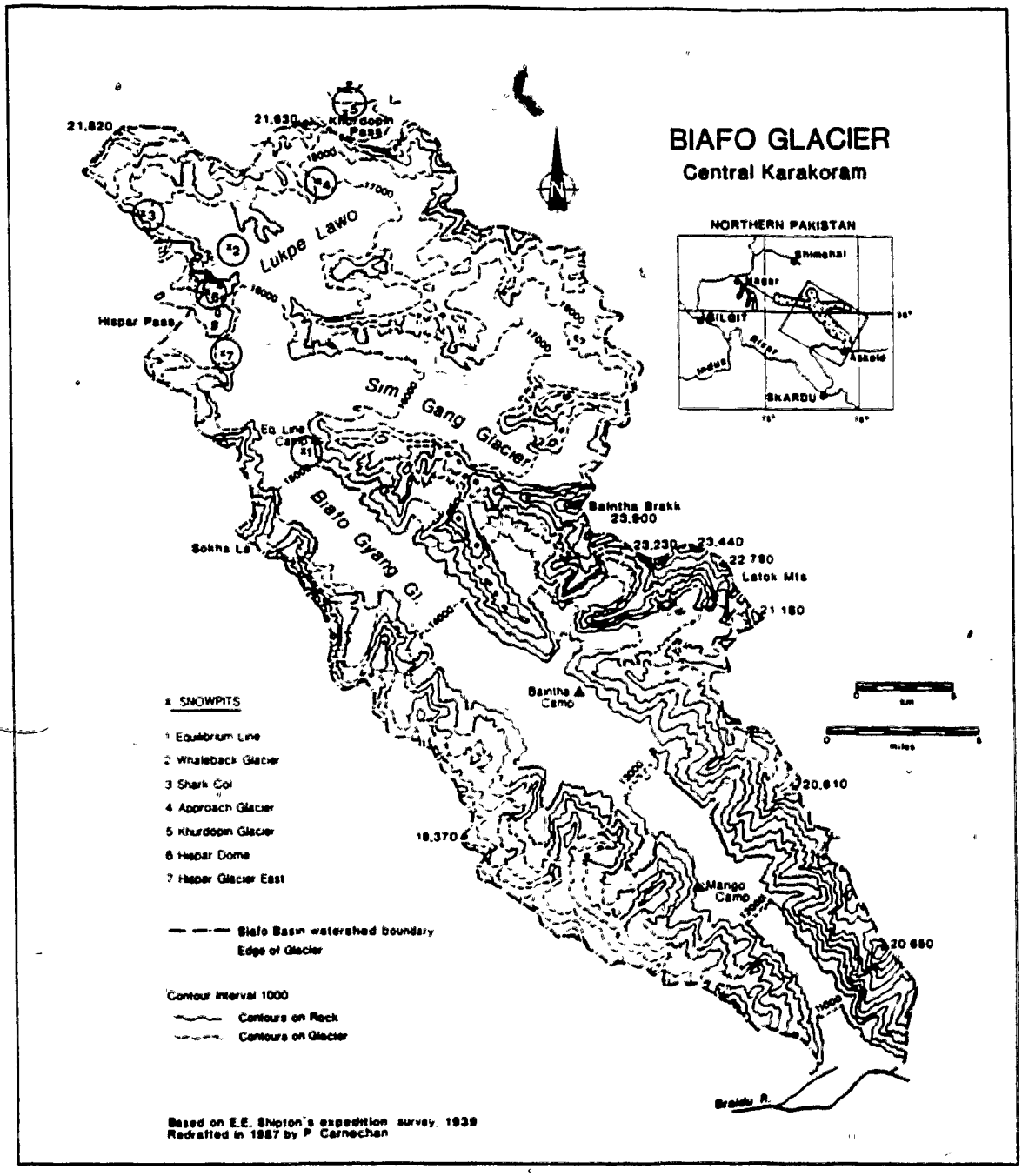
BIAFO GLACIER
Central Karakoram
NORTHERN PAKISTAN
Shimshal
Nagar
GILGIT
Askole
SKARDU
Khurdopin Pass
21,820
21,630
Lukpe Lawo
Hispar Pass
Simsa Gang Glacier
Eq. Line Camp
Biafo Gyang Gl.
Sokha La
Baintha Brakk 23,900
23,230
23,440
22,780
Latok Mts
21,180
Baintha Camp
20,810
18,370
Mango Camp
20,650
Braldu R.
SNOWPITS
1 Equilibrium Line
2 Whaleback Glacier
3 Shark Col
4 Approach Glacier
5 Khurdopin Glacier
6 Hispar Dome
7 Hispar Glacier East
Biafo Basin watershed boundary
Edge of Glacier
Contour Interval 1000
Contours on Rock
Contours on Glacier
Based on E.E. Shipton's expedition survey, 1939
Redrafted in 1987 by P Carnechan

FIGURE 2.6 HYPSOMETRIC CURVE FOR CONNECTED GLACIATED AREA OF THE BIAFO BASIN

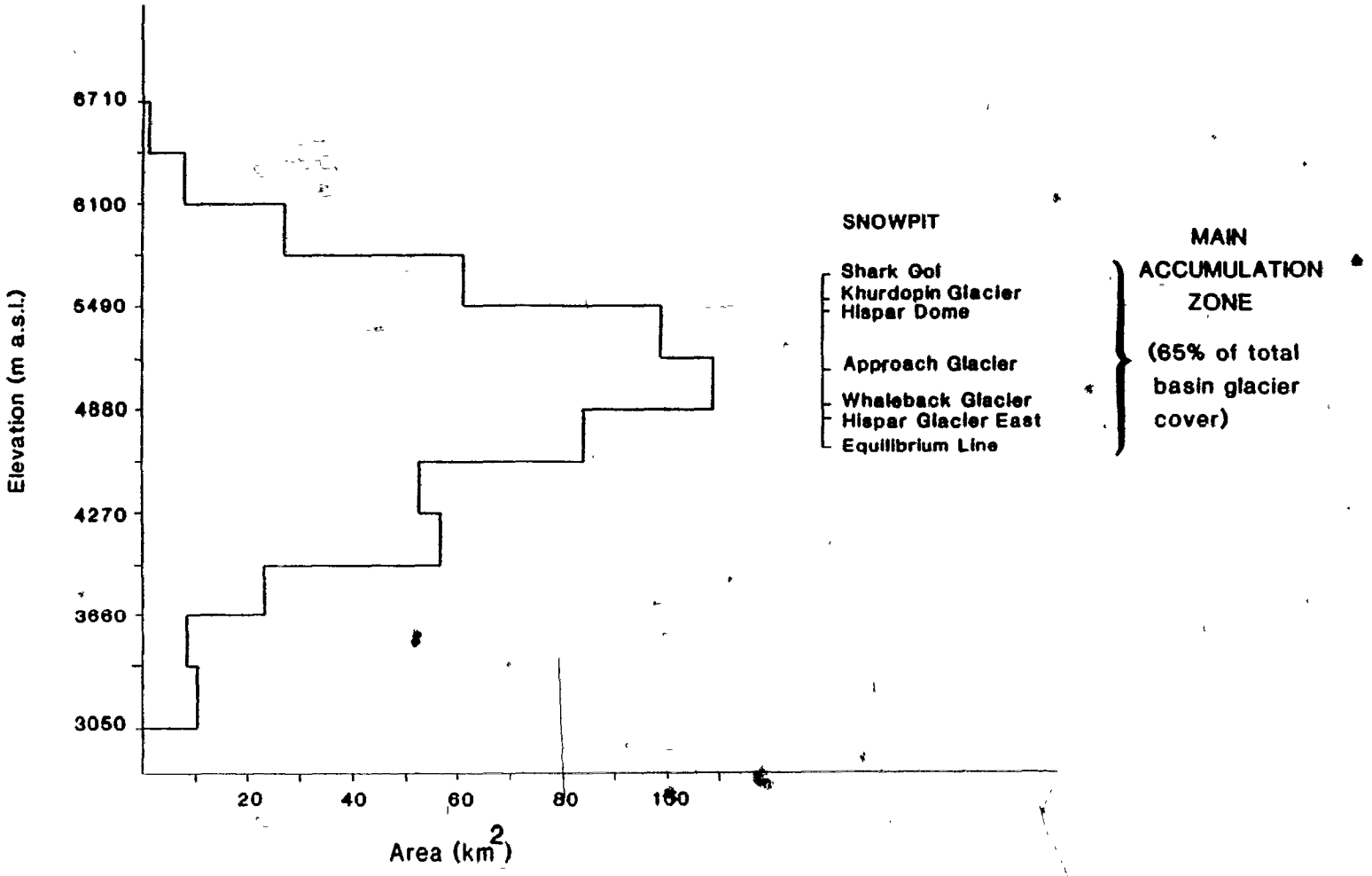

CHAPTER 3

METHODOLOGY AND PROCEDURE

3.1 FIELD WORK

During the 1986 summer field season two Canadians and four high altitude porters spent 2 months in the accumulation zone of the Biafo Glacier Basin. The snow accumulation field work was extremely successful due both to very good weather which dominated during our time above snowline, and to the combined effort of all party members.

Overall we examined and collected samples from 7 snowpits 5-10m deep, 15m of a snow/firn core drilled from the bottom of a 5m pit and collected fresh snow samples throughout the summer (Table 3.1). The seven snowpits cover an elevation range of 1010 m, from 4650 to 5660 m (Figure 3.1). This elevation band accounts for almost 85% of the glacier covered area in the accumulation zone. The elevation of each snowpit in relation to the hypsometric curve is shown in Figure 2.6. The geographic locations of the snowpits are illustrated in Figure 2.5. All but the Khurdopin Glacier site lie within the Biafo Glacier basin. In general the names which appear on the Royal Geographical Society map of the area (Mott, 1959) have been used to name the locations of the snowpits. Names assigned by us in areas for which no names existed have been placed in quotations throughout the text.

The importance of selecting suitable sites at which to collect data cannot be underestimated. Obtaining a 'representative' sample in an area that covers 370 km^2, over a range of elevations from 4500 to 6500 m is, to say the least, difficult. The problem is compounded by the remote nature of the

study area. Most of one's time is spent transporting logistical and scientific equipment to and from the various study sites, and therefore the number of snowpits that can be investigated is limited.

There exists strong local variation in accumulation due to aspect, local relief and the effects of avalanches. Sample sites can therefore not be chosen at random. Rather, it is through a familiarity of the physical processes that govern snow accumulation, and a familiarity with the region in general, that study sites are chosen in areas that are free from the redistribution of snow by avalanches and little affected by the local redistribution of snow by the wind.

In order to compare data among pit locations, some sites should have one common physical characteristic, such as elevation, aspect or location. The snowpack should, aside from the surface, remain below freezing for the entire year to limit the percolation of meltwater. Other things being equal, the higher the altitude the snowpit/core site is, the cooler the temperature. This increases the potential for preserving a chemical record unaltered due to meltwater percolation. Flow geometry is not a critical factor in the study of shallow snowpits.

Five of the seven snowpits, the exceptions being the 'Hispar Dome' and "Shark Col" sites, were dug in relatively flat, broad areas which appear to be representative of the surrounding basin. The Hispar Dome site was located on top of a large, gently sloping snowdome. Except for the "Shark Col" site, all of the snowpits were far removed from the influence of avalanches and showed little or no sign of heavy winds. In general winds were calm over the study

area throughout the summer.

At 5660 m, the "Shark Col" site is the highest sample location; however as a snowpit study site it has some severe limitations. The col is quite narrow; steep snow covered slopes rise sharply on the north and south sides. We recorded strong winds (>10 m/s) on 3 of the 5 days we were camped at the col. No avalanche debris was apparent at the col, however the possibility of avalanches from the surrounding steep slopes depositing snow at the col cannot be ruled out. While appealing due to its high elevation, caution must be used in interpreting the results of snow accumulation investigations at this site.

The seven snowpits were dug over a 45 day period, from June 15 to July 31. Work on the snowpits was preceded by three snowfall events on June 5 (16 cm of snow), June 11-12 (50 cm of snow), and June 14-15 (45 cm of snow). Accumulation from these three storms was about 0.30 m w.e. These were the only significant snowfall events (ie. greater than 10 cm of snow) that were witnessed through the entire snowpit study program. The site of the 'Equilibrium Line' snowpit is close to the firn line of the Biafo Glacier, where significant melting occurs. While most of this snowpack disappears during the course of the summer (snow depth on August 5 was 20-30 cm) little ablation had occurred prior to June 15, the day the pit was dug and sampled. The water equivalent measured on June 15 therefore closely represents annual accumulation at this elevation. The six snowpits dug above the firn line experience minimal ablation. The amount of meltwater produced and the depth to which it percolates is discussed in detail in Chapter 4. However, based on our observations in the field and interpretation of the

geochemical record, there is no significant change in the water equivalent of any of the annual layers due to the downward percolation of meltwater, in any of the six snowpits dug above the Equilibrium Line. This, combined with the lack of any significant precipitation events during the course of our work, implies that the data from all seven snowpits and be compared directly.

Losses due to evaporation are unknown. These are assumed to be equal for all of the snowpit locations as there is only minor variation in the intensity and time period of direct beam radiation and cloud cover between the sites (Wake, 1985). Any evaporation that does occur will not significantly alter the relative amount of net annual accumulation between snowpit sites. The effects of absolute losses due to evaporation will be investigated during the 1987 field season.

Snowpits were dug in 2 m intervals in order to simplify the sampling procedure. Snowpack stratigraphy was delineated on the basis of layer thickness, hardness, and colour, crystal size and shape, and the position of ice layers and debris bands. Density of each stratigraphic layer was measured using a 24 cm stainless steel tube with a cross-sectional area of 41.7 cm^2. Following collection, the cored snow sample was placed in a nylon stuff sack and weighed with a 2 kg Homs spring scale. In six of the snowpits, snowmelt samples were collected over 15 cm intervals. The complete interval of 15 cm was sampled in order to obtain a complete chemical record of the snowpack. A 30 cm sample interval was used at the 'Whaleback Glacier' pit. Extreme care was exercised at all times during sample collection to ensure the collection of uncontaminated samples. All sample bottles were rinsed 3 times, allowed to stand full for at least 24 hours, and rinsed another three times

with distilled, double deionized water that had subsequently been treated with a Milli-Q water purification system. A non-particulating clean suit in combination with an over the shoulder hood, particle mask and plastic gloves were worn by the sample collector. The north facing snowpit wall to be sampled was first scraped back approximately 30 cm with a lexan shovel and subsequently scraped clean with a plexiglass scraper. Samples were collected in 125 ml polypropylene wide mouth containers with polyethylene caps. Following melting, the samples were transferred into 2-20 ml linear polyethylene (LPE) scintillation vials.

At the Hispar Dome site a 15 m core was recovered from the bottom of the 5 m pit by hand drilling with a PICO auger. Before drilling the core, samples were collected from the snowpit wall using the methods described above. Subsequently, thirty centimetre samples from the wall of the 5 pit were scraped into ziplock bags using lexan scrapers. Thirty centimetre sections of the 15 m core were placed directly into ziplock bags after the stratigraphy had been analysed and the density measured. The resulting 68 samples in the ziplock bags were then melted and transferred into 20 ml scintillation vials and 500ml LPE containers for isotope and total beta activity analyses, respectively. The core was not sampled for ion analysis. The borehole remained dry throughout the entire drilling period. Temperature at the bottom of the borehole (20 m) was -4.5°C. Fresh snow samples were collected as soon as possible following the termination of a precipitation event. The sample site was approached from a downwind direction in order to avoid contamination of the fresh snow. The sampler wore a gortex suit, non-particulating clean hood, particle mask and plastic gloves. Samples were collected in 125 ml cups and were subsequently processed in the same

manner as the samples obtained from snowpit walls. Special care was taken to sample the complete depth of the fresh snow without sampling any of the underlying snow. In a few cases, 125 ml containers were opened and placed upwind from our camp at the beginning of the snow/rainfall event and left open for the duration of the storm. These were collected shortly after the the end of the storm. Overall 23 samples of fresh snow/rainfall were collected from seven different precipitation events. One suite of seven fresh snow samples were collected from the same storm over an elevation range from 5105 m to 5450 m. All sample containers shipped to Canada had their tops taped shut prior to their departure from the field to prevent leakage.

Seasonal Snowcover

While the focus of this research is the rate of snow accumulation within the area of perennial snowcover, two surveys were made of the seasonal snow cover in the lower half of the Biafo Glacier Basin. In addition the seasonal snowline in the lower half of the basin was photographed every week. On May 29th the seasonal snowline lay at ~4600 m on the south-west facing slopes behind Baintha Base camp. Snow depth increased to 0.80-1.00 m at 5055 m. Snowline elevation on the northeast facing slopes on the other side of the glacier was estimated at ~4000 m. From this elevation it was relatively easy to identify the transient snowline on the Biafo Glacier. Below 4000 m about 90% of the ice and supra glacial debris was exposed.

From 4000 to 4300 m snowcover on the glacier increased, until between 60% and 90% of the glacier surface was covered in snow. Snow was as deep as 0.5-1.0 m in hollows and on the north-east facing slopes of

the large medial moraines. At this time the snow in hollows was completely saturated with water. Above 4300 m the snow cover on the glacier exceeded 90%. This snow was relatively dry compared to the snow at lower elevations.

Three snowstorms between June 5 and June 15th deposited about 1.10 m of snow (0.30 m w.e.) at 4650 m. Only trace precipitation was recorded at Baintha Base Camp (4080 m) during the period from June 5 to June 15. On June 18, the transition zone of the water saturated, patchy snowcover lay in the range 4200–4400 m. Snow depth measurements were taken about every 600 m, between 4300 m to 4600 m. Table 3.2 lists the results. The physical characteristics of the snowpack above 4500 m suggested that relatively little melting had occurred at or above this elevation at this time. There is a sharp increase in snow depth from 4560 to 4590 m. This thought to reflect an increase of precipitation above 4560 m during the early June snowfall events. While this data is limited, it indicates that moisture input increases above 4080 m and perhaps even above 4560 m.

By the 30th of June the upper limit of the transition zone lay at about 4500 m. Above this elevation three large lakes had formed on the plateau beneath the icefall at 4560–4590 m. At this time the glacier showed 100% snow cover at this elevation.

Reconaissance Snowpit Studies in 1985

During the summer of 1985, two 4 m snowpits were dug and analysed in the accumulation area of the Biafo Glacier (Young, Hewitt and Wake, 1986). One of the snowpits was in the centre of Lukpe Lawo at about 4950 m, the other at 5060 m on Hispar Pass. For each snowpit the stratigraphy was

described and the density measured. Overall, the snowpack stratigraphy was quite similar in the two snowpits. Thick ice layers overlain with slightly dirty, hard granular snow containing lumpy ice were found at 330 cm in the Lukpe Lawo pit, and 325 cm in the Hispar Pass pit. These layers are interpreted as the previous summer's surface. This corresponds to a net annual accumulation of 1.60–1.80 m w.e. at the 5000 m altitudinal level, for the 1984–85 accumulation season.

3.2 LABORATORY WORK

Over 375 snowmelt samples were collected and returned for chemical and microparticle analyses. Anions (Chloride, sulfate and nitrate) have been analysed using a Dionex model 2010 ion chromatograph with an AS–4 column and 0.0021M $NaHCO_3$/0.0017M Na_2CO_3 eluent and a computer–driven autosampler. The detection limit for chloride, sulfate and nitrate is 0.5, 1.0 and 1.0 ppb (parts per billion). Ten percent of these samples were analysed in duplicate using two separately drawn samples. This procedure resulted in a relative deviation from the mean of 2% for chloride, nitrate and sulfate. (precision calculations after Skoog and West, 1976). Sodium was analysed by stabilized–temperature furnace atomic absorption spectrometry using a Perkin Elmer model 2280 equipped with a model 400 furnace. The detection limit for sodium, using this method, is 0.5 ppb. All of these samples were analysed in duplicate, resulting in a relative deviation from the mean of 3%. Both the anion and cation analyses were completed using the facilities of the Glacier Research Group at the University of New Hampshire. The oxygen isotope analyses were done by the Geophysical Isotope Laboratory at the University of Copenhagen

using gas source mass spectrometry. All of these samples were analysed twice. The relative deviation from the mean was 0.3%.

Forty samples from Hispar Dome 5m snowpit were also analysed for total conductivity and for microparticle concentrations in 15 different size ranges using a Coulter Counter TA II, by the Institute of Polar Studies at Ohio State University. Sixty-eight samples from the combined 5m snowpit and 15m snow/firn core from the Hispar Dome were analysed for oxygen isotope ratios and total β activity. The total β activity was measured at the University of New Hampshire, using a Canberra model 2404 alpha-beta-gamma counter with a 12 hour counting period for 47 cm Whatman SA-1 cation filters through which 500 ml samples had been gravity filtered twice.

As described below, two sets of field blanks, one set of transfer duplicates and one set of laboratory blanks were made to determine if snow samples collected in the Karakoram had been contaminated in any way during the sampling, transport and laboratory analysis phases of this project. Before leaving for the field, six 20 ml scintillation vials were filled with Milli-Q water at the University of New Hampshire. The blanks, termed 'UNH blanks', travelled with all of the other samples and remained sealed throughout the field program. As previously mentioned, samples were collected in 125 ml cups and, after melting, were transferred into 2-20 ml scintillation vials. Seven 'transfer blanks' were made by transferring Milli-Q water directly into the scintillation vials in the field at the same time the snow samples were transferred. The results appear in Table 3.3.

Six 'transfer duplicates' were made by transferring snow samples into a third 20 ml scintillation vial to test for ion contamination. The analytical results

of this set of duplicates is listed in Table 3.4. The results shown in Tables 3.3 and 3.4 indicate that, on the whole, the transfer process and the transport of samples introduced very little contamination.

One out of every ten samples analysed by ion chromotography and atomic absorption spectrometry was a sample of Milli-Q water. Throughout the laboratory procedure, these Milli-Q samples showed no signs of contamination indicating that the laboratory procedure did not contaminate the samples.

TABLE 3.1 SUMMARY OF SNOW PITS DUG IN THE CENTRAL KARAKORAM, SUMMER 1986

PIT NO.*	DATE	LOCATION	ELEVATION	ASPECT	DEPTH(m)
1	06/15	EQUILIBRIUM LINE	4650m/15,250'	SW	2.26
2	06/21	WHALEBACK GLACIER	4900m/16,070'	SE	4.50
3	06/26-27	SHARK COL	5660m/18,570'	E-W	7.75
4	07/4	APPROACH GLACIER	5100m/16,730'	E	4.80
5	07/5-6	KHURDOPIN GLACIER	5520m/18,100'	W	10.00
6	07/27-28	SNOW DOME (pit)	5450m/17,880'	-	5.00
		SNOW DOME (core)	--- " ---	-	15.00
7	07/31	HISPAR GLACIER	4830m/15,840'	E	4.80

* pit numbers refer to location of snowpits on Figure 1.

TABLE 3.2 SNOW DEPTHS ON THE BIAFO GLACIER, JUNE 18, 1986

ELEVATION (m)	KM FROM EQ. CAMP	SNOW* DEPTH(cm)	
4200	14	0-30	
4300	11	20-90	
4320	10	60	
4340	9.4	70	
4360	8.8	35	
4380	8.2	5	
4400	7.6	50	
4420	7.0	45	
4435	6.4	50	
4450	5.8	120	
4465	5.2	60	
4480	4.6	75	
4500	4.0	120	
4510	3.6	145	
4520	3.2	110	
4530	2.8	100	
4540	2.4	90	
4550	2.0	100	(below ice fall)
4590	1.5	200	(above ice fall)
4650	0	230	

*average of four soundings

+ snow density is assumed to be equal to mean snowpack density measured at the Equilibrium Line snowpit on June 15/86 (390 kg/m^3).

TABLE 3.3 RESULTS OF 'BLANK' ANALYSES

No.	TRANSFER BLANKS Cl (ppb)	Na (ppb)	UNH BLANKS Cl (ppb)	Na (ppb)
1	7	2	1	0
2	9	2	5	0
3	8	3	4	0
4	8	-	<1	0
5	12	-	2	0
6	3	<1	4	0
7	2	<1		
8	4	<1		

TABLE 3.4 ION TRANSFER DUPLICATES

Sample No.	Cl mean	Cl stnd dev(s)	NO_3 mean	NO_3 stnd dev(s)	SO_4 mean	SO_4 stnd dev(s)	Na mean	Na stnd dev(s)
169	53.1	1.5	146.7	0.9	82.8	0.5	12.9	2.43
188	20.2	0.7	71.9	0.6	46.7	0.5	5.8	0.2
280	26.1	1.1	45.9	2.5	40.8	0.5	13.9	1.0
20	--	--	--	--	--	--	3.0	0.0
40	--	--	88.5	0.8	119.9	0.9	--	--

FIGURE 3.1 ELEVATION RANGE OF SNOW PITS

CENTRAL KARAKORAM 1986

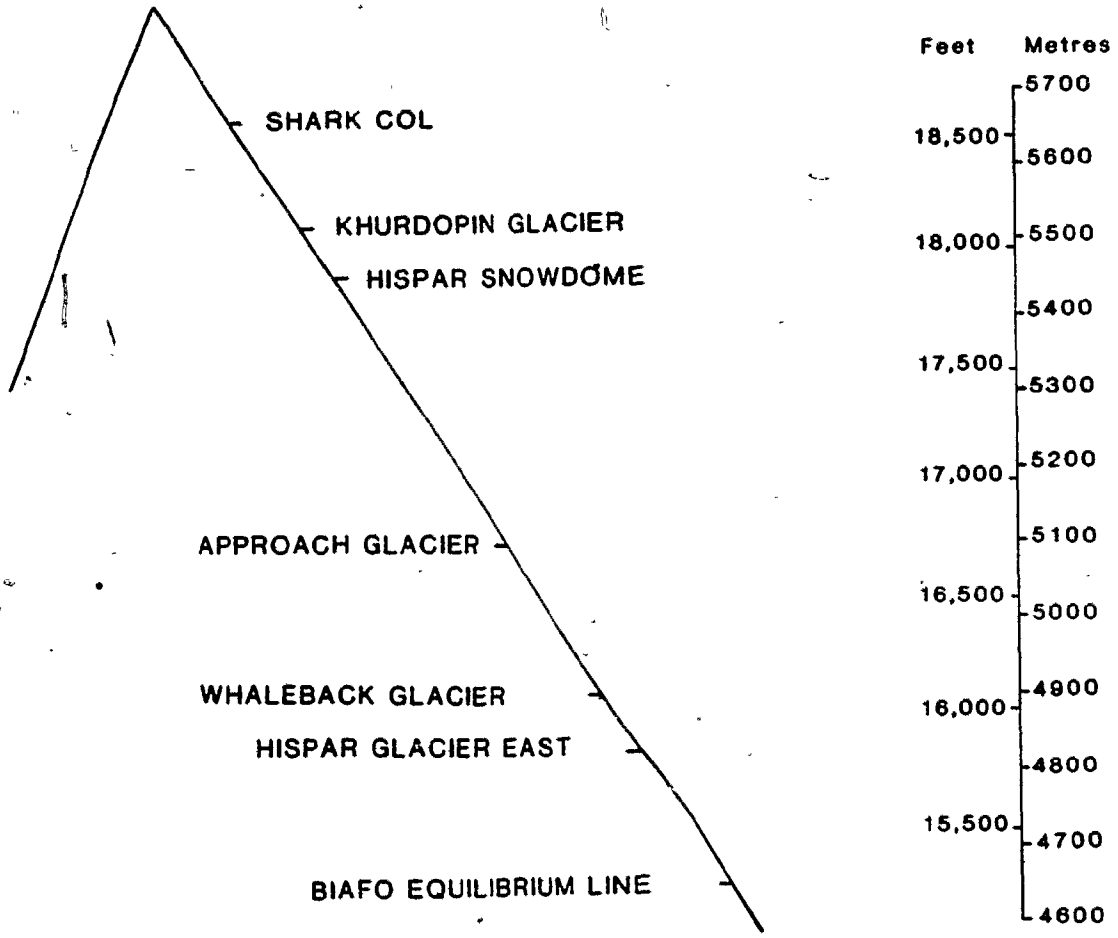

CHAPTER 4

POSTDEPOSITIONAL ALTERATION

4.1 POSTDEPOSITIONAL ALTERATION

An important consideration in all snow chemistry work is sample alteration due to post depositional changes. Post depositional processes, such as meltwater percolation, dry deposition, redeposition of snow by wind, gaseous transfer and recrystallization, can alter the chemical content of fresh and old snow. The extent of this alteration in snow and ice is of particular interest to chemical studies of cores recovered from glaciers. The majority of research on alpine snowpacks has been concerned with post depositional alteration caused by the percolation of meltwater through the snowpack. This research is briefly reviewed below, and provides a basis for interpreting the extent to which meltwater has effected the high elevation snowpack in the Central Karakoram.

The physical movement of water through snow is discussed in detail by Gerdel (1954) and Colbeck (1972, 1977). Upon the introduction of meltwater, three processes occur which drastically change the physical character of the snowpack. Initially, downward percolating meltwater develops its own vertical drainage tubes. Ice layers block the downward flow of water forcing it to follow a horizontal path. In fact, meltwater can also be temporarily ponded on top of the relatively impermeable layers. As more meltwater is introduced the network of vertical drainage becomes more intricate. Secondly, the presence of liquid water is accompanied by rapid grain growth until grain diameter reaches approximately 1 mm (Wakahama, 1968). This can cause an increase in the

permeability of the snowpack since permeability increases as the square of the average particular diameter (Shimizu,1970 cited in Colbeck, 1977). Thirdly, under the presence of large quantities of meltwater, the permeability of high density layers (ie. ice layers) increases rapidly. Associated with this is a morphological change and eventual breakdown of the high density layer. It is clearly the existence of free water itself which increases the ability of meltwater to travel through a snowpack.

A number of studies have looked at the effect of meltwater percolation on the isotopic record of a snowpack. Hattersley-Smith et al. (1975) studied the annual accumulation from a 32 m core retrieved from an ice cap on Northern Ellesmere Island. While this study is in a polar region, it addresses the role of oxygen isotopes as a tool for stratigraphic analyses within the zone of meltwater percolation facies. The stratigraphy revealed an extensive ice lens and pipe system. However, the snowpack continued to display strong seasonal variations in the $\delta^{18}O$ record. This implies that the formation of an ice lens and pipe structure was localized and did not effect the overall $\delta^{18}O$ values of the snowpack.

Ambach et al. (1972) studied the vertical profiles of the $\delta^{18}O$ content of old firn in the accumulation area of Kesselwandferner in the Oetztal Alps. These profiles show an enrichment of approximately 1.6 $^{o}/_{oo}$ due to fractionation processes occurring between percolating meltwater and the snow, which results in a slight smoothing of the $\delta^{18}O$ profile. The influence of meltwater is much greater on the large negative peaks in the $\delta^{18}O$ profile. Samples were also collected from January to May from a snowpack at 1600 m near Innsbruck, Austria (Ambach et al., 1972). In spite of the infiltration of

rain and meltwater the $\delta^{18}O$ vertical profile remained essentially unchanged.

Deuterium measurements from a snowpack in Upper Bavaria were undertaken from January to July by Moser and Stichler (1975). From January to March the stratification of the isotope profile was maintained. Heavy snowfall in April considerably increased the snow depth; the isotope composition of different precipitation events varied widely due to climatic conditions, and therefore did not produce a distinct pattern in the isotope profile. However, the deep layers retained their δD values over the complete seven month period. This compares favourably with the results of Ambach et al. (1972) and indicates that no significant variation in the isotope profile of lower layers occurs due to meltwater percolation.

Laboratory experiments by Moser and Stichler (1975) show that after a 10% weight loss of the snow sample due to melting, the $\delta^{18}O$ content is enriched by about 2 $^{o}/oo$. Moser and Stichler (1975) also investigated the diurnal variation in isotope content of surface snow for an eight day period at 2540 m in Switzerland. A general enrichment of approximately 10% in the deuterium content of the snow occurred during the day due to snow evaporation. This enrichment was partially offset by condensation during the night.

Two conclusions can be drawn from the studies discussed above. While the percolation of meltwater can alter the ratios of stable isotopes within the snowpack, it appears that limited meltwater percolation in alpine snowpacks does not remove the seasonal signature of the stable isotope profile. Studies that have recognized a smoothing of the $\delta^{18}O$ profile due to meltwater percolation indicate a change of 1-2 $^{o}/oo$. When considering annual variations

in the $\delta^{18}O$ profile in the Karakoram snowpack of 18 to 27 °/oo units (Table 5.1), a change of 1-2 °/oo is insignificant.

Experiments in the field and laboratory in Norway (Johannessen and Henriksen, 1978) indicate that impurities in the snowpack tend to become concentrated in the initial meltwater; 50-80% of the impurities leave the snowpack in the first 30-50% of the melt.

In addition to the fractionation process, the preferential elution of specific ions into the earliest portion of meltwater has been recognized (Davies et al., 1982; Brimblecombe et al., 1985; Tsiouris et al., 1985). These works examine the elution of ions in both field and laboratory snowpacks. The order of elution of ions varies somewhat between studies and even within single studies, but repeatable overall patterns are evident. Nitrate and sulfate elute quickly from the snowpack and are commonly present in the first meltwater fraction. Sodium and chloride on the other hand, are removed from the snowpack at a much slower rate. As the surface becomes depleted in ions, accumulation appears to take place at lower depths above low permeable layers.

Tsiouris et al. (1985) interpret the slow elution of chloride and sodium as a result of the importance of sea salt as condensation nuclei in the atmosphere. Much of the chloride and sodium occurs at the centre of the snow crystal, and is therefore removed slowly during melting. Ion species such as sulfate and nitrate that are associated with atmospheric pollution are attached to the surface of the snow crystals and could easily be removed in the first portion of meltwater.

The elution studies were undertaken in snowpacks which are both chemically and physically different from the snowpack in the Central Karakoram. The snowpacks investigated by Davies et al. (1982), Brimblecombe et al. (1985) and Tsiouris et al. (1985) suffered from the production and percolation of significant quantities of meltwater and show ion concentrations that are at least an order of magnitude greater than those in Central Karakoram snowpacks. The results of these elution studies must therefore be applied with caution to the snowpack in the Central Karakoram.

4.2 MELTING IN THE KARAKORAM

Direct solar radiation reaching the surface increases with elevation due to a decrease in the aerosol content and water vapour pressure of the atmosphere (Barry,1981). Shortwave radiation measurements during July and August at 4080 m showed repeatable maximum incoming short wave radiation of 1100-1300 W/m^2 which represents 80-95% of the solar constant (1360 W/m^2). The broad, relatively flat snow covered accumulation basins of the Biafo Glacier, combined with the surrounding steep snowcovered walls act as a heat trap, intensifying the effect of direct solar radiation. Maximum daytime temperatures recorded under clear sky conditions in the shade, within the broad basins at 4900m was 20°C. Minimum daily temperatures were always below freezing. Incoming solar radiation accounts for melting at the snow surface at higher elevations. The stratigraphy of the snowpits showed that 6-14% of the snowpack water equivalent was comprised of ice layers and lenses (Table 4.1), indicating that melting events do occur.

The studies dealing with the physical movement of water through the

snowpack, reviewed in Section 4.1, are primarily concerned with water movement through a ripe, isothermal snowpack. This type of snowpack does not exist above about 4800 m in the Central Karakoram. Of interest to this study are the distinct physical characteristics of the snowpack produced by percolating meltwater, such as vertical drainage tubes, homogeneous grain sizes and discontinuous ice layers. Very few vertical drainage tubes were observed in any of the snowpits in the Karakoram. Those that did exist were only of very local significance. Free water was never observed ponded on ice layers. Ice layers were characterized by a continuous layer visible on all four sides of a 2m by 2m snowpit. While they varied in thickness, they showed no discontinuities. A homogeneous distribution of grain sizes greater than 1 mm was observed at depths greater than 20 cm in three of the lower elevation snowpits. In the 'Whaleback Glacier' snowpit (4900 m), a soft, low density layer with medium grain size (1-2 mm) extended 62 cm below the upper snow surface, indicating that meltwater had percolated through the upper portion of the snowpack. However, significant meltwater percolation was limited to the upper 62 cm, as the soft, low density layer was underlain by a 1.5 cm continuous ice layer. A similar situation existed in the 'Equilibrium Line' (4650 m) and 'Approach Glacier' (5100 m) snowpits.

From a physical standpoint, there is little evidence for significant meltwater percolation in snowpacks above 4800 m in the Central Karakoram, although grain size distributions at the lower elevation sites suggest that some liquid water was present. However, the depth to which these grain size distributions exist indicate that the free water was limited to the upper stratigraphic layers.

Interpretation of glaciochemical data recovered from snowpits in which there has been melting, such as in the Karakoram, relies upon the assumption that the redistribution of ions due to meltwater percolation is limited to the uppermost stratigraphic layers. This assumption is supported by two separate lines of evidence. First, the snowpack temperature drops below freezing slightly beneath the air-snow interface. Upon encountering a below freezing layer, meltwater percolating down through the snowpack would theoretically freeze and form an ice layer. As the snow shows very low ion concentrations, even the elevated dissolved ion content in the initial meltwater would have little effect upon the freezing point of that water. The presence of ice layers in the top metre of all the snowpits analysed suggests that this is the case (Figures 5.1 through 5.3 show the vertical density profile for each snowpit. The ice layers are represented by thick black lines with a density greater than 700 kg/m^3). The ice layers thus formed may then act as a barrier to further meltwater percolation. Other physical characteristics of the snowpack, such as the lack of vertical drainage tubes, the lack of homogeneous grain size below 60 cm and ice layers that show no discontinuities, indicates that any meltwater that does form on the surface does not percolate to depths greater than about 60 cm.

Secondly, the chemical profiles from a snowpack in which there has been significant meltwater percolation, resulting in the mixing of ions from two different years of accumulation, would appear "washed out" and show weak, if any, seasonal variation (Mayewski et al., 1981). The ion concentration and $\delta^{18}O$ profiles from the high elevation sites (Figures 5.1 & 5.2) display distinct seasonal variations, and do not appear to have been significantly effected by meltwater percolation. Conversely, the ion concentration profiles

from the lower elevation sites (Figure 5.3) do not reveal a distinct seasonal pattern. It appears as though meltwater percolation during the summer at the lower elevation sites has effected the annual variation in the ion concentration profiles. However, the oxygen isotope profile for the lower elevation sites continues to show strong seasonal variations.

From the studies of Davies et al. (1982), Brimblecombe et al. (1985) and Tsiouris et al. (1985) it is expected that the effects of a smoothing process caused by the percolation of meltwater would be most pronounced in the sulfate and nitrate profiles. At the Hispar Dome pit (Figure 5.2 A & B) both the sulfate and nitrate profiles show relatively uniform concentrations in the upper 1.5 m. This could be attributed to the transfer of ions by meltwater. It is possible that this downward transfer of ions actually enhances seasonal variation, by increasing the thickness and magnitude of the peak ion concentration, while washing out the profile above this. This line of reasoning suggests that the process of ion redistribution by percolating meltwater could have produced the observed variation in the chemical profile. If this is the case, one would expect to find peak concentrations for all of the chemical species at the same depth, bordered by a washed out profile, for all of the snowpits. However, for the Hispar Dome site, this pattern does not occur in the sodium, chloride or oxygen isotope profiles. Also, this pattern is not evident for any of the snowpit profiles illustrated in Figures 5.1 through 5.3, indicating that percolating meltwater is not responsible for the observed variation with depth in most of the chemical profiles.

In summary, it is possible that in some of the snowpits the seasonal variation, especially in the sulfate and nitrate profiles has been enhanced by

the downward transfer of ions by percolating meltwater. This supports the view that sulfate and nitrate are eluted quickly from the snowpack. The observed variation in the ion and oxygen isotope records from the high elevation sites reflects seasonal variations in the chemical content of precipitation, and can therefore confidently be used to establish annual accumulation rates. For the lower elevation sites, the $\delta^{18}O$ profile is the only glaciochemical parameter which shows strong seasonal variation.

TABLE 4.1 PERCENTAGE OF ICE IN SNOWPITS

SNOWPIT	%ICE
Equilibrium	9%
Hispar Glacier East	10%
Whaleback Glacier	13%
Approach Glacier	7%
Hispar Dome	5%
Khurdopin Glacier	7%
Shark Col	7%

CHAPTER 5

ANALYSIS OF CHEMICAL AND PHYSICAL TIME-SERIES AND FRESH SNOW DATA

A summary of the chemical and physical attributes for each snowpit appear in Table 5.1. The snowpits are split into two distinct groups on the basis of elevation; the higher elevation sites (5450–5660 m) consist of three snowpits, while four snowpits make up the lower elevation sites (4650–5100 m; Figures 2.6 & 3.1).

Some important overall chemical features of the snowpits are apparent in Table 5.1. There is no trend in the oxygen isotope ratio with elevation. The low minimum ion concentration, especially for sodium and chloride, demonstrates that field sampling and subsequent analytical procedures have not introduced significant levels of contamination. This is consistent with the results of the two sets of blanks and single set of duplicate analyses discussed in Chapter 3.

5.1 ANALYSIS OF SNOWPIT DATA

The time-series profiles of the chemical properties (sodium, chloride, sulfate, nitrate, $\delta^{18}O$) and physical properties (density, debris and ice band locations) for all of the snowpits investigated, plus the total β activity, conductivity and microparticle concentrations profiles specific to the Hispar Dome site, appear in Figures 5.1 through 5.3. Seasonal trends can be identified

in all of the time-series profiles from the high elevation sites (Figures 5.1 & 5.2). Only the oxygen isotope profile shows good seasonal trends in the low elevation sites (Figure 5.3). The seasonal stratigraphy can be delineated in all of the snowpits. The oxygen isotope record is the single most useful profile, as it consistently displays a regular pattern of seasonal variations. Winter precipitation is characterized by a relative depletion in the heavy isotope content, which results in a more negative $\delta^{18}O$ value; summer precipitation is characterized by a relative increase in the heavy isotope content, which results in a less negative $\delta^{18}O$ value. More negative values, termed 'troughs', identify winter strata; less negative values, termed 'peaks', identify summer strata. Because of the strong seasonal pattern, distinct changes in the oxygen isotope profile are used as reference horizons to define summer and winter strata in all seven snowpits and the 15 m core. For the high elevation sites, seasonal cycles that are not clear in the oxygen isotope profile can be clarified through an analysis of the ion profiles. Confidence in the results increases with the greater the number of different profiles which display concurrent seasonal variation.

An analysis of the physical and chemical profiles from each snowpit are summarized in Tables 5.2 through 5.8. These tables contain considerable information in a condensed form and provide a simplification of the pattern displayed in the time-series profiles. In essence, the tables eliminate the 'noise' in the profiles and identify the major trends which identify summer and winter strata.

The format of Tables 5.2 through 5.8 are briefly discussed below. The first column identifies the parameter in question. The next four columns refer

to summer strata, while the four after that refer to winter strata. Variations in the parameter for summer and winter are described using four catagories: 1. characteristic (peak or trough); 2. timing of peak or trough (early, middle or late in the season); 3. intensity of the peak or trough (weak, medium or strong); and 4. thickness of the peak or trough (narrow, medium or broad). Underlining in certain cases identifies the predominant trend. The last column estimates the quality of the seasonal pattern (good, fair or poor). The bottom two lines of each table deal with the timing and existence of dirt and ice layers.

The following discussion only summarizes the data in Tables 5.2 through 5.8, and emphasizes some important points. The snowpits are discussed in order from the highest to the lowest elevation sites. The seasonal stratigraphy assigned to each snowpit appears on the right hand side of Figures 5.1 through 5.3.

5.1.I Highest Elevation Sites

Shark Col (5660m)

As previously discussed, 'Shark Col' is subject to the effects of high winds and avalanches which can alter the record of precipitation. Results from this site must therefore be viewed with caution. Despite this, seasonal snowpack stratigraphy can be determined from the time-series profiles (Figure 5.1A). A summary of the analysis of the profiles is listed in Table 5.2. The net annual accumulation at Shark Col, for the 3 years of record, is consistently 60% of the net annual accumulation at the Hispar Dome (Table 6.1A). This

suggests that the record of accumulation at Shark Col is, in fact, reliable.

The oxygen isotope record displays good seasonal variation. The ion and $\delta^{18}O$ profiles show medium to strong peaks during the summer. Sulfate and nitrate show peak values which tend to occur in mid to late summer. Peaks in the sodium and chloride profile occur before or concurrently with those of the sulfate and nitrate profile. The single most obvious ambiguity in the data from Shark Col is the discrepancy between the strong negative trend in the oxygen isotope profile between 4.5 and 5.9 m and the weak to moderate peaks in the sodium, chloride, sulfate and nitrate profiles between 5.0 and 5.5 m. The strong trend in the $\delta^{18}O$ profile is given more weight than the weak to moderate trend in the four chemical species. The layer is therefore interpreted as winter strata.

Khurdopin Glacier (5520m)

The profiles from the snowpit on the Khurdopin Glacier also display good seasonal trends (Figure 5.1B). A summary of the analysis of the profiles appears in Table 5.3. As with the Shark Col data, some ambiguities do exist between the various chemical profiles. The oxygen isotope profile shows good seasonal variation. Superimposed on the broad summer peaks are several narrow negative troughs. These are probably the result of a relatively colder air mass moving through the region during the summer. The broad trends in the oxygen isotope profile are given more weight than the narrow, relatively small scale discrepancies. Peaks in the sodium, chloride, sulfate and nitrate profile occur together during mid to late summer. While the oxygen isotope profile shows a strong negative trend from 3.8 and 5 m, the sodium, sulfate and nitrate profiles show moderate peaks from 4.3 to 4.6 m. More weight is

given to the oxygen isotope profile, and the layer is therefore considered as winter strata. An ice layer at 3.8 m also contains high concentrations for all four ions.

Hispar Dome (5450m)

The oxygen isotope, total β activity and density record from the combined 5 m snowpit and 15 m core at the Hispar Dome provide the deepest, and therefore the longest, record of snow accumulation. The record of ion concentrations, microparticle concentrations and conductivity extends only to 5.25 m below the surface. Similar and straightforward seasonal variations are evident in most of the time-series profiles (Figure 5.3 A & B). A summary of the analysis of the profiles is listed in Table 5.4.

As mentioned at the beginning of this chapter distinct trends in the oxygen isotope profile have been used as reference horizons to define summer and winter strata. The oxygen isotope profile shows strong seasonal variation for the first three summers. Ion concentrations also show good seasonal variation. The sulfate and nitrate profiles are characterized by strong, broad peaks which occur in mid to late summer. The chloride and sodium profiles show only a weak seasonal variation. Peaks tend to occur in mid to late summer, however solitary peaks are also evident in the winter portion of the profile. Peaks in the conductivity profile also occur in summer, but are generally narrower, and not nearly as strong as the sulfate and nitrate peaks. Peak concentrations in both the small (0.50-0.63μm) and total (0.50-12.7 μm) microparticles occur early in the summer; the small size particles display stronger peaks and a more distinct seasonal variation.

The total β activity profile displays distinct peaks in early to mid summer, for the first three summers. The peak values in the total β activity profile coincide with horizons containing visible dirt. The correlation coefficient between total β activity and total microparticle concentration is 0.72 at the 0.001 significance level (Appendix C). Unfortunately, the microparticle data stops at 5.25 m below the top of the snow pit, and therefore a concrete relationship between the microparticle concentrations and total β activity cannot be established. Only the physical, total β activity and oxygen isotope records are available below 5.25 m. The summer strata in 1984 is clearly identified by a sharp peak in the total β activity and a strong, broad peak in the oxygen isotope profiles. The interpretation of the chemical profiles below this is uncertain. The very weak peak in the oxygen isotope profile extending from 8.4 to 10.5 m can be interpreted as summer strata, bordered above and below by weak winter troughs. This interpretation results in net annual accumulation of 2.51 and 2.12 m water equivalent (w.e.) for 1983–84 and 1982–83, respectively. On the other hand the trough extending from 7.5 to 12.2 m could represent one winter's worth of precipitation, resulting in net annual accumulation of 4.63 m w.e. for 1983–84. This value seems very high when compared to the net annual accumulation of 1.20 and 0.65 m w.e for 1984–85 and 1985–86. The second interpretation is supported by the lack of any peak in the total β activity profiles. However, there is one sample missing from the β activity profile, and there is a conspicuous lack of a visible dirty horizon at this level in the snowpack. On the basis of consistency two annual layers are assigned to the snowpack from 3.6 to 12.2 m.

From 7 to 12 m below the surface, the seasonal variation in both the $\delta^{18}O$ and total β activity records from the core is reduced (Figure 5.3A). Both

record appear smoothed. Mass exchange by vapour diffusion can reduce the amplitude of seasonal variations. This is limited when the annual accumulation is greater than 0.25 m w.e. (Dansgaard et al., 1973), such as in the Karakoram (Table 6.1 A & B). However, melting events do occur. Therefore the 'smoothing' of the chemical records in the core below 7 m is probably due to both the percolation of meltwater, predominantly within summer strata, combined with compaction, and perhaps distortion, of the record with depth. Molecular diffusion in ice is a very slow process and would therefore not seriously effect shallow cores of this nature (Patterson, 1980).

A distinct transition occurs in the physical characteristics of the core at 12.2 m (Figure 5.2A). An abrupt contact marks the change from fine grained granular snow with a density of 590 kg/m^3, to a clear, icy layer containing enclosed air bubbles, with a density of 820 kg/m^3. Below 12.2 m the density profile shows a distinct pattern of alternating high density, clear, icy layers (represented by the stipled pattern) and lower density, white granular layers. These characteristics suggest that meltwater has played a role in the relatively shallow transition of firn to ice. Perhaps this portion of the core represents a period of accelerated melting. Other studies in the wet snow zone of glaciers have identified abrupt firn ice transitions at similar depths. Sharp (1951) recognized a sharp transition of firn to ice at a depth of 13 m on the Upper Seward Glacier. Vallon et. al. (1976) found an abrupt firn ice transition at 32 m in the Vallee Blanche in the Alps. Meltwater speeds up the transformation process by increasing the settling rate and sintering of snow crystals (Patterson, 1981).

Of special interest in the total β activity profile (Figure 5.3A) are the

two sharp peaks; one at 5.10–5.40 m (733 dph/kg) and the other at 19.1 to 19.4 m (1630 dph/kg), below the snow surface. The first peak at 5.1 to 5.4 m is of the same magnitude as the maximum total β activity peak (639 dph/kg) found at 15.4–15.96 m in the core from Sentik Glacier in the Ladakh Himalaya The peak in the total β activity profile from Sentik Glacier coincides with the 1963 thermo–nuclear test level. (Mayewski et al., 1984). The peak at 5.1 to 5.4 m in the Hispar Dome Core is assigned to the summer of 1984. This peak does coincide with a dirty, ice layer suggesting that the of the total β activity has been concentrated by surface melting and subsequent adsorption of beta active material onto dust particles (Prantl, 1973; Ambach, 1968).

The peak at 19.1–19.3 is extremely high. There appears to be no comparable peak in the Sentik Glacier core. This peak could be assigned to the Chinese nuclear weapons tests in the early 1970's or the early 1980's. Total β activity measurements of precipitation in Taiwan show a sharp peak in June of 1973, which is attributed to atmospheric nuclear weapon testing at Lop Nor (40 N; 90 W) in mainland China (Weng et al., 1977). Assigning this peak to increased atmospheric levels of total β activity in 1973, results in a mean annual accumulation rate from 1973 to 1982 of ~0.73 m w.e. This is low in relation to the mean annual accumulation rate from 1982–1986 of 1.62 m w.e. If the chronology for the total β activity peak at 19.1–19.4 m is correct, the data suggests that a portion of the record has been lost, presumably through intensive ablation at the Hispar Dome site. Assuming this period of intensive melting did occur, the resulting downward percolation of meltwater carrying with it radioactive material, provides an appealing mechanism for the concentration of beta active particles resulting in the large total β activity spike at 19.1–19.3 m.

High concentrations in the total β activity of air and precipitation samples were measured in 1981 by Health and Welfare Canada (Dr. Eaton, pers. comm.), presumably due to atmospheric nuclear weapons testing by the Chinese in October of 1980. Assigning the peak at 19.1-19.3 m to the winter of 1980 results in a mean annual accumulation rate of 2.90 m w.e. which is almost comparable to the rate of 2.51 m w.e. in 1983-84, but still much greater than the four year mean of 1.62 m w.e. This question remains unresolved.

The vertical distribution of ice layers, and horizons that contain visible debris is similar for all three higher elevation snowpits. The data is summarized at the bottom of Tables 5.2, 5.3 & 5.4. Only one out of twelve summer strata (Shark Col, summer 1985) does not contain at least one ice layer. On the other hand, six of the ten winter strata also contain ice layers. For the higher elevation sites, ice layers are considered a poor indicator of summer strata.

Horizons with visible debris are basically restricted to summer strata, but occur in only six of the twelve summer layers. While debris bands are characteristic of summer strata, their occurrence is not ubiquitous. Debris bands therefore help identify summer strata, but do not necessarily define summer horizons. Rather, debris bands are indicative of events such as pronounced surface ablation or an increase in the amount of debris transported to the site.

5.1.II Lower Elevation Sites

All of the four lower elevation snowpits display similar chemical profiles and are therefore discussed together. The chemical and density profiles are illustrated in Figure 5.3. A summary of the analysis of the chemical and physical records from each snowpit appears in Tables 5.5 through 5.8. As with the higher elevation sites, the oxygen isotope record from these four snowpits displays a strong, distinct pattern of seasonal variation. In the three snowpits above the Equilibrium Line, the end of the 1985 summer season is also identified by a horizon containing visible dirt, adjacent to an ice layer. Visible dirt layers occur nowhere else in the profiles. This is a strong indication that a physical analyses of snowpits at these elevations can accurately delineate annual snowpack stratigraphy for the most recent year of snow accumulation. This increases confidence in the results from the two snowpits investigated in 1985 (Young, Hewitt and Wake, 1986).

The investigation of the four low elevation snowpits over a 46 day period allows for an analysis of the evolution of the upper snow surface within Lukpe Lawo. The three snowpits investigated from June 15 to July 4 display no visible dirt at or near the surface despite clear, open sky conditions for most of this period. Only at the Hispar Glacier East snowpit, which was examined on July 31, was there a dirty horizon near the surface. This example suggests that in this elevation range, dirty horizons are formed only after a lengthy period of ablation, or perhaps during periods of increased debris transport. While samples from all four snowpits were analysed for their sodium content, only samples from three snowpits were analysed for their anion content. The one obvious characteristic which separates the lower

elevation sites from the higher elevation pits is the poor to non-existent seasonal pattern in all of the ion concentration profiles. Peak ion concentrations occur both in summer and winter strata, but do not reveal distinct, seasonal patterns.

There are three possible explanations for this. First, the lower elevation sites experience warmer air temperatures. Percolation of meltwater could have transported ions downward, thereby altering the chemical record in the snowpack. This appears to be the case in the Hispar Glacier East and Approach Glacier profiles (Figure 5.3 C & D). Second, three of the four snowpits show only one year of data. The short period of record makes it difficult to clearly decipher annual cycles. Thirdly, the source of chemical inputs could be different for the lower and higher elevation sites. Mayewski et al. (1983) collected a series of fresh snow samples over a range of elevations in the Ladakh Himalayas. All fresh snow samples were collected within 24 hours, following the end of the precipitation event. They noted a distinct change in the chemical content of fresh snow above and below 5300 m in the Ladakh Himalaya. This was attributed to precipitation from two discrete air masses with different chemical signatures.

5.2 ANALYSIS OF FRESH SNOW DATA

A summary of the time and location of fresh snow sample collection along with the chemical characteristics of the samples are listed in Table 5.9. Overall the samples show relatively low concentrations of sodium and chloride. That is characteristic of the winter and early summer strata displayed in all of

the chemical profiles (Figures 5.1 through 5.3). Nitrate and sulfate concentrations display considerable variation. Perhaps this accounts for some of the isolated peaks visible in records of these ions.

The suite of nine fresh snow samples collected over a range of elevations on July 28 provides a good comparative set of data. The storm that deposited this snow approached from the west. Cloud base was at the 5,500 m level. The mean sodium and chloride concentrations are low, 12 and 33 ppb, respectively. This indicates that air coming from the west holds relatively little sodium and chloride. The sulfate and nitrate content of the samples show a considerable increase in concentration with increasing elevation (Figure 5.4B). While there is some variation in the sodium and chloride concentrations with elevation, there is no obvious trend.

Three fresh snow samples were collected within 10 cm of each other on top of the Hispar Dome at 08:00, 11:00 and 14:30. July 28 was characterized by clear sky conditions; the maximum temperature was 12 ° C. Figure 5.4A clearly illustrates the elution of all four ions from the fresh snow on the surface. Chloride was eluted most quickly from the snowpack, and between 08:00 and 14:30 show a five fold decrease in concentration. Sulfate and nitrate eluted at about the same rate, and respectively show a three and two-fold decrease in concentration. Sodium shows a two-fold decrease in concentration.

TABLE 5.1 SUMMARY OF SNOWPITS INVESTIGATED IN THE CENTRAL KARAKORAM

	LOWER ELEVATION SITES				HIGHER ELEVATION SITES		
	EQUIL. LINE	HISPAR GLAC. E.	WHALEBCK GLACIER	APPROACH GLACIER	HISPAR DOME	KURDOPIN GLACIER	SHARK COL
DATE	June 15	July 31	June 21	July 4	July 27	July 5	June 26
ELEVATION (m/ft)	4650/ 15,250	4830/ 15,840	4900/ 16,070	5100/ 16,730	5450/ 17,880	5520/ 18,100	5660/ 18,570
ASPECT	SW	E	SE	E	-	W	E-W
DEPTH(m)	2.3	4.8	4.5	4.8	5.0	10.0	7.8
# of samp.	16	33	20	40	41	73	54
density(kg/m^3)							
mean	415	470	490	535	450	470	440
$\delta\ ^{18}O$							
mean	-14.0	-14.5	-18.1	-17.2	-13.0	-16.2	-13.9
min	-22.9	-26.3	-24.1	-26.8	-21.6	-29.7	-24.6
max	-4.9	-5.1	-3.2	-3.8	-2.9	-2.1	-0.5
Na:Cl							
mean	0.41	0.65	--	0.51	0.46	0.56	0.43
min	0.24	0.14	--	3.10	0.11	0.13	0.08
max	0.65	1.92	--	0.14	0.95	1.69	0.77
Na(ppb)							
mean	17	33	9	16	13	37	19
min	6	6	3	1	2	3	1
max	39	117	31	71	37	625	110
Cl(ppb)							
mean	40	50	--	19	28	50	44
min	20	10	--	1	9	10	11
max	88	143	--	80	52	370	220
NO_3(ppb)							
mean	218	224	--	96	154	167	197
min	73	9	--	3	22	33	41
max	503	430	--	299	475	625	1000
SO_4(ppb)							
mean	143	121	--	47	82	128	135
min	17	9	--	5	13	20	15
max	428	397	--	188	285	1210(?)	527

TABLE 5.2 SHARK COL (5660 m); 3.5 years of record

PARAMETER	SUMMER CHAR	SUMMER TIMING	SUMMER INTENSITY	SUMMER THICK.	WINTER CHAR.	WINTER TIMING	WINTER INTENSITY	WINTER THICK.	QUALITY OF SEASONAL PATTERN
$\delta^{18}O$	peak	all summer	strong	broad	trough	all winter	strong	broad	good
Na	peak	early, mid	medium	nar, med	trough	all winter	medium	broad	fair-good
Cl	peak	early, mid	strong	med	trough	all winter	weak	broad	fair-good
SO_4	peak	mid, late	strong	med, broad	trough	all winter	medium	broad	good
NO_3	peak	mid late	strong	med, broad	trough	all winter	medium	broad	fair
dirt layer	—	mid(2of4)	—	—	—	none	—	—	
ice layer	—	mid(3of4)	—	—	—	mid(1of3)	—	—	

NOTES: The strong negative trend in the oxygen isotope profile between 4.5 and 6.9 m is interpreted as winter strata. The weak to moderate peaks in the Na, Cl, SO_4, & NO_3 profiles between 6.0 and 5.5 m are considered as anomalous values

TABLE 5.3 KHURDOPIN GLACIER (5520 m), 2 years of record

PARAMETER	SUMMER CHAR.	SUMMER TIMING	SUMMER INTENSITY	SUMMER THICK.	WINTER CHAR.	WINTER TIMING	WINTER INTENSITY	WINTER THICK.	QUALITY OF SEASONAL PATTERN
δ^{18O}	peak trough+	all summer mid	strong weak	broad nar	trough	all winter	strong	broad	good
Na	peak	early, mid	strong	nar, med	trough	all winter	strong	broad	good
Cl	peak	early, mid	strong	nar, med	trough	all winter	strong	broad	good
SO_4+*	peak	early, mid	strong	med, broad	trough peak	all winter early 1985	weak strong	nar broad	good
NO_3+*	peak	mid	strong	med, broad	trough peak	all winter early 1985	strong strong	broad med	good
dirt layer	—	mid, late (2of4)	—	—	—	early(1of3)	—	—	
ice layer	—	mid(4of4)	—	—	—	mid(1of3)	—	—	

NOTES: + several narrow negative troughs occur within summer strata
* both SO_4 and NO_3 show two peaks every year.
Single strong peak in ice layer at 3.8 m in all ion concentration profiles

TABLE 5 4 HISPAR DOME (5450 m):
2 years of record for all parameters, >5 years of record for $\delta^{18}O$ & total β acivity

PARAMETER	SUMMER CHAR.	SUMMER TIMING	SUMMER INTENSITY	SUMMER THICK.	WINTER CHAR.	WINTER TIMING	WINTER INTENSITY	WINTER THICK.	QUALITY OF SEASONAL PATTERN
$\delta^{18}O$	Peak	all summer	strong	broad	trough	all winter	strong	broad	good
Na	peak	mid, late	weak	nar med	trough	all winter	strong	broad	fair
Cl	peak	mid, late	weak	nar, med	trough	all winter	strong	broad	fair
SO_4	peak	mid, late	strong	broad	trough	all winter	strong	broad	good
NO_3	peak	mid, late	strong	broad	trough	all winter	strong	broad	good
Cond.	peak	mid, late	strong	med	trough	all winter	strong	broad	good
small particles	peak	early, late	strong	nar	trough	all winter	strong	broad	good
total particles	peak	early mid	medium	med	peak	early	weak	broad	fair
β activity	peak	early mid	strong	med	trough	all winter	strong	broad	good
dirt layer	—	mid(2of4)	—	—	—	none	—	—	
ice layer	—	early, mid (4of4)	—	—	—	mid(4of4)	—	—	

TABLE 5.5 APPROACH GLACIER (5100 m); 1.5 years of record

PARAMETER	SUMMER CHAR.	SUMMER TIMING	SUMMER INTENSITY	SUMMER THICK.	WINTER CHAR.	WINTER TIMING	WINTER INTENSITY	WINTER THICK.	QUALITY OF1 SEASONAL RECORD
$\delta^{18}O$	peak	all spring	strong	broad	trough	all winter	strong	broad	good
					peak	mid	strong	broad	
Na	peak	mid	med.	narrow	peak	early	strong	broad	poor
					peak	mid	strong	med	
Cl	peak	mid	med.	narrow	peak	early	strong	med.	poor
SO_4	trough	all spring	med	broad	peak	early	strong	broad	poor
NO_3	trough•	all spring	med.	broad	peak	early	strong	broad	poor
Dirt layer	—	late (1of2)	—	—	—	none	—	good	
Ice layer	—	mid (2of2)	—	—	—	mid (1of1)	—	—	

NOTES: •possible redistribution of NO_3 due to percolating meltwater.

TABLE 5.6 WHALEBACK GLACIER (4900 m); 1 year of record

PARAMETER	SUMMER CHAR.	SUMMER TIMING	SUMMER INTENSITY	SUMMER THICK.	WINTER CHAR	WINTER TIMING	WINTER INTENSITY	WINTER THICK.	QUALITY OF SEASONAL RECORD
spb 1									
$\delta^{18}O$	peak	all spring	strong	broad	trough	all winter	strong	broad	good
Na	peak	early	weak	narrow	peak	mid	med	nar	poor
Dirt layer	—	late	—	—	—	none	—	good	
Ice layer	—	mid	—	—	—	mid	—	—	

TABLE 5.7 HISPAR GLACIER EAST (4830 m): 2 years of record

PARAMETER	SUMMER CHAR.	SUMMER TIMING	SUMMER INTENSITY	SUMMER THICK	WINTER CHAR.	WINTER TIMING	WINTER INTENSITY	WINTER THICK.	QUALITY OF SEASONAL PATTERN
$\delta^{18}O$	peak	all summer	strong	broad	trough+	all winter	strong	broad.	good*
		early	weak	narrow					
Na	peak	scattered	med	—	peaks	scattered	strong	—	poor
		early	weak	narrow					
Cl	peak	scattered	med	—	peaks	scattered	strong	—	poor
SO_4	trough	86 summer*	strong	broad					
$S\emptyset_4$	peak	85 summer	strong	broad	constant	all winter	strong	broad	poor
NO_3	trough	86 summer*	strong	broad					
$N\emptyset_3$	peak	85 summer	strong	broad	peak	mid	strong	narrow	poor
Diff layer	—	late(2of2)	—	—	—	none	—	—	good
Ice layer	—	early, late	—	—	—	none	—	—	—

NOTES: * possible redistribution of $S\emptyset_4$ and $N\emptyset_3$ due to meltwater percolation during summer 1986
+ winter 84-85 shows peak

TABLE 5.8 EQUILIBRIUM LINE (4650 m): 1 year of record

PARAMETER	SUMMER CHAR.	SUMMER TIMING	SUMMER INTENSITY	SUMMER THICK	WINTER CHAR.	WINTER TIMING	WINTER INTENSITY	WINTER THICK.	QUALITY OF SEASONAL PATTERN
$\delta^{18}O$	peak	all spring	strong	broad	trough	all winter	strong	broad	good
					peak	mid	strong	med.	
Na	peak	mid	strong	narrow	peak	early	strong	med.	poor
					peak	mid	strong	med.	
Cl	peak	mid	strong	narrow	peak	early	strong	med.	poor
					peak	mid	strong	med	
SO_4	peak	mid	strong	narrow	peak	early	strong	narrow	poor
$N\emptyset_3$	peak	early	strong	med.	peak	early	strong	broad	poor-fair
Diff layer	—	none	—	—	—	none	—	—	
Ice layer	—	early	—	—	—	none	—	—	

TABLE 5.9 SUMMARY OF FRESH SNOW SAMPLES COLLECTED FROM THE CENTRAL KARAKORAM, SUMMER 1986

SAMPLE	TIME OF PPT	TIME OF COLL	LOC/ELEV	COMMENTS	NA	CL	NO3	SO4	NA.CL	d18O
FSS2	Jun4/13-5/05	0900	BIAFO/4565m	snow 16cm	4	22	271	119	18	-11 8
FSS3	Jun 4/13-5/05	1230	EQ/4650m	snow 16cm	7	13	35	22	54	-11.8
FSS4	Jun 7, 15-16	1600	EQ/4650m	snow 1cm	16	78	334	560	21	-6 1
SP1-4	Jun 11-14	Jun 15 1400	EQ/4650m	snow 80cm	13	42	194	128	31	
FSS5	Jun15, 16	DURING PPT	EQ/4650m	rnd snow 1cm	76	>400	>900	>1000•		
FSS6	Jun16, 05-20	2000	EQ/4650m	snow 10cm	58	121	275	434	48	
FSS7	Jun16, 05-20	Jun17 0700	SOKHA LA/4750 m	snow 10cm	35	135	535	533	26	
FSS8	Jun16, 05-20	Jun 17 0800	SOKHA LA/4825m	snow 10cm	13	51	235	444	26	
FSS9	Jul 19, 09-11	DURING PPT	EQ/4650m	rain ?	45	>400	>600	>1000•		
FSS10	Jul 19/16-20/09	DURING PPT	EQ/4650m	rain & snow ?	50	98	491	473	51	
FSS11	Jul 21/20-22/06	DURING PPT	EQ/4650m	rain & snow 3cm	2	17	180	54	12	
FSS12	Jul 21/20-22/06	0600	EQ/4650m	rain & snow 3cm	4	24	236	79	17	-8 0
FSS13	Jul 23/18-24/15	DURING PPT	HISP P /5080m	snow-rain6cm	5	12			42	-16.1
FSS14	Jul 23/18-24/15	1500	HISP P /5080m	snow-rain6cm	2	6	77	25	33	-15.9
FSS15	Jul 24/15-16	DURING PPT	HISP P/5080m	rnd snow 1cm	19	46	289	74	41	-14 6
FSS16	Jul 27/13-14	Jul 28 0800	S DOME/5450m	snow 5cm	20	60	498	171	33	-6 8
FSS17	Jul 27/20-28/04	1100	S DOME/5450m	snow	10	22	435	161	45	-7 5
FSS18		1127	S DOME/5385m	snow	18	33	442	169	55	-7 5
FSS19		1132	S DOME/5335m	snow	12	29	405	149	41	-7 6
FSS20		1137	S DOME/5270m	snow	8	21	365	125	38	-6 9
FSS21		1143	S DOME/5210m	snow	19	44	272	83	43	-6.9
FSS22		1148	S DOME/5155m	snow	12	30	139	33	40	-6 8
FSS23		1156	S DOME/5105m	snow 1cm	21	42	113	29	50	
FSS24		1430	S DOME/5450m	snow	13	12	239	63	1 08	

• these samples appear to be contaminated

FIGURE 5.2 Ⓐ HISPAR DOME 5450 m

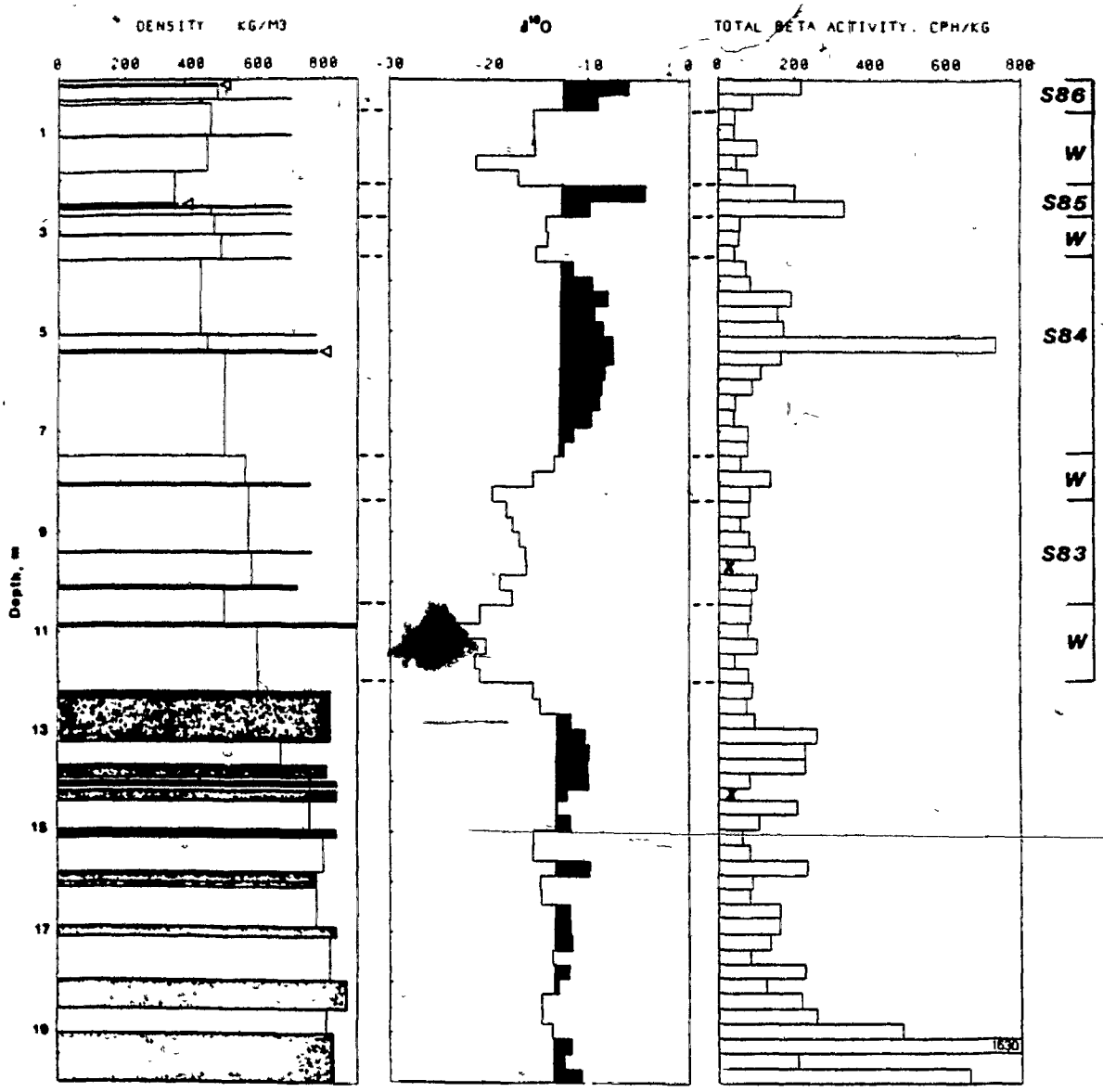

◁ Open triangles identifydirty horizons

FIGURE 5.2 (B)

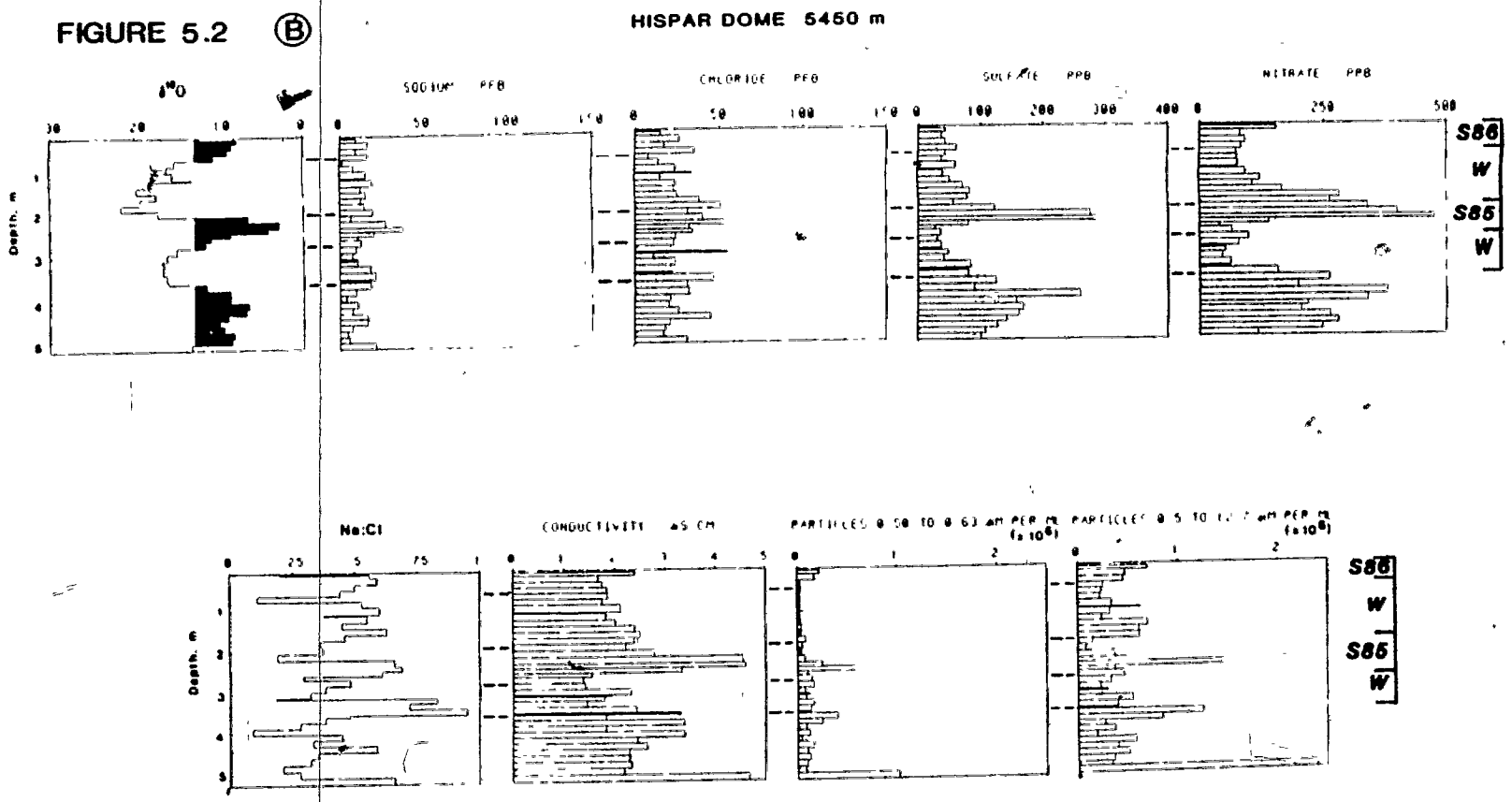
HISPAR DOME 5450 m
δ18O
SODIUM PPB
CHLORIDE PPB
SULFATE PPB
NITRATE PPB
Depth, m
S86
W
S86
W
Na:Cl
CONDUCTIVITY μS CM
PARTICLES 0.50 TO 0.63 μm PER ML (x 10⁶)
PARTICLES 0.5 TO 1.0 μm PER ML (x 10⁶)
S86
W
S86
W

FIGURE 5.4

FRESH SNOW SAMPLES - HISPAR DOME

July 28, 1986

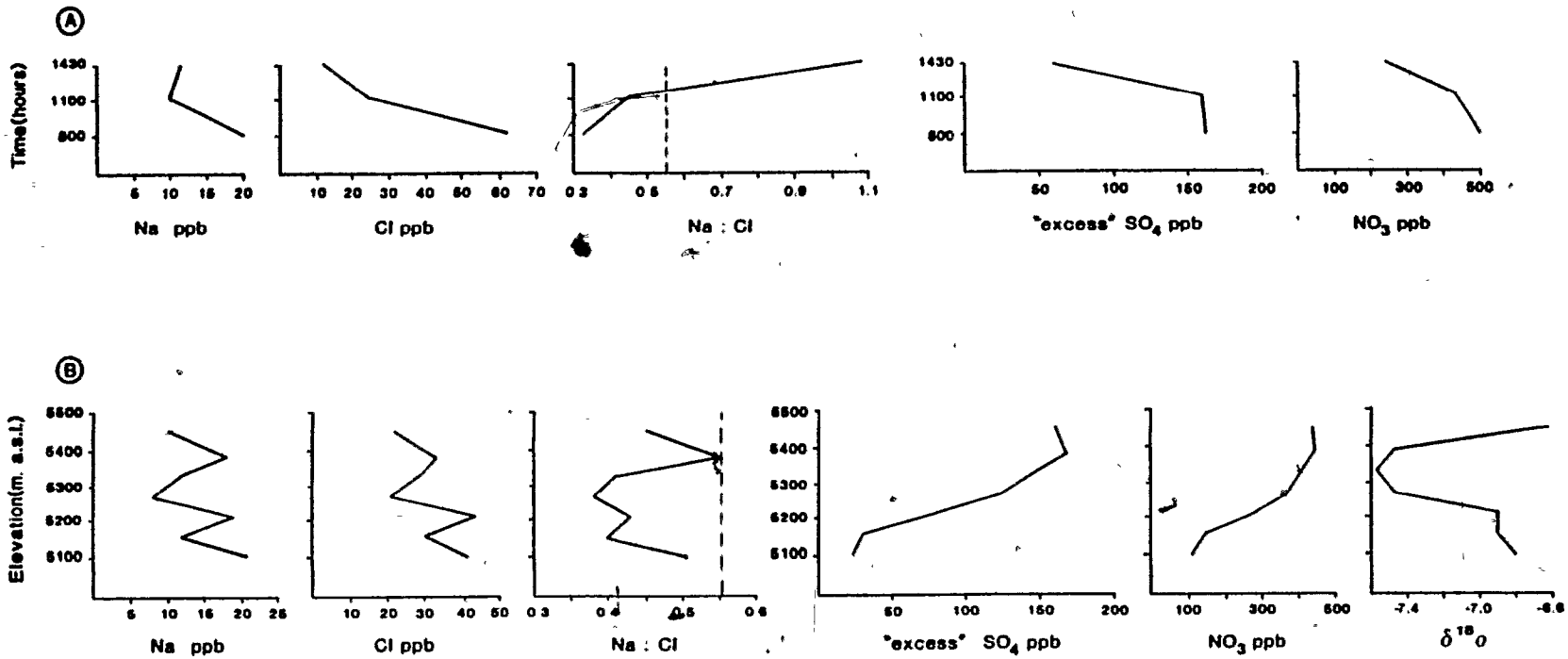

CHAPTER 6

DISCUSSION AND CONCLUSION

A detailed description and analysis of the time series profiles from the snowpits and core, as well an analysis of fresh snow data, is given in Chapter 5. The net seasonal and annual accumulation for each site, determined from the analysis in Chapter 5, appears in Tables 6.1, A & B. These results provide the basis for the interpretation of the altitudinal, lateral and temporal variation of snow accumulation within the Central Karakoram. The timing and source of chemical inputs and the effects of regional atmospheric circulation are also discussed below.

6.1 ALTITUDINAL VARIATION

In order to compare snow accumulation data from as wide a range of elevations as possible, this interpretation concentrates on the net annual accumulation for the 1985–86 accumulation year. On the basis of net annual accumulation, the study sites within the Biafo Glacier Basin can be separated into three distinct groups which represent three elevation bands (Table 6.2). There is a significant increase in net annual accumulation for the 'middle' elevation sites, as compared to the 'high' and 'low' elevation sites. Maximum accumulation in the Biafo Glacier Basin therefore occurs in the elevation band from 4900 to at least 5100 m. This band could extend as high as 5200 or 5300 m; unfortunately no data was collected at these elevations.

The zone of maximum accumulation from 4900–5100 m is best

explained by the combined effects of two different processes. Many sources, including Peattie (1936), Flohn (1974), Barrie (1981) and Price (1981), have identified an increase in the amount of precipitation with altitude in the Alps, the Rockies, the Himalayas and other temperate and subtropical mountain ranges throughout the world. Precipitation increases with altitude primarily because mountains obstruct the movement of air and cause it to rise. The effect of orographic lifting becomes stronger as the wind velocity increases with height (Flohn, 1974). The Alps show an increase in the amount of precipitation with height up to 3000–3500 m. In the Hindu Kush, the Pamirs and the northwestern Himalaya precipitation increases with altitude up to 3200–4200 m.

In 1973 the net annual accumulation at 4840 m in the accumulation zone of the Batura Glacier was 1.03 m water equivalent (w.e.), more than ten times the annual precipitation measured at 2680 m in the valley bottom (Batura Investigation Group, 1979). Three snowstorms in early June, 1986 deposited about 0.30 m w.e. of snow at 4650 m. However, during this period only trace precipitation was recorded at Baintha Base Camp (4080 m). As discussed in Chapter 3, the increase in snow depth with altitude on the Biafo Glacier, as measured on June 18, 1986 (Table 3.1), reflects the increase in precipitation with elevation. The increase in accumulation up to an elevation of 5100 m in the Biafo Glacier Basin can certainly be explained by an increase in precipitation with height, caused by orographic lifting. However, a second very important process, involving change in the pattern of deposition of snow due to the action of the wind, must also be considered.

Wind conditions in summer within the Biafo Glacier Basin are generally

moderate to calm in both the ablation zone, and in the broad, relatively flat areas of the accumulation zone, of the Biafo Glacier (see Chapter 2 for discussion). We know from our experience that during the summer, wind speed is considerably greater over exposed ridges and peaks at high elevations. Unfortunately, wind conditions at higher elevations in winter are unknown. However, Hewitt (pers. comm.) states that storms on the Biafo Glacier in the winter of 1961–62 occasionally resulted in high winds that were difficult to stand up in. Strong winter winds are certainly reflected by the wind-swept surface of large medial moraines, and the 2 to 3 m of wind-drifted snow that accumulates in hollows, within the lower half of the Biafo Glacier. One expects that these winds would be even stronger in exposed areas at higher elevations.

It is interesting that the zone of maximum accumulation from 4900–5100 m coincides perfectly with the broad, open areas in the accumulation zone of the Biafo Glacier, which accounts for the bulk of glacier cover in the basin (Figure 2.6). The strong relationship between snow accumulation and basin morphology, combined with a rough knowledge of wind conditions in winter, suggests that a portion of the snow accumulation in the elevation range from 4900–5100 m is due to the redistribution of snow by strong winds, both during precipitation and following deposition. This, in effect, creates an overcatch situation within the broad, flat, protected areas of Lukpe Lawo. This is a function of strong winds at high altitude, especially those accelerating over peaks and ridges, keeping snow in suspension, while the relatively sheltered, deeper air column over the broad, flat areas of the accumulation zone acts to trap snow.

The net annual accumulation for the Khurdopin Glacier (5520 m) for 1985–86 was 2.31 m w.e. This is much greater than the net annual accumulation of 0.71 and 1.20 m w.e. measured at Shark Col (5660 m) and Hispar Dome (5450 m), respectively. A similar relationship exists for net annual accumulation between the three sites in 1984–85 (Table 6.1A). This discrepancy between the rate of snow accumulation at the higher elevation sites can be explained by the obvious differences with respect to site characteristics. Both Shark Col and the Hispar Dome are relatively exposed sites at high elevations. While the Khurdopin Glacier site is also at a relatively high elevation, the snowpit was located in the broad, flat area of the accumulation zone. The basin is surrounded by steep walls. Morphologically, the accumulation zone of the Khurdopin Glacier is much like Lukpe Lawo, on a smaller scale and at a higher elevation. The similarity in basin morphologies, combined with the relatively high rate of snow accumulation in the broad, flat, protected areas of the accumulation zones within both glacier basins suggests that the elevation of maximum snow accumulation at both sites is dependent upon basin morphology.

In summary, elevations from 4900–5100 m represent the zone of maximum accumulation within the Biafo Glacier Basin. This zone probably extends as high as 5500 m in the Khurdopin Glacier Basin. The altitudinal variation of snow accumulation within the Central Karakoram is best explained by a combination of two processes: an increase in precipitation with elevation; and the redistribution of snow by strong winds resulting in an overcatch situation within the broad, protected areas of the accumulation zone. The elevations over which winds redistribute snow is dependent upon the area-altitude relationships of the glacier basin. As the amount of snow

deposited by direct precipitation is altered by the redistribution of snow by wind, a quantitative assessment of the increase in precipitation with elevation, or the identification of a zone of maximum precipitation, are doubtful possibilities, even with an increase in the number of data points. However, the data we have indicates that precipitation increases at least up to the 5000 m level, and net accumulation is greatest within the flat, broad protected areas of the accumulation zones of Central Karakoram glaciers.

6.2 LATERAL VARIATION

There is little variation in the net annual accumulation between the groups of lower and middle elevation snowpits. The Equilibrium Line and Hispar Glacier East snowpits, separated by 7 km, show a difference in net annual accumulation of 0.17 m w.e.. The difference between the Whaleback and Approach Glacier sites, separated by 5 km, is only 0.09 m w.e. The Hispar Pass and Lukpe Lawo snowpits investigated in 1985 show a difference of 0.15 m w.e. This suggests that accumulation for any given elevation band within the broad, flat areas in the accumulation zone of the Biafo Glacier is relatively uniform. Moreover, this is also a good indication that, within any elevation band, the snowpit locations chosen during 1985 and 1986 provide a 'representative' sample for the whole basin, in the sense that none seems subject to major disturbances by wind or avalanches.

On the other hand, we know there exists strong local variations in accumulation due to aspect, local relief or proximity to steep basin walls within the accumulation zone of the Biafo Glacier. Wind and avalanches play a

key role in the local redistribution of snow. However, as long as samples of net annual accumulation can be obtained that measure or predict average basin accumulation by elevation, we can then determine the large scale variation in accumulation, as opposed to small scale local variation.

With this stratified view of snow accumulation in the accumulation zone of the Biafo Glacier combined with area altitude relationships, a crude estimate of the moisture input during the 1985–86 accumulation year can be calculated (Table 6.3). Each elevation band covers 300 m. Snowpit data exists for 4 of the 7 elevation bands. These 4 elevation bands represent 90% of the glacier covered area in the basin. Moisture input in the accumulation zone of the Biafo Glacier is estimated to be on the order of 0.5 km^3 of water (Table 6.5). This represents 75% of the estimated meltwater production from melting ice in the ablation zone of the Biafo Glacier (Table 2.1). Accepting the relatively crude method of estimation, these results are promising. The error of such extremely simplified, large scale estimations is probably greater than the observed differences. However, these estimations provide us with a rough framework from which we can begin to quantify the various components of the hydrological system in the U.I.B. This represents a crucial step towards a better understanding of snow and ice hydrology in the U.I.B.

6.3 TEMPORAL VARIATION

This section deals with two different scales of temporal variation; seasonal and annual. The seasonal variation is interpreted using the data from all of the snowpits. Variations on the annual scale concentrate on the net annual accumulation data from the high elevation snowpits, and deals

especially with the 12.2 m of reliable data from the Hispar Dome site.

The data from all sites for 1985-86 sites show that 30-50% of the net annual accumulation occurs during the summer. However, the 1986 net summer accumulation listed in Table 6.1 does not include accumulation from a large snowfall event that we know occurred in early August. This suggests that the relative contribution of summer accumulation is possibly greater than 50%. This supports our original feelings, after witnessing large snowfall events during the summer of 1985 and 1986, that snow accumulation during the summer can be considerable.

Net summer accumulation at the Hispar Dome site in 1983 and 1984 was 3 and 6 times net summer accumulation in 1986, respectively. It has been demonstrated that summer snowfall in glacierized basins substantially decreases the rate of melting for short periods of time (Young, 1977). The experience of the Snow and Ice Hydrology Project during 1985 & 1986 at gauging stations in the U.I.B. indicates a dramatic drop in discharge during, and for some time after, extended summer storms, even though these storms are accompanied by heavy rainfall in and below the ablation zones (Figures D.1 & D.2). Summer precipitation from storms that extend over a few or more days is therefore inversely proportional to discharge. The reduction in discharge is most likely due both to the increase in cloud cover accompanying summer storms which decreases the amount of energy reaching the surface and therefore decreases the rate of melting (Wake, 1985), and an increase in the surface albedo, predominantly in the upper portions of the ablation zone. This type of response to precipitation within the U.I.B. demonstrates that melting snow and ice provide the predominant control on the temporal variation of

runoff.

With a significant increase in summer accumulation in 1983 and 1984, one might expect a corresponding decrease in annual discharge. The annual variation in discharge for three gauging stations in the U.I.B. are illustrated in Figure 6.1 and listed in Table 6.4. Contrary to the expected trend, all three stations show above average discharge in 1984; two of three stations show above average discharge for 1983. Therefore, as the summer of 1983 and 1984 show no reduction in annual runoff, it is unlikely that increased accumulation was caused by storms occurring throughout the summer. Rather, the high levels of summer accumulation were probably a result of an intensified period of precipitation, similar to our experience in August both 1985 & 1986 (Figures D.1 & D.2). The sharp decrease in the runoff hydrographs from the gauging stations in the U.I.B. on July 3 & August 8, 1983, and July 3 & August 18, 1984 (Figures D.3 & D.4) are indicative of intensive summer precipitation accompanied by extensive cloud cover. Therefore, data from 1983 through to 1986 suggests that increased summer accumulation is a result of low frequency-high magnitude precipitation events, on the seasonal scale. These storms result in a dramatic short term decrease in discharge. A more concrete relationship could be established by first, determining the variation in runoff for 5 day periods with respect to the long term mean, and second, by obtaining a longer term record of summer accumulation. In addition, a more complete chemical analysis of the snowpack would help identify the predominant source of moisture for these summer storms.

Finsterwalder (1960) stated that when the monsoon broke into the

Karakoram in the summer of 1959 snowstorms, which resulted in substantial accumulation of snow at higher elevations, were accompanied by very heavy precipitation in the valleys. The summer precipitation records for Karimabad (36 19 N; 74 40 E) in the Hunza Valley appear in Table 6.5. The 1983 and 1984 summers show below average values for summer precipitation. This reinforces the point that precipitation measurements at valley bottom stations, such at that at Karimabad, provide little indication of conditions at higher elevations.

A rough indication of the strength of the summer monsoon in the north-west quadrant of the subcontinent is provided by the summer rainfall records from Srinagar (34 05 N; 74 50 E). This data originates from the 'Monthly Climatic Data for the World' (NOAA, 1982-1986), and appears in Table 6.6. The 1983 and 84 summers show substantially more precipitation than the summers of 1985 and 1986. For the four summers from 1983-86, the variation in summer precipitation at Srinagar roughly corresponds to the variation in net annual accumulation at the Hispar Dome (Table 6.6). Concrete conclusions cannot be drawn due to the short time period represented by the data set. However, the data do suggest there is a relation between summer precipitation in Srinagar and summer accumulation in the Central Karakoram.

6.4 SOURCE OF VARIATION IN CHEMICAL INPUTS

Variations and timing of peak concentrations in the ion profiles with depth not only delineates seasonal layers, but can also potentially provide valuable information concerning the source of chemical inputs and atmospheric

circulation. This discussion focuses on the chemical records from the three higher elevation sites, although some chemical data from the lower elevation sites is also discussed. As previously mentioned, the ion concentration records from the lower elevation sites are difficult to interpret. The correlation between the various geochemical parameters with depth appears in Appendix C, and indicates that variations in sodium and chloride are well correlated, as are variations in sulfate and nitrate. These two groups of ions will be discussed separately.

Sodium and Chloride

Variations in sodium and chloride concentrations with depth are closely related; correlation coefficients for sodium and chloride for each snowpit are 0.83, 0.92, 0.61, 0.73, 0.71 & 0.81, at the 0.001 significance level (Appendix C). This close relationship between sodium and chloride suggests a common source. The mean sodium–chloride ratio for all samples from the Karakoram is 0.54, and is very close to the sodium chloride ratio of 0.56 calculated for seawater (Duxbury, 1979). It is apparent from the Na:Cl profiles in Figures 5.1 through 5.3 that the sodium–chloride ratio varies from sample to sample. However, this variation seldom results in a substantial deviation from the mean. The strong relationship between variations in sodium and chloride concentrations for all of the snowpits, combined with the bulk sodium–chloride ratio for all of the snow samples that is very close to the average sodium–chloride ratio in seawater strongly suggests a marine source for the bulk of sodium and chloride within the Central Karakoram snowpack. Sodium concentration does not increase in samples with visible dirt. Therefore crustal weathering of local material is not considered as an important source of

sodium in the Karakoram.

Sodium and chloride commonly show relatively low concentrations in winter, indicative of moisture derived from the west. A storm that approached from the west on July 27 deposited 5 cm of snow at the Hispar Dome site. Fresh snow samples collected from this snowfall show relatively low concentrations of sodium and chloride (Table 5.9). This provides further evidence that moisture brought to the region by the Westerlies are characterized by a low sodium and chloride content.

Interpretations by Mayewski et al. (1984) suggest that high concentrations of sodium and chloride in the Ladakh Himalayas occur in summer, and are due to moisture derived from the Arabian Sea. Peak concentrations of sodium and chloride commonly occur in mid summer in the Central Karakoram. The coinciding summer peaks in the sodium and chloride profiles for the Karakoram are therefore thought to reflect the influx of moisture from the Arabian Sea. Low winter concentrations, especially for chloride, are attributed to westerly marine sources more distant than the Arabian Sea, most probably the Atlantic Ocean or the Mediterranean Sea. Lower mean concentrations of sodium and chloride from the Central Karakoram, compared to those from Semtik Glacier in the Ladakh Himalaya (Table 6.7) demonstrates the greater influence Westerly derived moisture has on precipitation in the Karakoram. The concentration of chloride in a marine air mass decreases as a function of increasing distance from the coast (Eriksson; 1959 & 1960).

For the higher elevation sites, the sharp summer peaks in chloride and sodium, indicative of moisture derived from the Arabian Sea, commonly span a

vertical distance of only 15–45 cm (Figures 5.1 & 5.2). This suggests that during 1985 & 1986, only 15–45 cm of summer snowfall was derived from the Arabian Sea. The low sodium and chloride concentrations, which dominate in the winter portion of the snowpack, are also apparent in the summer strata. These low concentrations are indicative of moisture derived from the west. Summer snowfall therefore appears to originate from both the Atlantic Ocean and the Arabian Sea. Variations in the strength and intensity of the summer monsoonal circulation could account for the large variations in net summer accumulation that occurred during 1983 and 1984 in the Karakoram. As stated above, summer precipitation in the Central Karakoram appears to be related to the strength of the Indian Monsoon. This supports the conclusion of Mayewski et. al. (1980). They attribute the advances in Karakoram glaciers during the period 1890 to 1910 to strengthened circulation of the monsoon. This would have increased the influx of moisture to the Karakoram from the south.

Sulfate and Nitrate

The sources of sulfate and nitrate are numerous and often cannot be positively identified. The following is only meant to be a discussion of the possible sources of sulfate and nitrate for the high Karakoram.

Sulfate and nitrate display peaks which commonly occur in mid to late summer and tend to span a vertical distance greater than 60 cm. Sulfate and nitrate are well correlated in all of the snowpits (Appendix C). Both anions display a good, very similar seasonal pattern in the profiles from the higher elevation sites (Figures 5.1 & 5.2). Several studies have identified specific sources of sulfate in Greenland snow (Herron, 1982; Neftel et. al., 1985;

Mayewski, et. al., 1986). Sulfate originates from the ocean, volcanism, anthropogenic activity and biogenic emissions. Sulfate supplied by the ocean is transferred to the atmosphere by two principal mechanisms. Aerosol formation by injection of droplets into the atmosphere by breaking bubbles within whitecaps is well described by Blanchard (1963) and MacIntyre (1974). All dissolved ions in seawater are effected by this process. The degree of geochemical fractionation is variable, but recent work suggests that it is negligible for the major ions (MacIntyre, 1974; Hoffman et. al., 1980). Both sodium and chloride can be used as a reference to estimate the seasalt contribution of sulfate to marine aerosols. By multiplying the overall mean concentrations for sodium (24 ppb) and chloride (38 ppb) by the sodium–sulfate (0.25) and chloride–sulfate (0.14) ratios in seawater, respectively, the sea salt–associated sulfate can be estimated. The results indicate that, on average, only 5–6 ppb of sulfate is associated with sea-salt. While this obviously varies from sample to sample, it indicates that sea salt-associated sulfate represents a very small percentage of total sulfate in the samples, and can therefore not account for the seasonal variation in sulfate. Subtracting this sea salt–associated sulfate from the total sulfate results in "excess" sulfate.

Biological activity is sea surface waters supplies sulfur dioxide to the marine atmosphere (Nguyen et al., 1979). Excess sulfate concentrations of marine origins can be explained by the oxidation of marine sulfur dioxide (Bonsang et al., 1980). The biogenic sulfate flux is comparable to the sea salt production, indicating an enrichment of sulfate in marine aerosols by a factor of 2 (Bonsang et al., 1980).

While a volcanic source of "excess" sulfate in the high Karakoram cannot be ruled out, the random nature of volcanic events cannot account for the seasonal variation in the sulfate record. India is the closest source of anthropogenically produced sulfate. This sulfate could be transported into the Karakoram during the summer at the same time that moisture derived from the Arabian Sea is drawn into the region. Biogenic emissions are a source of both sulfate and nitrate and are therefore discussed together in the following paragraphs.

A variety of different sources for nitrate plus nitrite in the Ladakh Himalaya are reviewed by Lyons and Mayewski (1983). Their interpretations concerning the potential sources of nitrate in remote regions are, in a general sense, applicable to the Karakoram, with one exception. Above 5450 m, nitrate and sulfate concentrations in the Karakoram snowpack show a strong seasonal variation. Relatively broad peaks are characteristic of summer horizons. Recent studies in tropical to semi-tropical rain forests (Lawson and Winchester, 1979; Stallard and Edmont 1981) indicate that both sulfur and nitrogen are injected into the atmosphere by biological emissions, primarily from plant exudates. Nitrogen gases are also more readily liberated from the soil during the warm season (Yaalon, 1964). The valley bottoms in the Karakoram are in a semi-arid region which experiences a short growing season. Biological output is seasonally controlled. Intensive plant growth is restricted to villages in the main river valleys below about 3000 m. Open pasture is common up to 4000 m and extends above 4600 m. If the biological activity of the crops and pastures is sufficient to produce a substantial portion of the nitrate and sulfate content measured in the snowpack above 4650 m, then seasonally controlled biological emissions could account for the observed seasonal

variation in the sulfur and nitrate profiles (Figure 5.1 & 5.2). The extensive use of natural fertilizer during the summer is another possible seasonal source of nitrate.

A second difference is apparent between the nitrate records from the Sentik Glacier and the Central Karakoram. The mean nitrate concentration of the samples from the Karakoram is almost 3 times the mean nitrate plus nitrite concentration of the Sentik Glacier core samples (Table 6.7). It is tempting to attribute this excess nitrate in the Karakoram to biological emissions, as it would conveniently explain the seasonal nitrate signal in the Karakoram snowpack. This subject deserves further investigation.

6.5 CONCLUSIONS

This research provides the first detailed assessment of snow accumulation in the Karakoram, and its variation with respect to space and time. Net annual accumulation is determined at seven different sites in the Central Karakoram through an analysis of the chemical and physical characteristics of the snowpack. The sites cover a range of elevations from 4650 to 5660 m a.s.l., over a wide geographic area (Figure 2.5). The deepest record shows reliable data for a four year period from 1982 to 1986. The results (Table 6.1, A & B) provide information on a number of different aspects of snow accumulation in the Central Karakoram.

For the Biafo Glacier Basin maximum accumulation occurs in the elevation band from 4900–5100 m, and for 1985–86 net annual accumulation was 1.90 m water equivalent. This probably extends as high as 5500 m in the

Khurdopin Glacier Basin. This zone of maximum accumulation is thought to result from a combination of two processes. First, precipitation increases with increasing elevation, at least up to 5100 m. Second, the Biafo Glacier and Khurdopin Glacier Basins are relatively protected from the strong winter winds which are characteristic of the area. This creates an overcatch situation where blowing snow, originating both during precipitation events and resuspended following deposition, is trapped within the broad, flat areas.

For any given elevation band, accumulation in the broad flat portions in the accumulation area of the Biafo Glacier is relatively uniform. This is a good indication that the locations chosen for the snowpits within the basin are representative of the basin in general. Crude estimates were calculated for moisture input in the accumulation zone of the Biafo Glacier, using the snow accumulation data presented in this study. For the 1985-86 season, moisture input was on the order of 0.5 km^3 of water. If this value is correct it represents about 0.7% of annual runoff from the Upper Indus Basin.

Net summer accumulation appears to have increased substantially during 1983 and 1984. Interpreting a wide range of hydrological and meteorological data, in relation to summer precipitation events, suggests that increased summer accumulation is due to one or two intensive storms, as opposed to a large number of storms occurring throughout the summer.

The timing and strength of peak concentrations in the sodium and chloride profile indicate that precipitation from westerly air masses dominate during winter and spring. The data also suggests that air masses derived from the Arabian ocean deposit precipitation in the Karakoram each summer. Net

summer accumulation during 1985 and 1986 accounted for about 30% of the total. The large increase in the amount of summer precipitation during 1983 and 1984 could be attributed to strengthened monsoonal circulation, however this needs further investigation.

Evaluation of Techniques

The results demonstrate that glaciochemical dating is an efficient and effective method by which to determine the spatial and temporal variation of net annual accumulation in remote, high altitude, temperate alpine environments, such as the Karakoram. Especially important in regions for which no data exists, this technique enables one to produce paleoclimatic records for use in both climatic and hydrological investigations. In addition, the chemical records provide valuable data concerning the source of moisture.

The oxygen isotope record represents the single most useful time-series profile because in consistently shows a recognizable pattern of seasonal variation for each and every snowpit. At depths greater than 7-8 m below the surface at the Hispar Dome site, the extent of seasonal variation is reduced making it difficult to delineate seasonal stratigraphy.

The total β activity time-series profile shows strong seasonal variation for 3 years of accumulation. Conversely, from 7-18 m below the surface the profile lacks a recognizable pattern of seasonal variation. The sharp peak at 19.1-19.3 m has not been positively assigned to any one series of atmospheric nuclear weapons testing. However, peaks of this magnitude have the potential to act as reference horizons from which a chronology for the snowpit or core can be established.

The conductivity profile shows a good seasonal variation and displays the same trend as the ion profiles, especially sulfate and nitrate. Microparticle concentrations, both small (0.50–0.63μm) and total (0.50–12.7 μm), display seasonal variation but do not strongly identify summer and winter strata. The good relationship between total microparticle concentrations and total β activity is worthy of further investigation.

The sodium and chloride records prove to be the most valuable for determining the source of moisture in the Karakoram. This is a reflection of the limited potential sources of these two ions.

For the lower elevation sites (4650–5100 m) the oxygen isotope record shows strong seasonal variation. However, the ion concentration profiles display no recognizable seasonal pattern. The breakdown of the seasonal signature in the ion concentration profiles below 5100 m is most likely due to the redistribution of ions by meltwater percolation. The position of dirty horizons adjacent to ice layers within the snowpack at the lower elevation sites clearly identifies the 1985 summer surface. While this is promising, the short period of record from the low elevation sites prohibits the development of a concrete relationship between dirty horizons and annual layers.

6.6 RECOMMENDATIONS FOR FUTURE RESEARCH

A number of questions raised by this study cannot be answered with confidence due to the short period of record. A longer term record of snow

accumulation in the Karakoram is a crucial component of hydrological research in the U.I.B. The glaciochemical analysis of a deeper core would result in the production of a longer term record of snow accumulation. This is essential if we are to confidently determine the relationship between snow accumulation and runoff, as well as the role the summer monsoon plays in the hydrology of the region.

The possibility that portions of the snow accumulation record have been lost below 12.2 m at the Hispar Dome is of considerable interest to future glaciochemical research in the region. The Hispar Dome is a strong positive feature at a relatively high elevation. Because of this it receives sunlight for longer periods of time than the broad, flat basins of the Sim Gang Glacier, Khurdopin Glacier and Lukpe Lawo. The distinct morphology has probably resulted in increased rates of ablation at the site. The Hispar Dome is therefore probably not representitive of melting conditions of the region in general. There is no other data to confirm or deny that portions of the snow accumulation record have been lost at other locations in the Karakoram. This question should be answered prior to the investigation of a deeper core.

The investigation of lateral variation could be complimented with similar studies on different scales. Local variability could be studied by investigating a series of snowpits over a relatively small area. On the other hand, a knowledge of the lateral, as well as altitudinal, variation of snow accumulation over the whole mountain range is desirable for obvious reasons.

TABLE 6.1A SEASONAL AND ANNUAL NET ACCUMULATION - HIGH ELEVATION SITES

SHARK COL (5660m)

SEASON	SNOWPACK DEPTH(m)	W.E.(m)	% OF ANNUAL ACC.(m)	NET ANNUAL ACC.(m)
S86	0-1.05	0.34+	48%	0.71
W85-86	1.05-1.95	0.37	52%	
S85	1.95-2.30	0.13	32%	0.41
W84-85	2.30-2.98	0.28	68%	
S84	2.98-4.35	0.63	44%	1.42
W83-84	4.35-5.90	0.79	56%	

KHURDOPIN GLACIER (5520m)

SEASON	SNOWPACK DEPTH(m)	W.E.(m)	% OF ANNUAL ACC.(m)	NET ANNUAL ACC.(m)
S86	0-2.70	1.12+	48%	2.31
W85-86	2.70-5.60	1.19	52%	
S85	5.60-8.92	1.73	85%	2.04
W84-85	8.92-9.54(?)	0.31(?)	15%	

HISPAR DOME (5450m)

SEASON	SNOWPACK DEPTH(m)	W.E.(m)	% OF ANNUAL ACC.(m)	NET ANNUAL ACC.(m)
S86	0-0.70	0.32+	27%	1.20
W85-86	0.70-2.05	0.88	73%	
S85	2.05-2.70	0.22	34%	0.65
W84-85	2.70-3.60	0.43	66%	
S84	3.60-7.50	1.95	78%	2.51
W83-84	7.50-8.40	0.56	22%	
S83	8.40-10.50	1.10	52%	2.12
W82-83	10.50-12.20	1.02	48%	

TABLE 6.1B SEASONAL AND ANNUAL NET ACCUMULATION - LOW ELEVATION SNOW PITS

APPROACH GLACIER (5100m)

SEASON	SNOWPACK DEPTH(m)	W.E.(m)	% OF ANNUAL ACC.(m)	NET ANNUAL ACC.(m)
S86	0-1.35	0.65+	35%	1.88
W85-86	1.35-3.75	1.23	65%	

WHALEBACK GLACIER EAST (4900m)

SEASON	SNOWPACK DEPTH(m)	W.E.(m)	% OF ANNUAL ACC.(m)	NET ANNUAL ACC.(m)
S86	0-2.15	0.88+	49%	1.79
W85-86	2.15-4.10	0.91	51%	

HISPAR GLACIER EAST (4830m)

SEASON	SNOWPACK DEPTH(m)	W.E.(m)	% OF ANNUAL ACC.(m)	NET ANNUAL ACC.(m)
S86	0-0.92	0.49+	46%	1.07
W85-86	0.92-2.10	0.58	54%	

EQUILIBRIUM LINE (4650m)

SEASON	SNOWPACK DEPTH(m)	W.E.(m)	% OF ANNUAL ACC.(m)	NET ANNUAL ACC.(m)
S86	0-0.70	0.28+	31%	0.90
W85-86	0.70-2.25	0.62	69%	

+ Net summer accumulation for 1986 is incomplete as snowpit investigations were completed prior to a large snowfall event in August. Accumulation at 4900m in the Barpu Glacier Basin (see Figure 2.4 for location) was greater then 50 cm of wet snow.

1984-85 SNOWPITS

LOCATION	ELEVATION (m)	SNOWPACK DEPTH(m)	NET ANNUAL ACC.(m)
Lukpe Lawo	4950	0-3.65	2.02
Hispar Pass	5060	0-3.47	1.83

TABLE 6.2 1985-86 NET ANNUAL ACCUMULATION

Relative Elevation	Snowpit	Accumulation m w.e.
High	Shark Col (5660 m)	0.71
	Hispar Dome (5450 m)	1.20
Middle	Approach Glacier (5100 m)	1.88
	Whaleback Glacier (4900 m)	1.79
Low	Hispar Glacier East (4850 m)	1.07
	Equilibrium Line (4650 m)*	0.90

* Value for annual accumulation only

TABLE 6.3 ROUGH ESTIMATE OF MOISTURE INPUT IN THE ACCUMULATION ZONE OF THE BIAFO GLACIER (1985-86)

ELEVATION BAND	AREA (km^2)	NET ANNUAL ACC(m w.e.)	10^6 m^3 WATER
4572-4877*	84.0	1.0	84.0
4877-5181*	109.5	1.8	197.1
5181-5486*	99.2	1.5	148.8
5486-5791*	61.8	1.0	61.8
5791-6096	27.6	0.8 (?)	22.1
6096-6401	8.6	0.6 (?)	6.2
6401-6706	1.3	---	----
			519 TOTAL

*elevation bands for which data exists.

TABLE 6.5 KARIMABAD (2400 m)
SUMMER PRECIPITATION (JUNE-SEPT)

YEAR	PPT(mm)	DEPARTURE*
1979	57	-18
1980	86	+11
1981	96	+21
1982	51	-24
1983	42	-33
1984	40	-35
1985	23	-52

*mean=75 mm

TABLE 6.6

SRINAGAR (1518 m)

YEAR	SUMMER PPT(mm)	DEPARTURE*
1982	158	-33
1983		229
1984	200	+9
1985	109	-82
1986	142	-49

*mean=191 mm

HISPAR DOME (5450 m)

SUMMER ACCUMULATION (mm)	

+38	1100
1950	
220	
320	

TABLE 6.7 COMPARISON OF CHEMICAL CHARARTERISTICS IN SNOWPACKS FROM THE CENTRAL KARAKORAM AND LADAKH HIMALAYA

	All 1986 Snowpits Central Karakoram	Sentik Glacier Ladakh Himalaya (Mayewski et. al., 1984)
Na	24 ppb (251)	104 ppb^{+} (114)
Cl	38 ppb (265)	72 ppb^{+} (114)
Na:Cl	0.54 (246)	0.70 (114)
SO_4	111 ppb (246)	---
NO_3	178 ppb (243)	62 ppb^{+}(103)*
$\delta\ ^{18}O$	-14.9 ^{o}/oo (272)	-16.1 ^{o}/oo (19)
Total β act.	164 (66)	225 (21)
Microparticles		
0.50-0.63 μ m	132 X 10^3/ml (41)	680 X 10^3/ml (114)
1.00-1.25 μ m	50 X 10^3/ml (41)	40 X 10^3/ml (114)
8.00-10.00 μ m	200/ml (41)	60/ml (114)

Numbers in (brackets) represent number of samples analysed.
$^{+}$(μmol/l) x (molecular weight) = ppb or μg/l.
* from Lyons and Mayewski (1983).

FIGURE 6.1

UPPER INDUS BASIN
VARIATION IN ANNUAL DISCHARGE

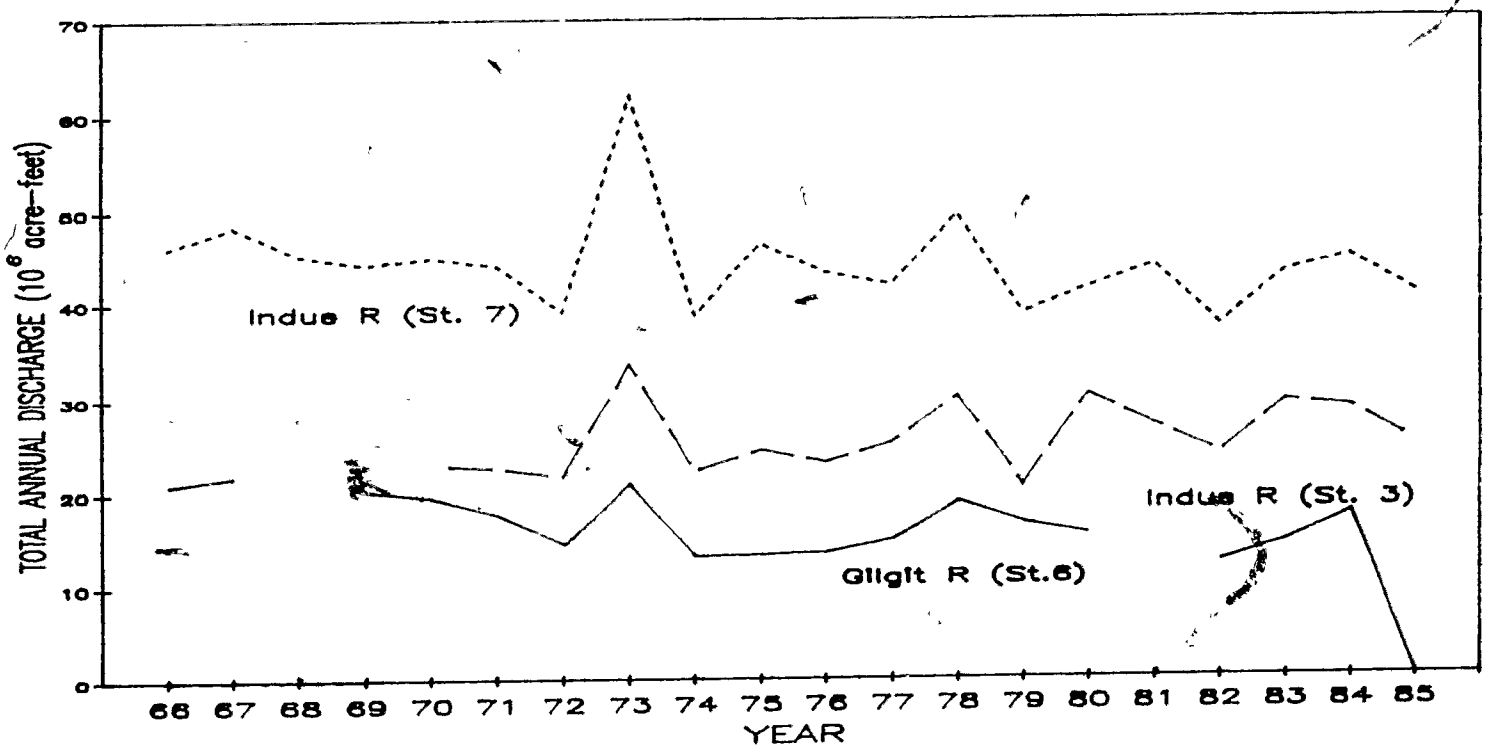

TABLE 6.3 VARIATION IN ANNUAL DISCHARGE OF THE UPPER INDUS BASIN

STATION•	MEAN ANNUAL DISCHARGE (1000 A-ft)	PERCENTAGE OF MEAN ANNUAL DISCHARGE 1966	67	68	69	70	71	72	73	74	75	76	77	78	79	80	81	82	83	84	85
3 Indus R at Katchura	25,210	—	—	—	—	88	86	82	131	85	94	91	99	120	81	121	107	94	118	115	98
6 Gilgit R at Alam Br	16,610	122	127	—	119	114	104	85	122	77	77	81	90	114	100	93	—	74	87	100	—
7 Indus R at Partab Br	43,160	104	110	102	100	101	100	88	140	87	105	100	97	115	90	96	102	87	100	104	94

•Station Number refers to Figure 2.1

REFERENCES

Ambach,W., Eisner, H., and Pessl, K. 1972. Isotopic oxygen composition of firn, old snow and precipitation in alpine regions. Zeitschrift fur Gletscherkunde und Glazialgeologie, Vol. 8, pp.125-135.

Ambach, W., Eisner, H., Elsasser, M., Loschhorn, U., Moser, H., Rauert, W., and Stichler, W. 1976. Deuterium, Tritium and Gross-Beta-Activity on Alpine Glaciers (Otztal Alps). Journal of Glaciology, Vol. 17, no. 77, pp. 383-400.

Barry, R.G. 1981. Mountain Weather and Climate. Methuen, New York. 313 p.

Barry, R.G. and Chorely, R.J. 1982. Atmosphere, Weather and Climate, 4th edn. Methuen, New York. 407 p.

Batura Glacier Investigation Group, 1979. The Batura Glacier in the Karakoram Mountains and its variations. Scientia Sinica, Vol. 22, pp. 958-974.

Blanchard, D.C. 1963. The electrification of the atmosphere by particles from bubbles in the sea, in M. Scars (ed) Progress in Oceanography. Pergamon Press, N.Y., Vol. 1, pp.71-202.

Bonsang, B., Nguyen, B.C., Gaudry, A. and Lambert, G. 1980. Sulfate enrichment in marine aerosols owing to biogenic gaseous sulfur compounds. J. Geophys. Res. vol. 85, pp.7410-7416.

Boucher, K. 1975. Global Climate. John Wiley and Sons, Inc., New York.

Boutron, C. 1979. Alkali and Alkaline earth enrichments in aerosals deposited in Antarctic snows. Atmospheric Environment, Vol. 13, pp. 919-924.

Boutron, C. and Lorius, C. 1979. Trace metal in Antarctic snows since 1914. Nature, Vol. 277, pp. 551-554.

Brimblecombe, P., Tranter, M., Abrahams, P. W., Blackwood, I., Davies, T. D., Vincent, C. E., 1985. Relocation and preferential elution of acidic solute through the snowpack of a small, remote, high-altitude Scottish catchment. Annals of Glaciology, Vol. 7, pp.141-147.

Butler, D., Lyons, W., Hassinger, J., and Mayewski, P. 1983. Shallow core snow chemistry of Athabasca Glacier, Alberta. Canadian Journal of Earth Sciences, Vol. 17, No. 2, pp. 278-281.

Butz, D. 1987. Irrigation agriculture in high mountains: the example of

Hopar Villages, Nagyr, Karakoram Himalaya. Unpublished Masters Thesis, Wilfrid Laurier University.

Butz, D. and Hewitt, K. 1986. A note on the Upper Indus Basin weather stations, in K. Hewitt (ed), Snow and Ice Hydrology Project Annual Report and Scientific Papers, 1985. Wilfrid Laurier University, pp. 64-76.

Colbeck, S. C. 1972. A theory of water percolation in snow. Journal of Glaciology, Vol. 11, No.63, pp.369-385.

Colbeck, S. C. 1977. Short term forecasting of water runoff from snow and ice. Journal of Glaciology, Vol. 19, No. 81 pp.571-588.

Dansgaard, W. 1964. Stable isotopes in precipitation. Tellus, Vol. 16, pp. 436-468.

Dansgaard, W., Johnson, S.J., Gundestrop, N., Clarsen, H.B., 1973. Stable Isotopes in Glaciology. Medd. Groenl, Vol. 197, No. 2, pp.1-53.

Davies, T.D., Vincent, C.E., and Brimblecombe, P. 1982. Preferential elution of strong acids from a Norwegian ice cap. Nature, Vol. 300, pp. 161-163.

Epstein, S. and Sharp, R.P. 1959. Oxygen isotope variations in the Malaspina and Saskatchewan glaciers, Journal of Geology, Vol. 67, pp. 88.

Eriksson, E., 1959. The yearly circulation of chloride and sulfur in nature; Meteorological, geochemical, and pedological implications, I. Tellus, Vol. 11, pp.375-403.

Eriksson, E. 1960. The yearly circulation of chloride and sulfur in nature; Meteorological, geochemical, and pedological implications, II. Tellus, Vol. 12, pp.63-109.

Ferguson, R. 1984. Sediment Load at the Hunza River in K. Miller (ed) The International Karakoram Project, Vol. 2, Cambridge University Press, Cambridge, pp.581-598.

Ferguson, R. 1986. Parametric modelling of daily and seasonal snowmelt using snowpack water equivalent as well as snowcovered area. IAHS Publ. no. 155, pp. 151-165.

Flohn, H. 1974. A comparative meteorology of mountain areas, in J.P. Ives and R.G. Barry (eds), Arctic and Alpine Environments. Methuen: London. pp.55-71.

Friedman, I. and Smith, G.I. 1970. Deuterium content of snow cores from Sierra Nevada area. Science, Vol. 169, pp. 467-470.

Finsterwalder, R. 1960. German glaciological and geological expedition to the Batura Mustagh and Rakaposhi Range. Journal of Glaciology, Vol. 3, No. 28, pp. 787-788.

Gaggeler, H., von Gunten, H.R., Rossler, E., Oeschger, H., and Schotterer, U. 1983. Pb-dating of cold alpine firn/ice cores from Colle Gnifetti, Switzerland. Journal of Glaciology, Vol. 29, No. 101, pp.165-77.

Gerdel, R. W. 1954. The transmission of water through snow. Transactions, American Geophysical Union, Vol. 35, No. 3, pp.475-485.

Gilbert, O., Jamieson, D., Lister, H., and Pendlington, A. 1969. Regime of an Afghan glacier. Journal of Glaciology, Vol. 8, No. 52, pp.51-65.

Godwin-Ansten, H.H. 1864. On the Glaciers of the Mustagh Range. Journal of the Royal Geographical Society, Vol. 34, pp.19-56.

Goudie, A.S. and others 1984. The geomorphology of the Hunza Valley, Karakoram Mountains, Pakistan, in K. Miller (ed), The International Karakoram Project, Vol. 2, Cambridge University Press, New York. 635 pp. 359-410.

Haeberli, W., Schotterer, U., Wagenbach, D., Haeberli-Schwitter, H., and Bortenschlager, S. 1983. Accumulation characteristics on a cold, high alpine firn saddle from a snow-pit study on Colle Gnifetti, Monte Rosa, Swiss Alps. Journal of Glaciology, Vol. 29, No. 102, pp. 260-271.

Hattersley-Smith, G., Krouse, H.R., and West, K.E. 1975. Oxygen isotope analysis in accumulation studies on an ice cap in northern Ellesmere Island, NWT. IAHS Publ. No. 104, pp. 123-128.

Herron, M.M. 1982. Impurity sources of F, Cl, NO3 and SO4 in Greenland and Antartic precipitation. Journal of Geophysical Research, Vol. 87, No. C4, pp.3052-3060.

Hewitt, K. 1961. Studies in the Geomorphology of the Upper Indus Basin. 2 vols. unpublished Ph.D dissertation, University of London.

Hewitt, K. (1964) A Karakoram ice-dam. Indus (Pakistan), Vol. 5, pp.18-30.

Hewitt, K. 1982. Natural Dams and Outburst Floods of the Karakoram Himalaya. IAHS Pub. No. 138, pp.259-269.

Hewitt, K. 1985. Snow and ice hydrology in remote, high mountain basins: the Himalayan sources of the Indus. Snow and Ice Hydrology Project working paper No. 1, 28 p.

Hewitt, K. 1986. The Upper Indus Snow Belts: Snowfall and Sources of Water Yield in K. Hewitt (ed) Snow and Ice Hydrology Project - Annual Report and Scientific Papers 1985, Wilfrid Laurier University, pp.58-63.

Hoffman, E.J., G.L. Hoffman, and R.A. Duce, 1980. Particle size dependence of alkali and alkaline earth metal enrichment in marine aerosols from Bermuda, J. Geophys. Res. Vol. 85, pp.5499-5502.

Holdsworth, G., Pourchet, M., Prantl, F.A., and Meyerhof, D.P. 1984. Radioactivity levels in a firn core from the Yukon Territory, Canada. Atmospheric Environment, Vol. 18, No. 2, pp.461-466.

Huebert, B.J. and Lazrus, A.L. (1980). Tropospheric gas-phase and particulate nitrate measurements. Journal of Geophysical Research, Vol. 85, pp.7322-7328.

Johannessen, M., and Henriksen, A. 1978. Chemistry of snow meltwater: changes in concentration during melting. Water Resources Research, Vol. 14, No. 4, pp. 615-619.

Jouzel, J., Merlivat, L., and Pourchet, M. 1977. Deuterium, tritium, and beta activity in a snow core taken on the summit of Mont Blanc (French Alps). Determination of the accumulation rate. Journal of Glaciology, Vol. 18, No. 80, pp. 465-470.

Judy, C., Meiman, J.R. and Friedman, F. 1970. Deuterium variations in an annual snowpack. Water Resources Research. Vol. 6, No. 1, pp.125-129.

Junge, C.E. 1977. Processes responsible for the trace content in precipitation. IAHS Pub. No. 118, pp.63-77.

Koerner, R. M. and Fisher, D. 1982. Acid Snow in the Canadian high Arctic. Nature, Vol. 295, pp.137-140.

Lawson, D.R. and J.W. Winchester, 1979. Sulfur, potassium and phosphorus associations in aeosols from Southern American tropical rain forests, Journal of Geophysical Research, Vol. 84, pp.3723-3727.

Lockwood, L.G. 1965. The Indian monsoon - a review. Weather, Vol. 20, pp.2-8.

Lyons, W.B. and Mayewski, P.A. 1983. Nitrate plus nitrite concentration in a Himalayan ice core. Geophysical Research Letters, Vol. 10, No. 12, pp. 1160-1163.

Lyons, W.B., Mayewski, P.A., Thompson, L.G., and Allen, B. 1985. The glaciochemistry of snow-pits from Quelccaya ice-cap, Peru, 1982. Annals of Glaciology, Vol. 7, pp. 84-88.

MacIntyre, F. 1974. The top millimeter of the ocean. Sci. Am., Vol. 230, No. 5, pp.62-77.

Macpherson, D.S. and Krouse, H.R. 1967. 018/016 ratios in snow and ice of the Hubbard and Kaskawulsh glaciers, in Isotope Techniques in the Hydrological Cycle, American Geophysical Union Monograph No. 11, pp. 180-194.

Mayewski, P.A., Lyons, W.B., and Ahmad, N. 1981. Reconnaissance glaciochemistry studies in the Indian Himalaya. Proceedings of the Eastern Snow Conference, 38th annual meeting, pp. 45-48.

Mayewski,P.A., Lyons, W.B., and Ahmad, N. 1983. Chemical composition of a high altitude fresh snowfall in the Ladakh Himalayas. Geophysical Research Letters, Vol. 10, No. 1, pp. 105-108.

Mayewski, P.A., Lyons, W.B., Spencer, M.J., Twickler, M., Dansgaard, W., Koci, B., Davidson, C.I., and Honrath, D.E. 1986. Sulfate and Nitrate Concentrations from a South Greenland Ice Core. Science, Vol. 232, pp.975-977.

Mayewski, P.A., Lyons, W.B., Ahmad, N., Smith, G., and Pourchet, M., 1984. Interpretation of the chemical and physical time-series retrieved from Sentik Glacier, Ladakh Himalaya, India. Journal of Glaciology, Vol. 30, No. 104, pp. 66-76.

Mercer, J.H. 1975. Glaciers of the Karakoram, in W.O. Field, Mountain glaciers of the northern hemisphere, Vol. 2, CRREL, Hanover, N.H., pp.371-409

Miller, M.M. 1965. Tritium in Mt. Everest ice-annual glacier accumulation and climatology at great equatorial altitudes. Journal of Geophysical Research, Vol.70, No.16, pp.3885-3888.

Moser, H. and Stichler, W. 1975. Derterium and oxygen 18 contents as an idex of the properties of snow cover. IASH Publication No. 114, pp.122-135.

Mott, P.G. 1950. Karakoram survey, 1939. A new map. The Geographical Journal, Vol. 116, No. 1-3, pp. 89-95.

NOAA 1982-1986. Monthly Climatic Data for the World. Vols. 35-39.1 National Climatic Data Centre: Asheville, North Carolina (also available at AES in Downsview, Ontario.)

Neftel, A., Beer, J., Deschger, H., Zurcher, F., and Finkel, R. C., 1985. Sulphate and nitrate concentrations in snow from South Greenland 1895-1978. Nature, Vol. 314, pp.611-613.

Niewondniczanski, J., Grabczak, J., Baranski, L. and Rzepka, J. 1981. The altitude effect on the isotopic composition of snow

in high mountains. Journal of Glaciology, Vol. 27, No. 95, pp. 97-111.

Oerter H., Rauert W. 1982 Core drilling on Vernagtferner (Oetztal Alps, Austria) in 1979: tritium contents. Zeitschrift fur Gletscherkunde und Glazialgeologie Vol. 18, pp.13-22.

Oerter H., Reinwarth O., Rufli, H. 1982 core drilling through a temperate Alpine glacier (Vernagtferner, Oetztal Alps) in 1979. Zeitschrift fur Gletscherkunde und Glazialgeologie Vol. 18, pp.1-11.

Oerter, H., Baker, D., Stichler, W., and Rauert, W. 1985. Isotope studies of ice cores from a temperate alpine glacier with respect to the meltwater flow. Annals of Glaciology, Vol. 7, pp.90-93.

Oeschger, H., Stauffer, B., Haeberli, W., and Rothlisberger, H. 1978. First results from alpine core drilling projects. Zeitschrift fur Gletscherkunde und Glazialgeologie. Vol. 13, pp.193-208.

Peattie, R. 1936. Mountain Geography. Greenwood Press Publishers, New York. 257 p.

Picciotto, E. and Wilgain, S. 1963. Fission products in Antartic Snow, a reference level for measuring accumulation. Journal of Geophysical Research, Vol. 68, No. 21, pp.5965-5973.

Prantl, F.a., Ambach, W. and Eisner, H. 1973. Alpine glacier studies with nuclear methods. The Role of Snow and Ice in Hydrology. Proceedings of the Banff Symposia, 1972. pp. 299-312.

Price, L.W. 1981. Mountains and Man: A Study of Processes and Environment. University of California Press: Berkeley. 508p.

Rahn, K.A. and McCaffrey, R.J., 1979. Compositional differences between Arctic Aerosol and Snow. Nature, Vol. 200, pp.479-480.

Raina, V.K., Kaul, M.K., and Singh, S. 1977. Mass-balance studies of Gara Glacier. Journal of Glaciology, Vol. 18, No. 80, pp. 415-423.

Schotterer, U., Haebern, W., Good, W., Oeschger, H., and Rothlisberger, H. 1981. Datierung von kaltem firn und Eis in einem Bohrkern vom Colle Gnifetti, Monte Rosa. Jahrbuch an Schweizerischen Naturforschenden Gesellschaft, Wissenschaftlicher Teil, pp.48-57.

Sharp, R.P. (1951) Features of the Upper Seward Glacier, St. Elias Mountains,, Canada. Journal of Geology, Vol. 59,

pp. 599-621.

Sharp, R.P., Epstein, S. and Vidziunas, I. 1960. Oxygen isotope ratios in the Blue Glacier, Olympic Mountains, Washington. Journal Geophysical Research, Vol. 63, No. 12, pp.4043-4059.

Skoog, D.A. and West, D.M. 1976. Fundamentals of Analytical Chemistry. Holt, Rinehart and Winston, Toronto.

Sugden, D.E. and John, B.S. 1976. Glaciers and Landscape. Edward Arnold, London. 376 p.

Stallard, R.F. and J.M. Edmond, 1981. Geochemistry of the Amazon 1. Precipitation chemistry and the marine contribution to the dissolved load at the time of peak discharge. Journal of Geophysical Research. Vol. 86, pp.9844-9858.

Stichler, W., Baker, D., Oerter, H., Trimborn, P. 1982 Core drilling on Vernagtferner (Oetztal Alps, Austria) in 1979: deuterium and oxygen-18 contents. Zeitschrift fur Gletscherkunde und Glazialgeologie Vol. 18, pp.23-35.

Spencer, M.J., Mayewski, P.A., Lyons, W.B. and Hendy, R.H. 1985. A preliminary assessment of the potential application of glaciochemical investigations on Heard Island, South Indian Ocean. Journal of Glaciology, Vol. 31, No. 109, pp. 233-236.

Thompson, L.G., Hastenrath, S., Morales Arnao, B. 1979. Climatic ice core records from the tropical Quelccaya Ice Cap, Science, Vol. 203, pp.1240-1243.

Thompson, L.G., Moseley-Thompson, E., Grootes, P.M., Pourchet, M., and Hastenrath, S. 1984. Tropical glaciers: potential for ice core paleoclimatic reconstructions. Journal of Geophysical Research, Vol. 89, No. D3, pp. 4638-4646.

Thompson, L.G., Mosely-thompson, E., Dansgaard, W., and Grootes, P.M. 1986. The Little Ice Age as recorded in the stratigraphy of the tropical avelccaya ice cap. Science, Vol. 234, pp.361-364.

Tsiouris, S., Vincent, C. E., Davies, T. D., and Brimblecombe, P., 1985. The elution of ions through field and laboratory snowpacks. Annals of Glaciology, Vol. 7, pp.196-201.

Vallon, M., Peht, J.r. and Fabre, B. 1976. Study of an ice core to bedrock in the accumulation zone of an alpine glacier. Journal of Glaciology, Vol. 17, pp. 13-28.

Wakahama, G. 1968. The metaporphism of wet snow. IAHS Pub. No. 79, pp.370-379.

APPENDIX A

PAKISTAN GLACIER INVENTORY+

MOUNTAIN AREA Karakoram GLACIER Biafo Gyang

SOURCES:

Map Title and Number Hispar-Biafo Glacial Regions (The Geographical Journal; July-September 1950)

Compiled by E.E. Shipton Date 1950 (Surveyed 1939)

Scale 1:253,440 Contour Interval 250 feet

Map Title and Number India and Pakistan (Jammu and Kashmir) Topographic Series; Maps NJ 43-15 and NI 43-3

Compiled by U.S. Army Map Service Date 1953 (Compiled from Survey of India;1945)

Scale 1:250,000 Contour Interval 500 feet

TERMINUS CO-ORDINATES:

Longitude 75°55' E

Latitude 35°40' N

MID-BASIN CO-ORDINATES:

Longitude 75°43' E

Latitude 35°55' N

ORIENTATION:

Basin Long Axis 145° (SSE) Ablation Area 145° (SSE)

Accumulation Area Lupke Lawo 180° (S) Sim Gang 270° (W)

ELEVATIONS:

Maximum Basin Elevation 7,286 m Glacier Terminus Elevation 3,110 m

Basin Elevation Range 4,176 m Ablation Line Elevation 4,650 m

Mean Accumulation Area Elevation (a) 5,968 m* (b) 5,271 m*

Mean Ablation Area Elevation (a) 3,880 m* (b) 4,146 m*

LENGTH AND AREA:**

Maximum Glacier Length 59 km Mean Main Stream Width 2.5 km

Maximum Length Ablation Area 45 km Maximum Length Accumulation Area 14 km

Total Basin Area 852.52 km² Glaciated Area 544.09 km²

Connected Glacier Area 535.87 km²

Ablation Area 32 % 173.18 km² Accumulation Area 68 % 370.91 km²

SLOPE-ASPECT DATA: TOTAL BASIN

North facing 17.95 % 153.01 km² South facing 38.19 % 325.54 km²

East facing 21.64 % 184.46 km² West facing 22.22 % 189.51 km²

SLOPE-ASPECT DATA: GLACIATED SLOPES

Average Glacier Slope Biafo 1:15.719 Sim Gang 1:19.833

North facing 17.11 % 93.21 km² South facing 40.79 % 221.93 km²

East facing 21.69 % 117.96 km² West facing 20.41 % 111.01 km²

+ Prepared by David Butz.

* Ablation and accumulation area elevations are calculated in two ways: (a) average of highest and lowest elevations; and (b) mean of area-altitude calculations above and below ablation line.

**All area data refers to plan area.

Condensed From
PAKISTAN GLACIER INVENTORY

AREA-ALTITUDE RELATIONSHIP

MOUNTAIN AREA Karakoram

Total Basin:

2,440-2,743m		km²	%
2,743-3,048m		km²	%
3,048-3,353m	12.33	km²	1.45 %
3,353-3,658m	13.05	km²	1.53 %
3,658-3,962m	34.63	km²	4.06 %
3,962-4,267m	89.92	km²	10.55 %
4,267-4,572m	112.33	km²	13.18 %
4,572-4,877m	147.48	km²	17.30 %
4,877-5,181m	159.18	km²	18.67 %
5,181-5,486m	149.13	km²	17.49 %
5,486-5,791m	86.65	km²	10.16 %
5,791-6,096m	36.70	km²	4.30 %
6,096-6,401m	9.59	km²	1.12 %
6,401-6,706m	1.33	km²	0.16 %
6,706-7,010m	0.19	km²	0.02 %
7,010-7,315m		km²	%
7,315-7,620m		km²	%
7,620-7,925m		km²	%
7,925-8,230m		km²	%
8,230-8,535m		km²	%

GLACIER Biafo Gyang

Glaciated Area:

2,440-2,743m		km²	%
2,743-3,048m		km²	%
3,048-3,353m	10.38	km²	1.91 %
3,353-3,658m	8.63	km²	1.59 %
3,658-3,962m	23.12	km²	4.25 %
3,962-4,267m	57.04	km²	10.48 %
4,267-4,572m	53.01	km²	9.74 %
4,572-4,877m	83.98	km²	15.43 %
4,877-5,181m	109.53	km²	20.13 %
5,181-5,486m	99.15	km²	18.22 %
5,486-5,791m	61.75	km²	11.35 %
5,791-6,096m	27.64	km²	5.08 %
6,096-6,401m	8.57	km²	1.58 %
6,401-6,706m	1.29	km²	0.24 %
6,706-7,010m		km²	%
7,010-7,315m		km²	%
7,315-7,620m		km²	%
7,620-7,925m		km²	%
7,925-8,230m		km²	%
8,230-8,535m		km²	%

APPENDIX B

SURFACE VELOCITY OF THE BIAFO GLACIER, 1985-86

INTRODUCTION

As part of the overall glaciological program conducted on the Biafo Glacier during the summers of 1985 and 1986, lines of wooden stakes were drilled into the ice in profiles transverse to the direction of glacier flow and were surveyed by theodolite to determine rates of ice movement. While most of the information obtained during these surveys applies to flow rates during the "summer", two stakes from the 1985 survey were resurveyed during the 1986 survey allowing for the calculation of "winter" flow rates. In conjunction with depth sounding along the same profiles, the ice flux through the transverse sections will be estimated; the flux at the equilibrium line will give a first approximation of the annual mass balance of the glacier.

LAYOUT OF SURVEY POINTS

Two excellent theodolite survey stations were established at the Mango, Baintha, and Equilibrium Line profiles. These stations were set up on prominent, stable locations some 50-200m

above glacier surface level. The stations are identified by large cairns and each set of stations is clearly intervisible. The Sim Gang set of survey points is marginally adequate. The distance between the survey points is small (356m) and access is difficult and at times dangerous. However, unless one climbs up very high, these are the only apparent locations for survey stations in the equilibrium zone of the glacier.

All stake profiles were positioned on a line at right angles to glacier flow from the primary survey station. It was this station which was used at the beginning and end of the survey period to determine the angular movement and hence the distance each stake moved. Angles measured from the secondary survey station were taken at the start of the survey period to fix the initial locations of the stakes.

STAKE PROFILE LAYOUT

Figure A.1 illustrates the position of the stake profiles in relation to the Biafo Glacier. The 1985 and 1986 Baintha stake profiles were the most detailed, consisting of 9 stakes placed at approximately 300m intervals (see surface velocity profiles, Figure A.1). The glacier is some 3.3km wide at this location.

The other three profiles were not as detailed. The Sim Gang

profile consisted of 4 stakes each separated from the other by 600m. The glacier is approximately 3.0 km wide at this profile. The Equilibrium Line profile originally consisted of 6 stakes. Unfortunately stake 6, positioned 700m from the NW edge of the glacier was not sighted during the July 20/86 survey. Therefore surface movement at this profile is limited to the SE half of the glacier. Glacier width here is approximately 2.3 km. The Mango profile was established on ice which was far more difficult to travel on than the other three profiles due to large amounts of supra-glacial debris and significantly greater relief of the ice surface. Stakes were drilled in clean ice commencing 450m from the NW edge of the glacier; 250m separates stakes 1 & 2 and 2 & 3; 110m separates stakes 3 & 4. Glacier width at this profile is approximately 1.8 km.

Profiles consisted of 2m hardwood stakes drilled vertically almost 2m into the ice. These were redrilled when necesary in order to prevent the stakes from falling over.

BASE LINE LAYOUT AND SURVEY STATION COORDINATES

Temporary baselines were established on relatively flat sections of the glacier. The Mango (100.00m) and the Baintha (260.08m) baselines were measured with a 50m steel tape; the

Equilibrium Line (100.0m) and Sim Gang (106.5m) profiles were measured with a 50m climbing rope. All four baselines were measured at the same time that angles to the survey points were made. Coordinates of survey stations and stakes were subsequently calculated in arbitrary northings and eastings relative to the baselines. The calculated distances between survey stations for the Mango, Baintha, Equilibrium Line and Sim Gang sites are 1203.1m, 911.0m, 674.9m, and 356.5m, respectively.

Baseline measurements are assumed good to within 0.10m. Checks on the calculations have shown that, despite the unsatisfactory necessity of surveying and setting up base lines on glacier ice, the coordinates of the survey stations are good to within approximately 1.0m. Total movement measurements are therfore certainly good to within 0.10 and movement per day calculations good to within 0.01. Confidence in the results is therefore high.

DISCUSSION

The results of the 1985 and 1986 surveys are listed in Table A.1. The Baintha profile, and to a lesser extent the other three profiles, show that a wide section in the middle of the glacier is moving at approximately the same rate (Figure A.1); there seem

to be rapid increases in the movement rates within a few hundred meters of the glacier margins. In the case of the Mango and Baintha profiles this largely coincides with the zones of heavy supra-glacier debris cover.

Other things being equal one would expect that surface movement rates at the Equilibrium Line would be substantially greater than at any other location on the Biafo glacier. In fact, flow rates are not substantially different from the Baintha profile. This, in combination with the fact that the glacier is actually narrower by at least 1 km at the Equilibrium Line would imply that the glacier is perhaps twice as deep at the Equilibrium Line than at Baintha.

Two stakes from the 1985 Baintha profile were resurveyed during the 1986 survey. The results, listed in Table A.2, are not entirely representative of seasonal movement as the "winter" season, defined by the last survey of 1985 on August 12 and the first survey of 1986 on May 29, includes some "summer" movement. This indicates that, at the very least, summer flow rates are twice as high as those in winter on the Biafo Glacier.

TABLE B.1 BIAFO GLACIER SUMMER SURFACE MOVEMENT

STAKE PROFILE	LENGTH OF SURVEY	STAKE #	TOTAL MOVEMENT(m)	MEAN DAILY MOVEMENT (m)
1985				
BAINTHA (4085m/ 13,400')	23 DAYS	1	8.1	0.35
		2	11.4	0.50
		3	12.3	0.53
		4	12.9	0.56
		5	13.0	0.57
		6	13.4	0.58
		7	13.0	0.57
		8	11.9	0.52
		9	9.1	0.40
1986				
MANGO (3885m/ 12,750')	39 days	1	22.4	0.58
		2	24.1	0.62
		3	23.7	0.61
		4	23.7	0.61
BAINTHA (4085m/ 13,400')	63 days	1	30.8	0.49
		2	39.5	0.63
		3	39.0	0.62
		4	38.0	0.60
		5	37.8	0.60
		6	37.7	0.60
		7	37.3	0.59
		8	34.2	0.54
		9	25.3	0.40
EQUILIBRIUM LINE (4650m/ 15,250')	41 days	1	27.0	0.66
		2	30.4	0.74
		3	32.6	0.80
		4	35.0	0.85
		5	36.5	0.89
SIM GANG GLACIER (4800m/ 15,750')	41 days	1	10.7	0.26
		2	12.9	0.31
		3	11.8	0.29
		4	9.6	0.23

TABLE B.2 "SUMMER" & "WINTER" SURFACE GLACIER MOVEMENT
BAINTHA PROFILE, BIAFO GLACIER

DATES	LENGTH OF SURVEY	STAKE #	TOTAL MOVEMENT (m)	MOVEMENT PER DAY (m)
20/7-12/8/85 ("summer")	24 days	2	11.4	0.50
		4	12.9	0.56
12/8/85-29/5/86 ("winter")	313 days	2	65.1	0.22
		4	86.7	0.30
29/5-30/7/86 ("summer")	63 days	2	40.0	0.63
		4	38.0	0.60

FIGURE B.1

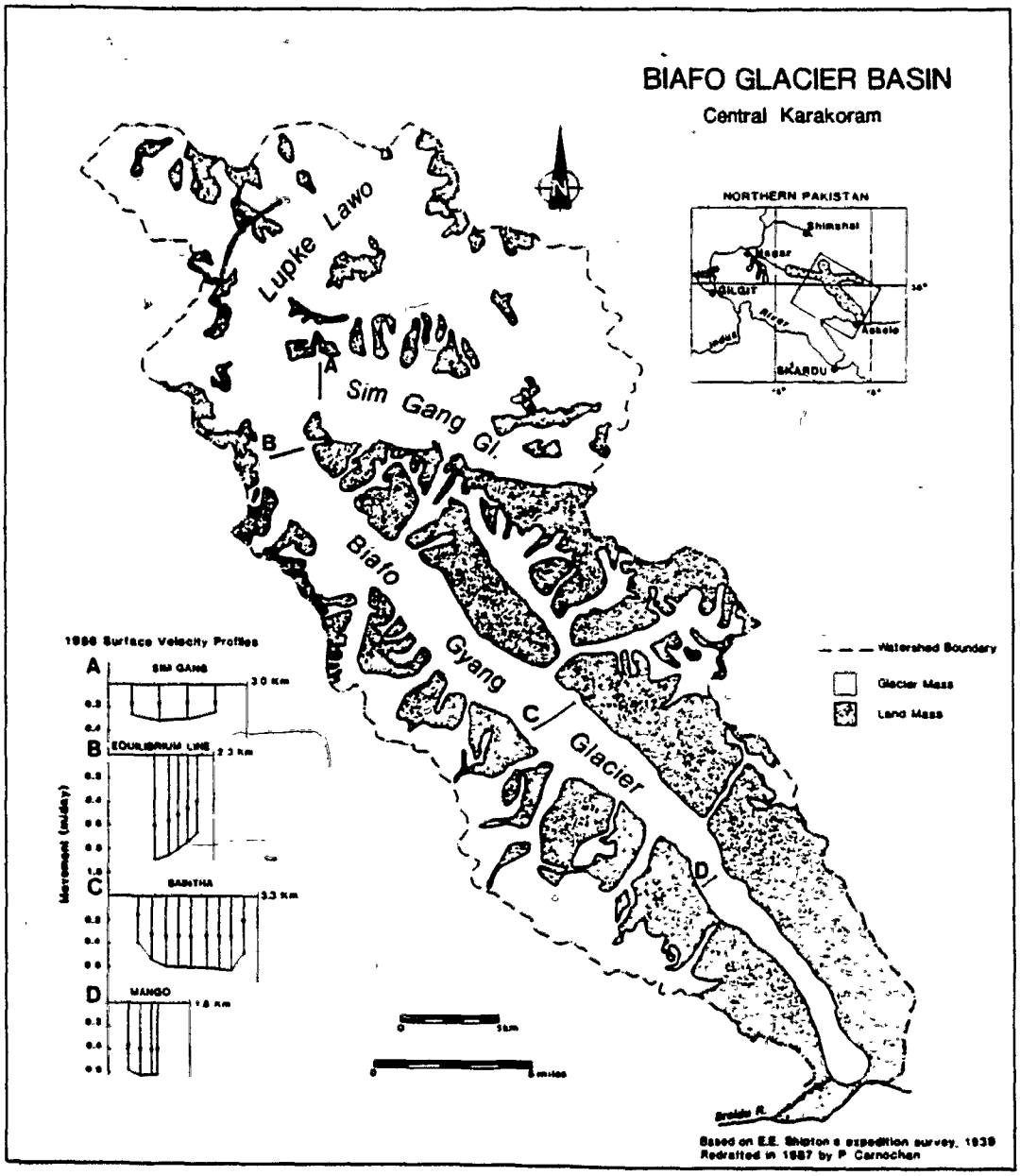
BIAFO GLACIER BASIN
Central Karakoram
NORTHERN PAKISTAN
Shimshal
Hasar
GILGIT
Askole
SKARDU
Lupke Lawo
Sim Gang Gl.
Biafo
Gyang
Glacier
A
B
C
D
1986 Surface Velocity Profiles
SIM GANG
3.0 Km
EQUILIBRIUM LINE
2.3 Km
BARATHA
3.3 Km
MANGO
1.8 Km
Movement (m/day)
Watershed Boundary
Glacier Mass
Land Mass
Based on E.E. Shipton's expedition survey, 1939
Redrafted in 1987 by P Carnochan

APPENDIX C

CORRELATION COEFFICIENTS BETWEEN GLACIOCHEMICAL PARAMETERS, WITH DEPTH

Shark Col. (5660m) n=42

	$\delta^{18}O$	Na	Cl	NO_3	SO_4
$\delta^{18}O$	1.00	----	----	0.49*	0.48*
Na		1.00	0.83+	0.41*	0.45*
Cl			1.00	0.71+	0.68+
NO_3				1.00	0.82+
SO_4					1.00

Khurdopin Glacier (5520m) n=67

	$\delta^{18}O$	Na	Cl	NO_3	SO_4
$\delta^{18}O$	1.00	----	0.20$	0.32*	0.30*
Na		1.00	0.92+	----	0.26$
Cl			1.00	0.26$	0.33$
NO_3				1.00	0.42+
SO_4					1.00

Hispar Dome (5450m) n=35

	$\delta^{18}O$	Na	Cl	SO_4	NO_3	Cond.	Part.	Beta.
$\delta^{18}O$	1.00	----	----	0.61+	0.56	0.38$		0.28$
Na		1.00	0.61+	0.50+	0.30$	0.56+	0.42*	0.32$
Cl			1.00	0.28$	0.36$	0.68+	----	----
SO_4				1.00	0.86+	----	----	----
NO_3					1.00	0.59+	----	----
Cond.						1.00	0.42*	0.48*
Part.							1.00	0.72+
Beta								1.00

Approach Glacier (5100m) n=32

	$\delta^{18}O$	Na	Cl	SO_4	NO_3
$\delta^{18}O$	1.00	---	---	---	---
Na		1.00	0.73+	0.29$	0.36$
Cl			1.00	0.50$	0.63+
SO_4				1.00	0.69+
NO_3					1.00

Hispar Glacier East (4830m) n=25

	$\delta^{18}O$	Na	Cl	SO_4	NO_3
$\delta^{18}O$	1.00	---	---	---	---
Na		1.00	0.78+	0.56*	0.44$
Cl			1.00	0.62*	0.57$
SO_4				1.00	0.72+
NO_3					1.00

Equilibrium Line (4650 m) n=13

	$\delta^{18}O$	Na	Cl	SO_4	NO_3
$\delta^{18}O$	1.00	----	----	0.53$	0.66*
Na		1.00	0.81+	0.52$	---
Cl			1.00	0.53$	0.66*
SO_4				1.00	0.56*
NO_3					1.00

Significance Levels

$ 0.10
* 0.01
+ 0.001

Low correlation coefficients with significance levels above 0.10 have been omitted from the tables.

APPENDIX D

UPPER INDUS BASIN HYDROLOGICAL RECORDS 1983-1986

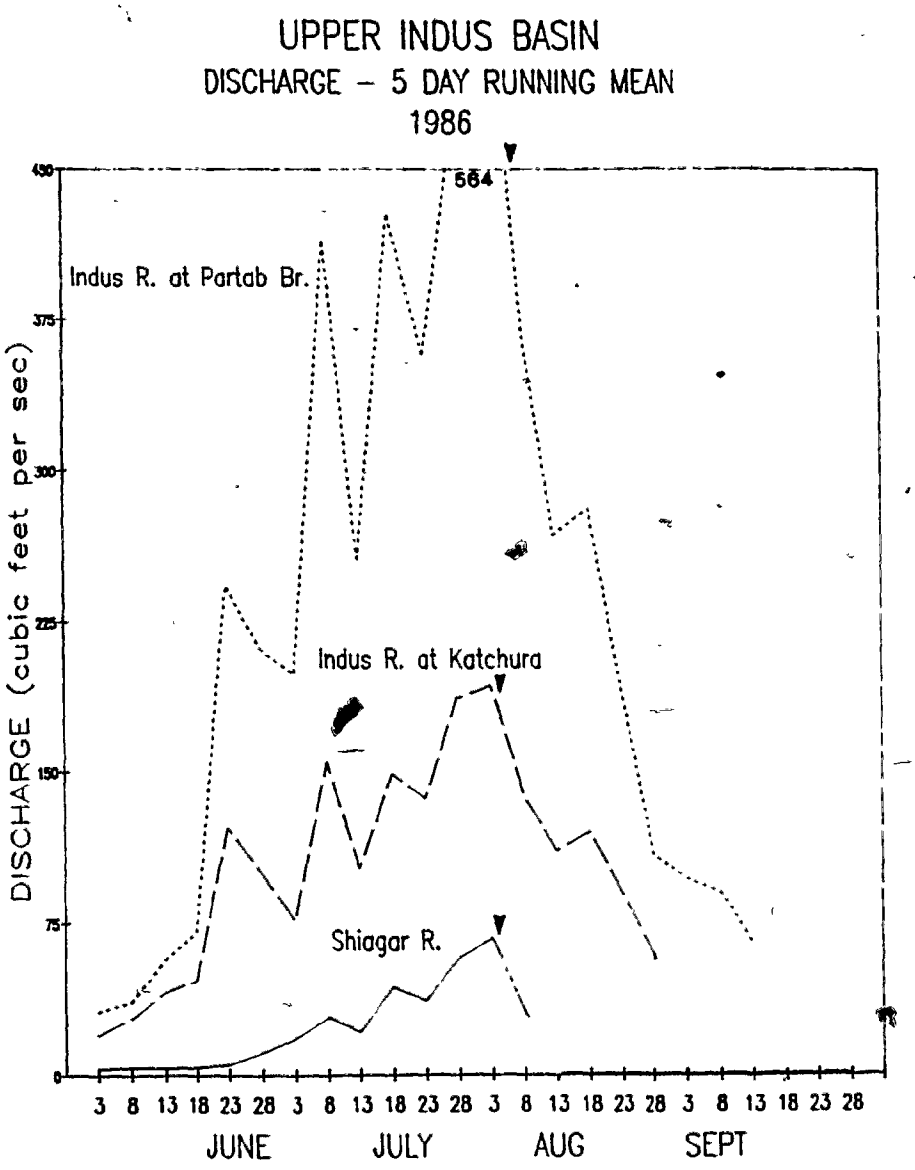

FIGURE D.1 The solid black arrows correspond to an extended period of precipitation (August 3-9) that was accompanied by extensive cloud cover. Note the sharp decrese in discharge at all gauging stations. The location of the gauging stations is shown in Figure 2.1.

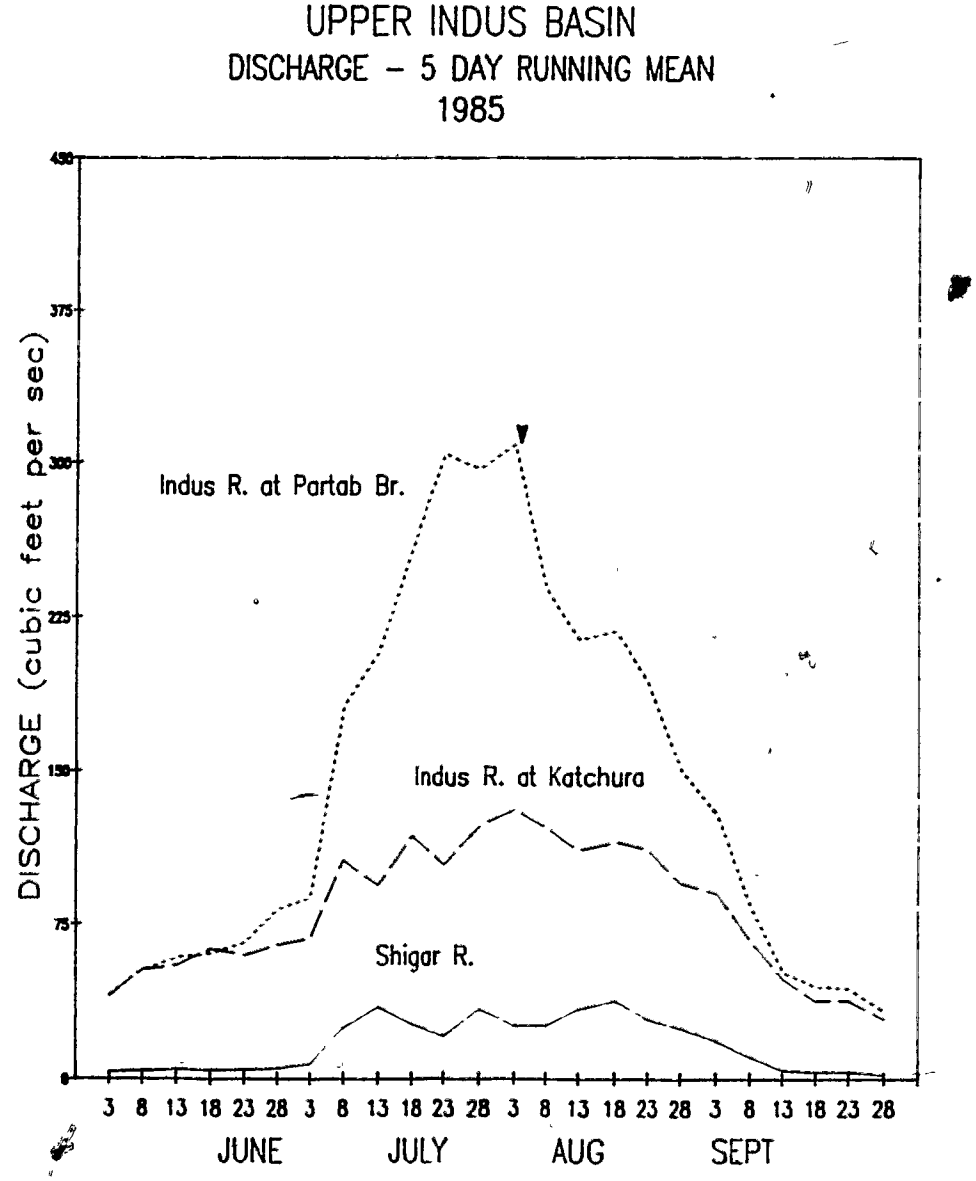

FIGURE D.2 The solid black arrows correspond to a period of heavy snowfall (August 2–7) at 4900 m which was accompanied by rainfall and heavy cloud cover at lower elevations. Note the sharp decrease in discharge for the Indus River at Partab Bridge gauging station.

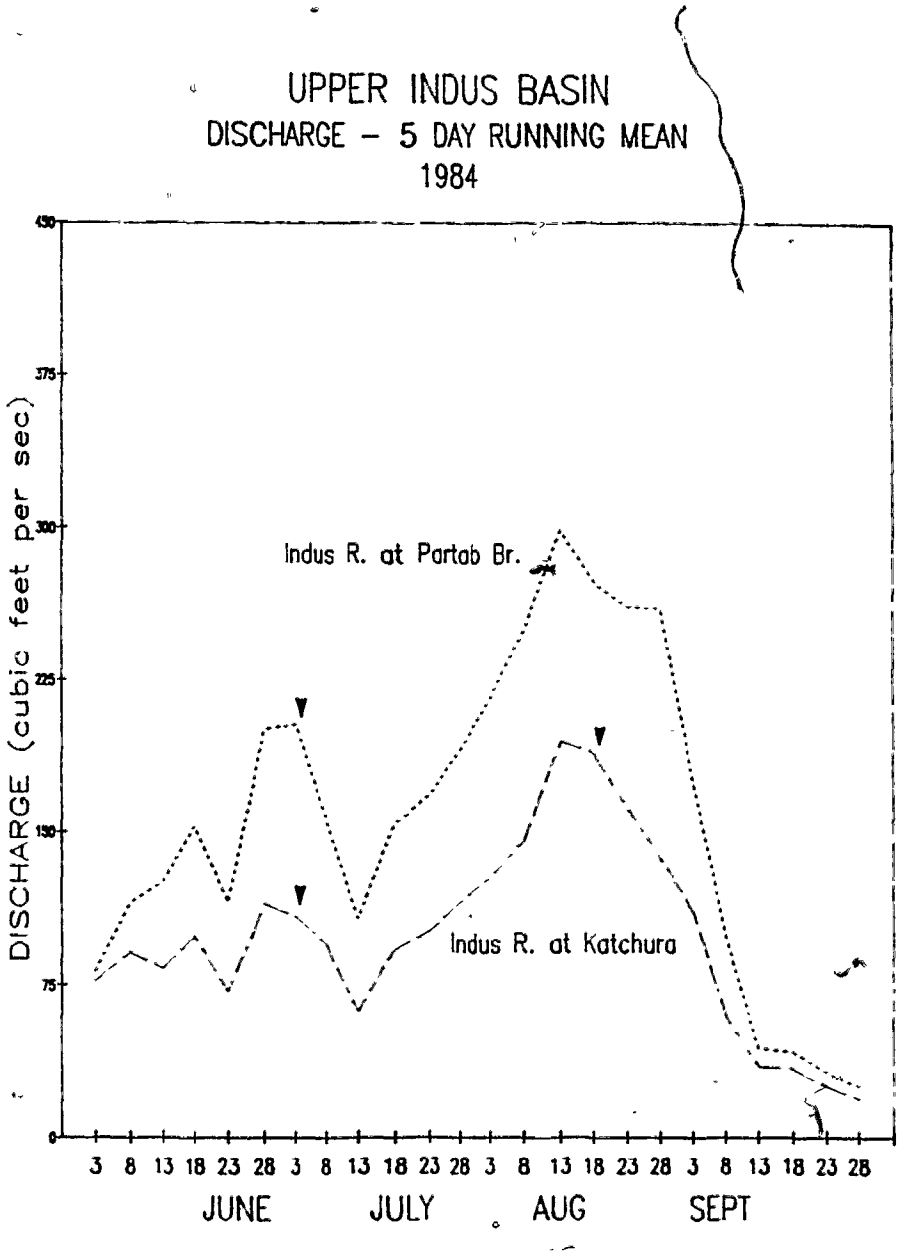

FIGURE D.3 The solid black arrows highlight sharp decreases in discharge, indicative of extended periods of summer precipitation accompanied by extensive cloud cover. There exists no 1984 data for the Shigar River gauging station.

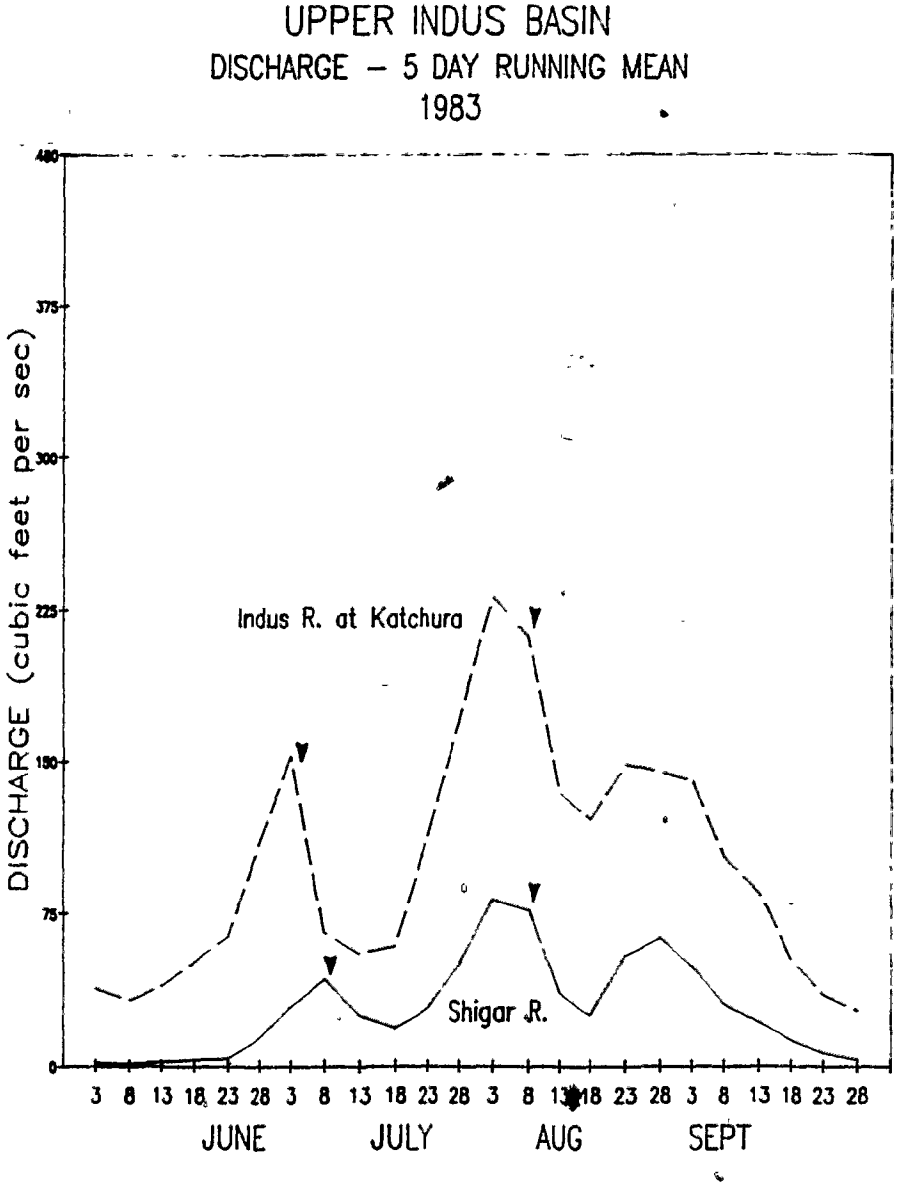

FIGURE D.4 The solid black arrows highlight sharp decreases in discharge, indicative of extended periods of summer precipitation accompanied by extensive cloud cover. There exists no 1983 data for the Indus River at Partab Bridge gauging station.

APPENDIX E

PHOSPHATE & NITRITE

Along with the analysis of chloride, sulfate and nitrate, the samples were also analysed for nitrite and phosphate. For all of the nitrite samples and most of the phosphate samples, concentrations were equal to or less than the detection limit of 5 and 20 ppb, respectively. The horizons that did show phosphate concentrations above 20 ppb are listed in Table E.1. The lack of any recognizable pattern in the distribution of phosphate makes an interpretation concerning the source of this ion difficult.

TABLE E.1 PHOSPHATE CONCENTRATIONS (ABOVE 20 PPB) IN SNOWPITS

SNOWPIT	DEPTH	THICK	TIMING	PO_4	Na	Cl	SO_4	NO_3
Shark Col.	745	15	summer	2[illegible]	27	70	24	84
	760	15	summer	58	41	75	70	122
Khurdopin Glacier	85	15	early summer	47	75	105	74	99
	175	15	all summer	30	38	65	68	87
	190	15	all summer	44	112	119	36	65
	205	15	all summer	46	143	205	119	88
	220	15	all summer	35	91	118	144	124
	280	15	late winter	24	48	64	63	95
	993	7ice	summer	36	140	224	271	351
Hispar Dome	310	3ice	mid winter	172	11	58	13	52
	355	5ice	late summer	22	12	25	18	43
Hispar Glacier E.	265	15	mid winter	27	60	117	238	228
	340	20	late summer	100	40	74	49	75
	435	10ice	early summer	23	24	43	75	23

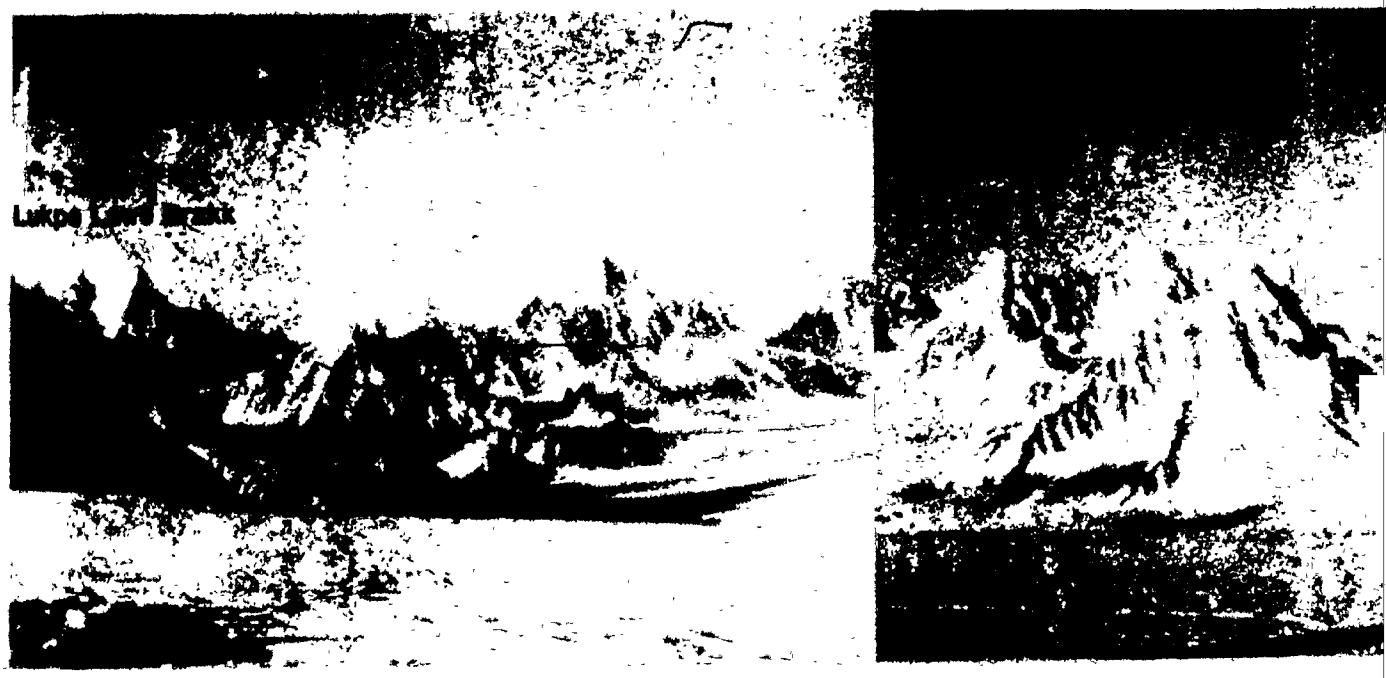

Lukpe Lawo ('Snow Lake') and the Sim Gang Glacier

Glacier looking west from Hispar Dome

FIGURE 5.1

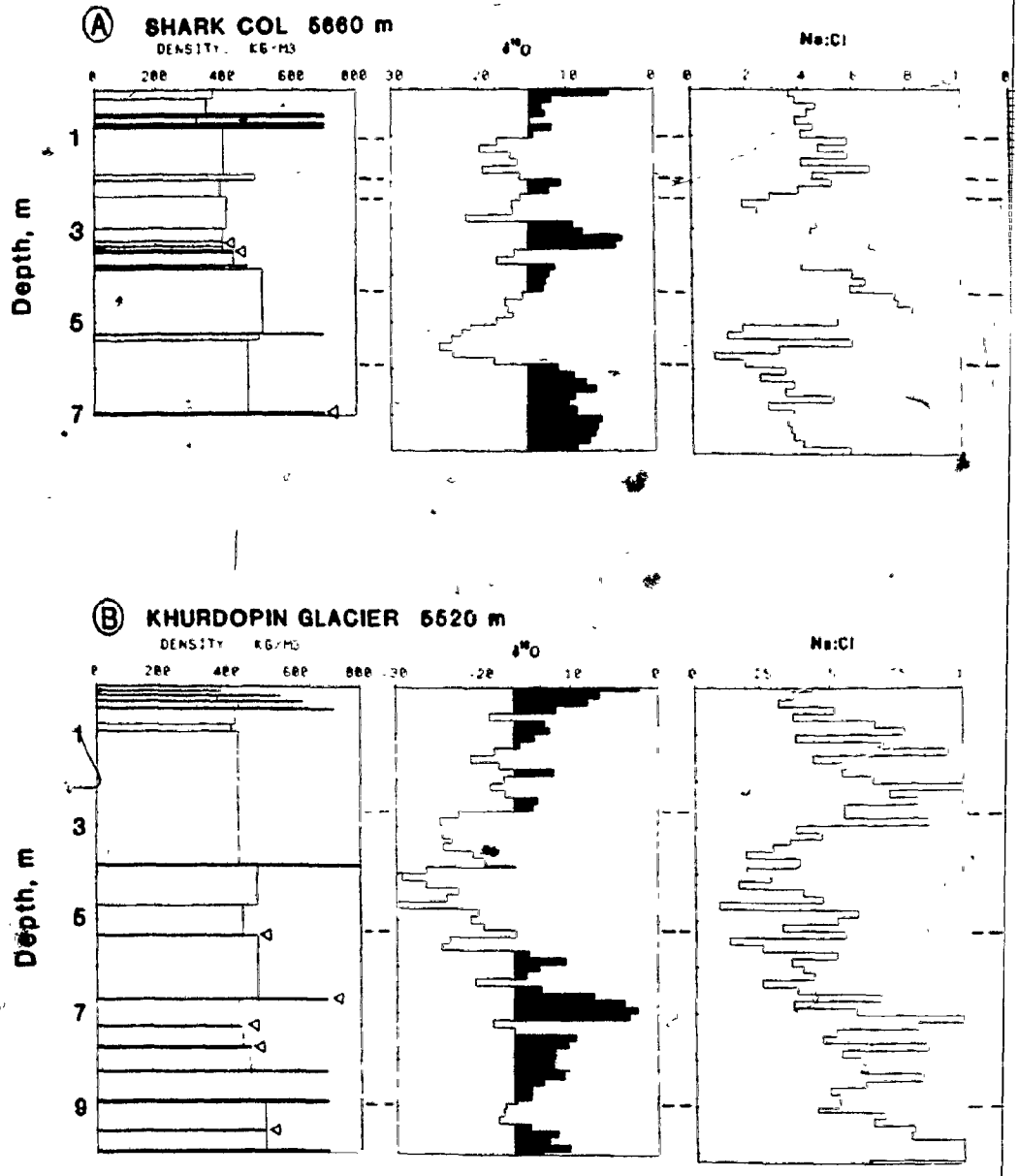

◁ Open triangles identify dirty horizons

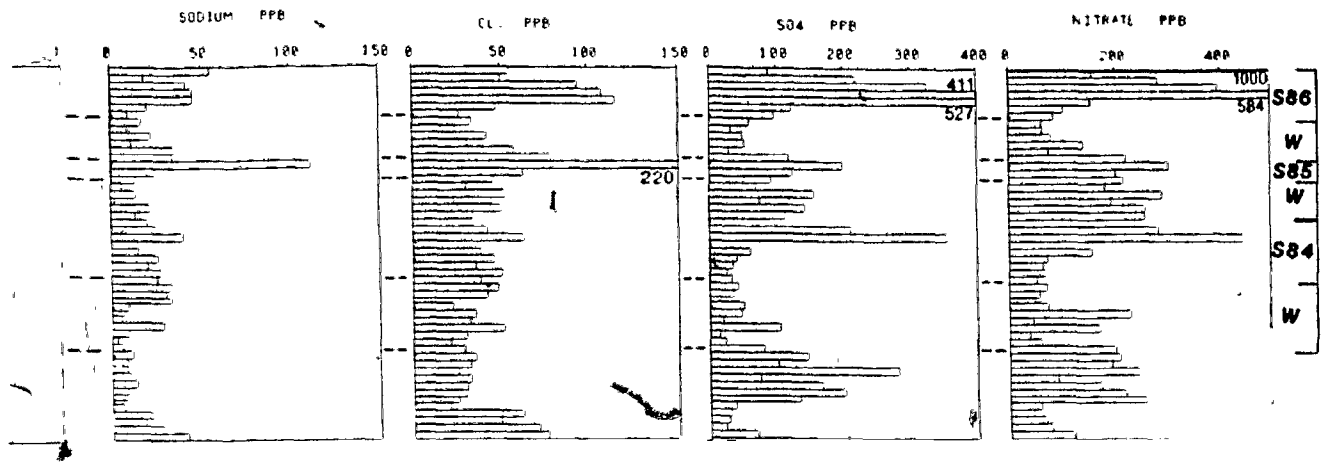
SODIUM PPB
CL. PPB
SO4 PPB
NITRATE PPB
0 50 100 150
0 50 100 150
0 100 200 300 400
0 200 400
220
411
527
1000
584
S86
W
S85
W
S84
W

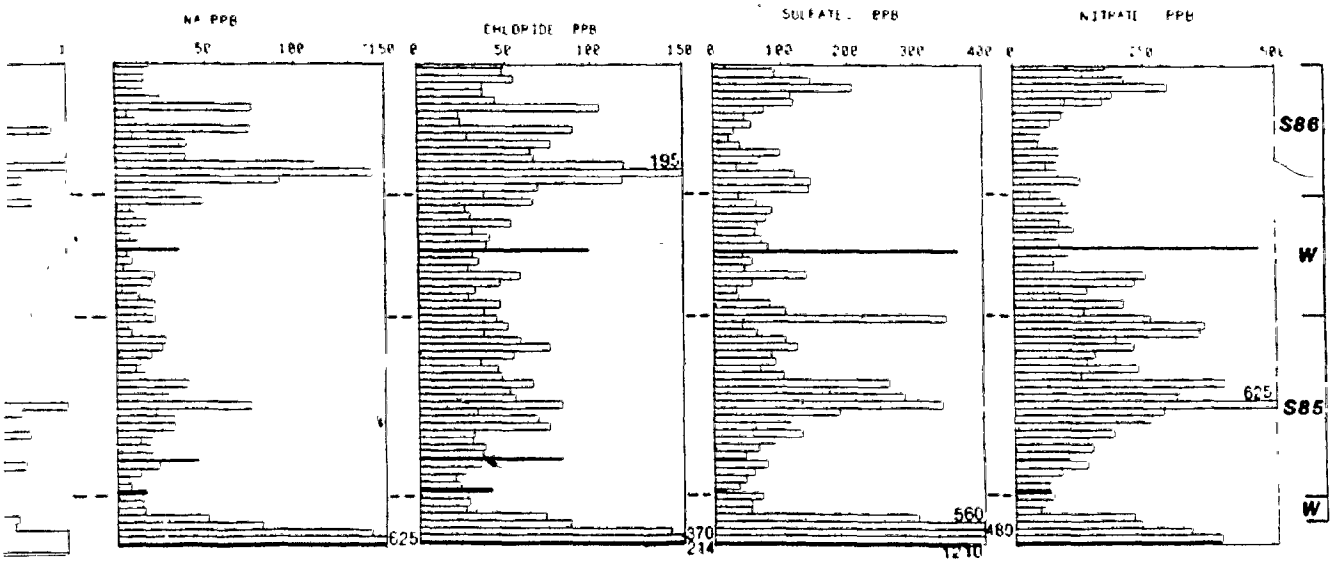
NA PPB
CHLORIDE PPB
SULFATE PPB
NITRATE PPB
50 100 150
0 50 100 150
0 100 200 300 400
195
625
370
214
560
1210
480
625
S86
W
S85
W

FIGURE 5.3

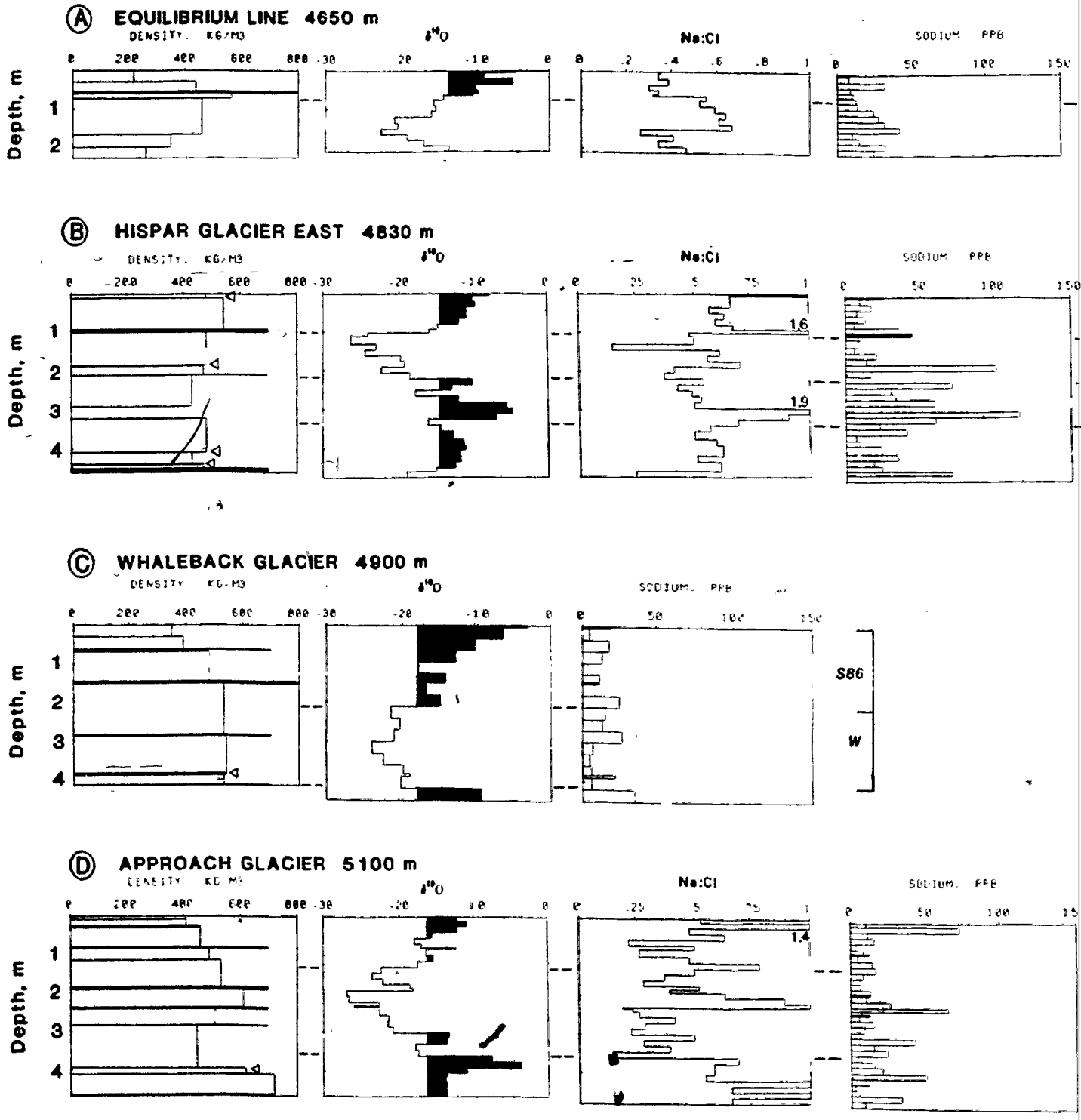

◁ **Open triangles identify dirty horizons**

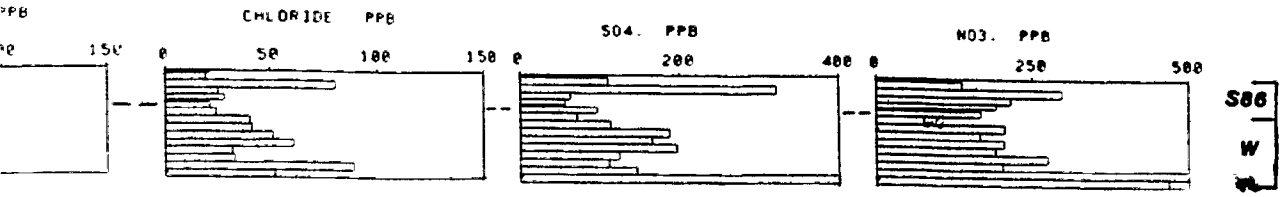
CHLORIDE PPB
0 50 100 150
SO4. PPB
0 200 400
NO3. PPB
0 250 500
S86
W

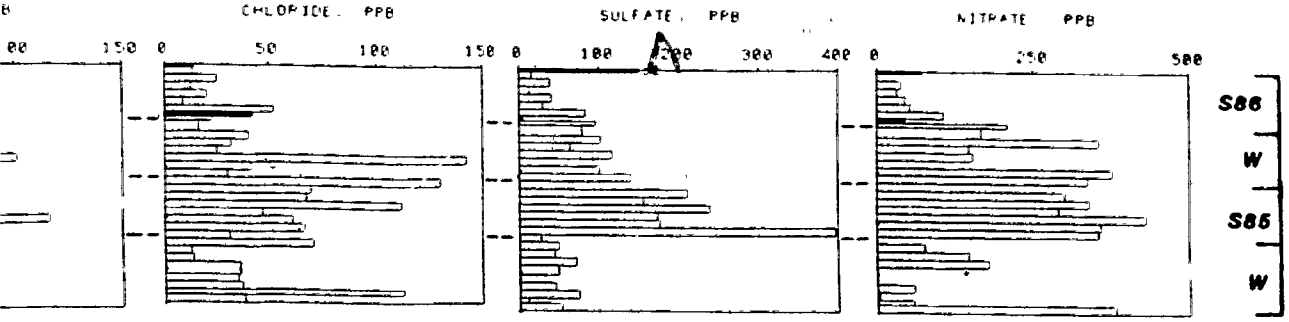
CHLORIDE PPB
0 50 100 150
SULFATE PPB
0 100 200 300 400
NITRATE PPB
0 250 500
S86
W
S86
W

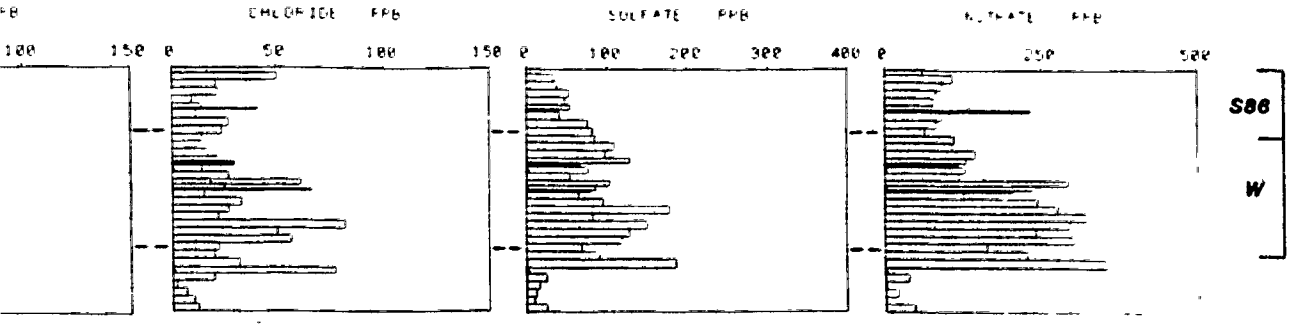
CHLORIDE PPB
0 50 100 150
SULFATE PPB
0 100 200 300 400
0 250 500
S86
W